Høgskulen på Vestlandet

Master Thesis

ING5002

Predefinert informasjon

Startdato:	24-05-2018 10:33	**Termin:**	2018 VÅR
Sluttdato:	01-06-2018 14:00	**Vurderingsform:**	Norsk 6-trinns skala (A-F)
Eksamensform:	Masteroppgave		
SIS-kode:	203 ING5002 1 MOPPG 2018 VÅR		
Intern sensor:	(Anonymisert)		

Deltaker

Navn:	Johan Kristian Møller
Kandidatnr.:	11
HVL-id:	127667@hvl.no

Informasjon fra deltaker

Tittel *:	Effects of ventilation on evacuation in tunnel fires
Engelsk tittel *:	Effects of ventilation on evacuation in tunnel fires

Tro- og loverklæring *:	Ja	**Inneholder besvarelsen konfidensiell materiale?:**	Nei
Jeg bekrefter at jeg har registrert oppgavetittelen på norsk og engelsk i StudentWeb og vet at denne vil stå på vitnemålet mitt *:	Ja		

Jeg godkjenner avtalen om publisering av masteroppgaven min *

Ja

Effects of ventilation on evacuation in tunnel fires

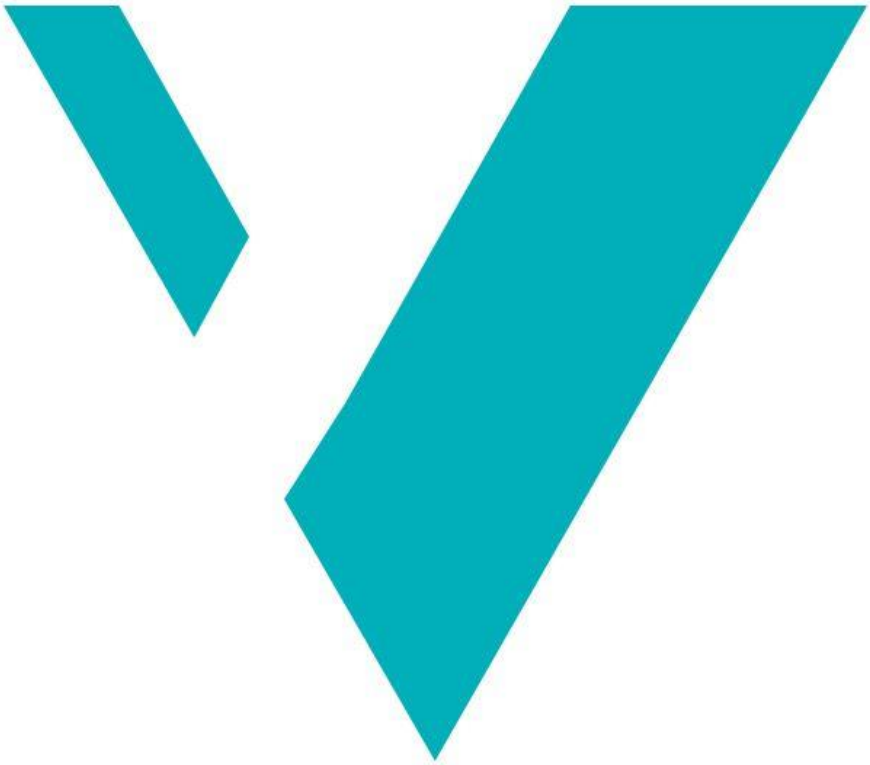

Johan Kr. Møller

WESTERN NORWAY UNIVERSITY OF APPLIED SCIENCES

Master Thesis in Fire Safety Engineering

Haugesund
June, 2018

Western Norway University of Applied Sciences

Effects of ventilation on evacuation in tunnel fires

Master thesis in Fire Safety Engineering

Author: Johan Kr. Møller	Author sign. I am the author of this document 2018.05.31 23:19:03+02'00'
Thesis submitted: Fall 2018	Open thesis
Tutor: Xiaoqin Hu External tutor:	
Keywords: Fire; Tunnel; Ventilation; Dilution; Toxic gases; Life safety; Evacuation; Egress; Safety	Number of pages: 61 + Appendix: 16 Haugesund, June 1, 2018 Place/Date/year

This thesis is a part of the master's program in Fire Safety engineering at Western Norway University of Applied Sciences. The author(s) is responsible for the methods used, the results that are presented, the conclusion and the assessments done in the thesis.

Western Norway University of Applied Sciences

Preface

This master thesis concludes a two-year master program on fire safety at Høgskolen Vestlandet (HVL).

The report focus on the effect of longitudinal ventilation systems on downstream egress conditions in bidirectional road tunnels (single bore tunnels). The overall results are however believed to be universal, i.e. they also give important input to situations in multi bore tunnels with evacuees downstream a fire as well as rail and metro tunnels when accounting for differences such as cross section, fuel type, fire growth rate, heat release rate and distance between exits.

The study includes fire and egress simulations with input data based on results from full-scale tunnel fire tests. Results from the simulations are reviewed in light of these full-scale fire tests and state-of-the-art tunnel fire safety knowledge.

Western Norway University of Applied Sciences

Acknowledgements

This study has been made possible due to my very understanding and supportive family. Thank you to my three girls at home and the rest of our family for all the support during the last two years of late nights and travels.

A very special thanks to my dear colleague and friend Geir Jensen, a true inspirator, motivator and a living definition of what a mentor should be. My academic perspective within fire research in general and special interest for tunnel fire safety origins from this one-of-a-kind inventor and researcher. I am forever grateful for your company that has made my carrier so interesting and fruitful.

Also many thanks to David and Kasper for discussions and collaboration during my three first years exploring fire safety, Vicky my tutor for asking the difficult questions and helping me communicating my work through this thesis, other lecturers at HVL and colleagues at COWI Fire.

Western Norway University of Applied Sciences

Summary

Norwegian road traffic, including transport of goods, is growing and so has the need and ability to build long and deep tunnels. A tunnel fire has a catastrophic potential, so technical measures including ventilation systems are used as replacement for emergency exits or additional tunnel tubes which are very expensive. Originally, tunnel ventilation systems were implemented to handle waste gases and dust from the tunnel, but later this has become one of the most important mitigating measures during fire.

The most commonly used ventilation system in Norway are longitudinal ventilation driven by jet fans in the ceiling and using tunnel portals as supply and exhaust. The reason for this is mainly the cost and the fact that transverse systems with vertical shafts are unwanted in densely populated areas, unpractical for tunnels deep into rock and not feasible for sub-sea tunnels. The transverse systems with ducts increase the required tunnel cross-section and become overly expensive.

Longitudinal ventilation systems that achieve critical velocity are able to create a smoke-free environment upstream the fire, but often evacuees get trapped at the downstream side of the fire. The issue of downstream evacuation has raised discussions in the tunnel fire safety community and the industry regarding ventilation strategies. This has led to the use of several ventilation strategies, ranging from the ventilation system not starting at all before evacuation is completed to systems running at full power from start. The arguments for not starting the ventilation system is that this can diminish smoke stratification whilst on the other side, arguments are based on the dilution of smoke to an extent that visibility and toxicity does not severely affect the evacuation.

This thesis investigate the effects of various ventilation velocities on downstream evacuation conditions using fire- and egress simulation models FDS and STEPS. Fire input data of the simulations are based on full scale tunnel fire test data, including the effect of forced ventilation on the fire growth rate. The egress simulations provide data which is used to calculate FED values on an individual level when combined with the fire simulation results, including the effect of reduced visibility on the walking speed.

The results are unambiguous during the important initial phase of evacuation; increased air velocity worsen the downstream conditions severely compared to lower or no ventilation. This is based on measurements in 2 m height downstream the fire for visibility, temperature and CO concentrations. Egress calculations including upstream evacuation show that low air velocities delay the backlayering and downstream smoke propagation sufficiently to allow for safe evacuation at both sides of the fire.

The maximum CO concentration was found to be higher for low air velocities, including a no-ventilation scenario. However, for the first 10-14 min at 200 m distance downstream of a relatively severe HGV fire, the highest air velocities caused significantly higher CO concentrations at 2 m height. Simulations with the same fire growth rate for high and low air velocities further confirm this. At 600 m downstream, the difference between high and low air velocities increases. Here, the CO concentration for lower air velocities remain well below the higher air velocities for the duration of the simulations.

The somewhat surprising results, at least for some, are believed to be caused by two main phenomena's which should be investigated closer, potentially, through full scale fire tests so that more explicit recommendations can be given for ventilation strategies;

A. Forced air movement, induced from jet fans placed in the ceiling, push smoke towards the floor at an increasing rate with increased velocity. This is both a result of the location of the jet fans

and the dilution of smoke that cools it down and makes it descend faster. The friction between the smoke and air increase with increased velocity and disperse the smoke so that it is both diluted and that the direction is changed from a uniform horizontal flow to include vertical directions as well, but in smaller scale.

B. Increased ventilation velocity spreads the smoke faster downstream the tunnel. Even if it does not obtain the same maximum CO levels as the smoke from lower ventilation velocities, visibility is reduced at an earlier stage and exposure time is increased for evacuees.

Western Norway University of Applied Sciences

Sammendrag

Trafikken på norske veier, inkludert godstrafikk, vokser i takt med vår evne til å bygge lengre og dypere tunneler. En tunnelbrann representerer et katastrofepotensiale så tekniske tiltak, inkludert ventilasjonssystemer, benyttes som erstatning for nødutganger eller ekstra tunnelløp som er svært kostbare tiltak. Opprinnelig ble tunnelventilasjon installert for å redusere mengden eksos og støv, men i senere tid har dette vist seg å være et av de viktigste branntiltakene som benyttes i tunneler.

Det vanligste ventilasjonssystemet som brukes i Norge er langsgående ventilasjon som drives av impulsvifter montert i taket. Tunnelåpningene fungerer da som forsynings- og avkast åpninger. Årsaken til at dette systemet er mest utbredt er hovedsakelig kostnader og det faktum at tverrgående vertikale ventilasjonssjakter er uønsket i tettbebygde strøk, upraktisk i dype fjelltunneler og svært vanskelig å få til i undersjøiske tunneler. Tverrgående ventilasjonssystemer med langsgående kanaler øker tverrsnitts arealet av tunnelen og blir dermed uforholdsmessig dyrt.

Langsgående ventilasjon som oppnår kritisk hastighet gir en røykfri side av brannen (oppstrøms), men ofte befinner det seg også personer på den andre siden av brannen. Dette problemet har skapt diskusjoner både i brannmiljøet og på byggherre-/entreprenørsiden angående valg av ventilasjonsstrategier. Dette har ført til at det benyttes ulike ventilasjonsstrategier som varierer fra å ikke benytte ventilasjonssystemet i det hele tatt før evakuering er fullført og til å slå på systemet med full styrke fra start. Argumentene for å ikke starte ventilasjonssystemet er at man ikke ønsker å ødelegge røyksjiktningen, mens man på den andre siden baserer seg på at røyken blir såpass uttynnet at sikt og toksisitet i røyken ikke blir et problem.

Denne rapporten undersøker effekten av ulike ventilasjonshastigheter på rømningsforholdene nedstrøms en brann ved hjelp av brann- og rømningssimuleringer i FDS og STEPS. Inngangsdata for brannsimuleringene er basert på resultater fra fullskala brannforsøk i tunneler og inkluderer effekten som ventilasjonen har på brannvekstraten. Resultater fra rømningssimuleringene kan benyttes til å beregne FED-verdier på individ-nivå når de kobles opp mot resultatene fra brannsimuleringene og inkluderer effekten som nedsatt sikt har på ganghastigheten.

Resultatene for den tidlige evakueringsfasen viser tydelig at økt lufthastighet forverrer forholdene nedstrøms brannen sammenlignet med lavere lufthastigheter eller situasjon uten ventilasjon. Dette er basert på målinger av sikt, temperatur og CO konsentrasjon i 2 m høyde. Rømningssimuleringene, som inkluderer evakuerende oppstrøms brannen, viser at lave lufthastigheter forsinker røykspredningen oppstrøms såpass at rømning kan foregå trygt på begge sider av brannen.

Den maksimale CO konsentrasjonen var høyere med lav lufthastighet og ingen ventilasjon, men under de første 10-14 minuttene 200 m nedstrøms en relativt kraftig vogntogbrann, gav de høyeste lufthastighetene betydelig høyere konsentrasjoner av CO i 2 m høyde. Simuleringer ulike lufthastigheter og hvor brannvekstraten ble holdt konstant understøtter disse resultatene. 600 m nedstrøms brannen er forskjellen enda større. Der holdes CO konsentrasjonen for de lavere lufthastighetene godt under nivåene for de høyere lufthastighetene gjennom hele simuleringstiden.

De, for noen, relativt overraskende resultatene antas å ha to hovedårsaker som bør undersøkes nærmere, potensielt også gjennom fullskalaforsøk slik at man kan gi mer utvetydige anbefalinger for bruk av tunnelventilasjon under brann:

A. Tvungen luftstrøm fra impulsvifter plassert i taket presser røyk ned mot bakken med økende styrke jo høyere lufthastigheten er. Årsaken til dette er både plasseringen av impulsviftene og uttynningen av røyken som gjør den blir kald og raskere faller ned. Friksjonen som oppstår mellom røyk som presses nedstrøms og luften foran øker med økt lufthastighet og sprer røyken slik at den både tynnes ut og delvis forandrer retning fra en uniform horisontal retning til at også vertikal retning for deler av den oppstår.
B. Økt ventilasjonshastighet øker spredningsfarten på røyken nedstrøms brannen. Selv om uttynningen medfører lavere maksimale CO konsentrasjoner i forhold til lavere ventilasjonshastigheter, reduseres sikten på et tidligere tidspunkt og de evakuerende blir derfor utsatt for røyk over lengre tid.

Western Norway University of Applied Sciences

Table of contents

Table of figures

List of tables

Abbreviations

CFD – Computational fluid dynamics (used to refer to a number of softwares)

FDS – Fire dynamics simulator (an open and free CFD software with focus on fire induced fluid dynamics)

HGV - Heavy goods vehicle

HRR - Heat release rate

FGR – Fire growth rate

FED – Fractional effective dose

PUR/PU - Polyurethane

1 Introduction

Despite increased environmental focus, Norwegian road traffic including goods traffic, has been growing rapidly for the last decades and still are. The need and ability to build long and deep tunnels such as sub-sea tunnels, has been present for over 30 years, starting with the subsea Vardøtunnel in Norway in 1983 [1]. Traffic and regulations has been substantially developed since the early 1980's, whereas the overall physical design of tunnels has changed less. The interior has however changed dramatically, both with regards to installations and materials used.

1.1 Tunnel fire safety

For Norwegian tunnels, it is a requirement that tunnel owners facilitate for evacuation to happen in a safe manner if a fire were to occur [2]. What this really means in practice is not specified, but one thing is for sure, the facilitation requirements for evacuation in tunnels are lower than in buildings. Normally one assess egress facilitation by studying available safe egress time (ASET) and required safe egress time (RSET). If the available time is longer than the required time to evacuate, egress safety is maintained. This is the requirement for Norwegian buildings [3], but no such requirement exists for tunnels.

In public buildings the maximum recommended length to a protected evacuation route or exit is 30 m whilst in a Norwegian tunnel the corresponding length can be up to 10 000 m for new tunnels with traffic figures below 8 000 vehicles on average per day according to section 3.6 of [4]. This is, however, not in alignment with the appendix referred to in §8 of [5] (bullet point no. 2.3.6), which states that emergency exits shall be in place when the traffic volume exceeds 4000. At the same time, even higher traffic volumes are allowed for existing tunnels of equivalent lengths without such exits [5]. For comparison, the American and internationally used standard NFPA 502 [6], requires emergency exits to be provided in tunnels longer than 300 m and with a maximum distance between exits of 300 m. As one can see, there is a gigantic difference in the egress requirements for buildings and tunnels and for tunnels between countries. Higher ceiling and good overview of the "fire compartment" in the vicinity of a fire in a tunnel cannot account for this difference.

The probability of tunnel fires are increasing with increased traffic. According to [7], there was 25 fires on average in the 1130 Norwegian road tunnels every year between 2007-2015, i.e. the probability of a fire in a specific tunnel is 0,022. In comparison, there was 3092 building fires in 2016 [8] divided on approximately 4 100 000 buildings [9], i.e. the probability of a building fire is 0.00075 and even lower for public buildings. This means that the likelihood of a tunnel fire is 29 times higher than for a building fire. Even so, the number of fire fatalities in buildings has been relatively steady for the last four decades, with an average of 58 fatalities per year since 2000 [8]. Mathematically, the corresponding annual death rate due to fire in tunnels are then 0.47. Historical data however, show that no one has died in a Norwegian tunnel due to fire for the last couple of decades. The occupancy is of course a big difference when comparing buildings and tunnels, but vehicle fires in a tunnel requires persons to be present and active. Even when accounting for the fact that many who dies in building fires are asleep, the Norwegian statistics are still surprising when looking at it in general. However, international tunnel fire catastrophes show that there is a big potential risk.

An important aspect of tunnel fire safety is the potential for "catastrophic" fires in tunnels (> 4 fatalities [10]), considering the facilitation when only looking at yearly average traffic figures. The "missing link" in

the requirements for specific measures and limits, and ways to enforce this, with regards to peak hours due to ferry lines or convoys during winter, reinforces this problem. In all cities, there are peak hours that result in queuing inside tunnels. City tunnels often have high traffic figures anyways, and get a higher safety level with respect to distance between emergency exits and other safety installations than tunnels in the outskirts with lower annual traffic, which there are many of in Norway. A peculiarity for the outskirts of Norway are the fjords and the high mountains, resulting in sub-sea tunnels and/or ferry lines connected with tunnels. For tunnels located in mountain areas, convoys during winter is not uncommon. This result in high traffic volumes within a limited time and close to no traffic in between these hours. As one can imagine, a tunnel fire of a certain magnitude necessitates a vehicle inside the tunnel, so whenever the possibility of a fire is there, there is also a lot of other vehicles inside the tunnel and a potential for a catastrophic outcome is in place. One catastrophic fire can turn the statistics for the last decade upside down. With increasing traffic, long and deep tunnels, a catastrophic tunnel fire is by many perceived as an event just waiting to happen, it is just a matter of time.

1.2 Why fire in tunnels are a problem

Tunnels have a considerably longer lifetime than what has been, and still are, normal to account for when designing emergency exits for them. Typically, calculated traffic figures 20 years ahead are used to determine the risk level [4]. This creates a major challenge when considering fire and life safety in existing tunnels, as more traffic are increasing the risk while the overall expectations to fire and life safety (regulations) has also increased. The requirement for emergency exits was not implemented in single tube road tunnels until 2006[1] [11] [12], resulting in many existing tunnels today with long egress pathways. These pathways are of course the same as for the smoke that travels from a fire so there is a need to evacuate in smoke, which is a big problem.

The only feasible way to adapt old tunnels to heightened traffic numbers and keep an acceptable risk level are in many instances limited to implementing technical measures. Physical changes to the design, e.g. construction of an additional tunnel tube or dedicated emergency exits, are often impossible, and in all cases very expensive. Neither is this a requirement when upgrading existing tunnels according to Norwegian tunnel safety regulations, which is based on the EU-directive of 2004/54/EF on minimum safety requirements in road tunnels, referenced in [5].

The economic aspects, both of keeping goods traffic and adding an extra tunnel tube or emergency exits (emergency exit tunnels), limits the possibilities of measures that can effectively reduce risk. Many other measures, such as signage, barriers, lighting, walkways, water for firefighting and ventilation are implemented, but does not pose the same effectiveness and robustness as an actual exit. Fixed firefighting systems, such as sprinklers and water mist, have become more frequently used in the later years, but not in Norway. This is an effective measure to reduce fire spread to other vehicles and the maximum HRR [13]. For now, ventilation seems to be the main and most used measure to mitigate the risk for people inside a tunnel in case of a fire.

Many tunnel owners are facing, what they call, an irrational risk perception for tunnel fires in the society. When looking at the statistics [14], this can be understandable, and efforts and resources should instead

[1] It is noted that Statens vegvesen handbook 021 for road tunnels of 2004 is not publicly available (withdrawn from server; https://www.vegvesen.no/binary?id=14123).

be used on fire prevention in private homes where most lives are lost [8]. Tunnel fires however, represent potential catastrophic emergencies, and people do not expect to be put in such situations when using public roads or infrastructure. Furthermore, why should authorities use money, funded by the public, to build tunnels, or other structures, exposing the public for such risk? The potential risks of tunnel fires have not been fully visible until the joint work of several countries was started in the 1990's and early 2000 with specific tunnel fire safety programs that disclosed much higher HRR's in tunnel fires than was believed to be the truth up until then [15] [16]. Some of the programs was a result of the catastrophic tunnel fires in Mt. Blanc (1999), Tauern (1999) and St. Gothard (2001), whilst others was proven relevant after these fires. Also, the channel tunnel fires between UK and France (1996 and 2008), surprised many with respect to what HRR's one can obtain in a tunnel fire [15]. For most of these tunnel fires and the scenarios representing a potential catastrophic outcome, heavy goods vehicles (HGV's) are a common denominator.

The focus on HGV fires is not only due to the potential high HRR they represent, but also the fact that 44 % of all tunnel fires in Norway (2008-2011) happened in tunnels with a gradient of above 5 %, even though only one out of twenty five tunnels have this kind of gradient. Such steep gradients are typical for subsea tunnels, but also many existing tunnels in Norway. More than half of these fires involved HGV's [17]. In total, HGV's represented 40 % of all tunnel fires in Norway between 2008-2015 whilst the HGV share of the total traffic was 14 % [14].

1.3 Objective of this thesis

For a long time, ventilation systems was mainly used to remove pollution from traffic exhaust in tunnels. Later, these systems has become one of the most important fire safety measures in tunnels [15]. Improvements has been made to the systems to cope with heightened amount of exhaust from increasing traffic and to handle larger fires. Research and experience has shown that tunnel fires can have a much greater heat release rate than one expected in the 1990's though [18], creating a problem in existing tunnels.

Ventilation as a measure to reduce the consequences of a fire was originally, and are still to a large extent, intended to aid the fire service in approaching fires, providing a safe and unobstructed line of attack and retreat. Recently, additional focus has been on the internationally accepted cornerstone of life safety in tunnels; the concept of self-evacuation. This means the tunnel safety strategy rest upon the assumption that people are enabled to get out of a tunnel during a fire on their own.

The positive outcome after several major incidents in Norwegian road tunnels for the last 5-7 years, Oslofjordtunnelen (2011/2017), Gudvangatunnelen (2013/2015) and Skatestraumtunnelen (2015) [2], has publicly been described as pure luck. It is however of great interest for the tunnel fire safety community to investigate this in an academic way. May ventilation systems in these tunnels have impacted the outcome in positive direction, considering many has been evacuating for long distances downstream of the fire? Road authorities in Norway has experience supporting this, as fire tests in Byfjordtunnelen (1998) and Bømlafjordtunnelen (2000) gave non-lethal CO and NO_X concentrations downstream of the fires with the use of longitudinal ventilation (Nilsen, A. R., Lindvik, P. A. & Log, T., 2001, referenced in [19]). A general perception that longitudinal ventilation will dilute smoke and toxicity

downstream a tunnel fire was strengthened by this study. However, the documentation of these tests are not publicly available and so it is a challenge to verify the findings.

Still, there are no clear approach on how a ventilation system are best applied to assist persons downstream of the fire. Several strategies are used and even more are proposed in literature, including:

- delayed start or no ventilation at all until fire brigade has arrived
- start of ventilation on low velocities (until evacuation is finished)
- use of the ventilation direction and velocity which was dominant on the time of fire
- full capacity of the ventilation system in a predefined direction or in a specific direction depending on where the fire is

This has made operation of the ventilation systems difficult and unpredictable, and often the chosen strategy, whatever it has been, has been criticized after incidents. The challenge lies in the fire dynamics; increased ventilation rates can increase the intensity of a fire and make it grow and spread faster. At the same time it is desirable to obtain a ventilation rate that prohibits backlayering, the rate referred to as the critical velocity, to aid firefighting and rescue. Furthermore, the gradient, or vertical alignment of the tunnel and other geometrical parameters of the tunnel, outside natural wind conditions, temperature, pressure differences etc. will influence the conditions within the tunnel. This is somewhat troublesome, since ventilation also can make the situation inside the tunnel worse, especially for those downstream the fire.

This master thesis is dedicated to those who are so unlucky to end up on "the wrong side" of a tunnel fire with longitudinal ventilation. This is a relevant issue in single bore tunnels with bidirectional traffic and multi bore tunnels where traffic congestion or other aspects gives scenarios with evacuees downstream the fire. The question is really how increased ventilation velocity influences the conditions, and especially toxicity of the smoke downstream the fire, when also considering the ventilation's effect on fire intensity, growth rate and spread. The objective is to establish a new set of knowledge of these physics for designers and operators to make better use of the ventilation systems in case of tunnel fires. This can give a cost-effective rise in safety level for existing and new tunnels by using systems already in place in a more optimized way. The work is based on investigating the following hypothesis;

"*Increased longitudinal ventilation velocity will increase the probability of surviving an evacuation downstream a tunnel fire*".

1.4 Investigations using fire and evacuation simulations

The hypothesis will be investigated by looking at downstream toxicity for different ventilation velocities using CFD simulations in Fire dynamics simulator (FDS) [20]. Theoretical data, based on full scale fire experiments, will be used to account for the influence of ventilation velocity on the fire growth rate (FGR). This is further described in chapter 5 and is based on a tunnel fire scenario given in chapter 4. The production of smoke, i.e. toxic gases, is directly linked to the HRR and the material burning so the change of ventilation velocity will influence both the FGR and the downstream conditions [21]. To obtain valid results it is therefore of vital importance to account for these dependencies.

Toxicity at different distances downstream the fire will be evaluated as well as full evacuation scenarios, further described in chapter 6. The evacuation simulations include the influence of reduced visibility on walking speed and log the uptake of toxic gases. The effect of toxic exposure is investigated on an individual level. This is done by importing FDS results to the evacuation simulation program STEPS [22]. Logging toxic gas exposure for individuals, which is also affected by visibility (walking speed), enables calculations of fractional effective doses (FED) which can give valuable input to how many will be incapacitated in the different ventilation scenarios for comparison. FED values are often used to assess survivability in the far field of a fire since it accounts for high concentration exposure to toxic gases during short periods as well as low concentrations during longer periods (Bukowski & Tubbs, chapter 56 in [23]). Further explanation of this is given in chapter 7.

Chapter 2 gives an overall presentation of state-of-the-art on tunnel fire research, whilst chapter 3 present the methodology used to investigate the effect that ventilation has on the downstream conditions. Results from the FDS and STEPS simulations are given in chapter 8 and further discussed in chapter 9. Conclusions, based on the findings in this report are given in chapter 10. The need for further work is presented in chapter 11.

It is the sincere hope that the results of this work can bring more focus and research to how longitudinal ventilation systems can be best used during fire evacuation in tunnels.

2 Tunnel fire dynamics

There are still a lot of unknowns when considering characteristics of tunnel fires and research on the specifics of tunnel fire dynamics are ongoing work. Ingason and several associates of him has undertaken extensive research and performed a number of full scale tunnel fire experiments such as the Runehamar tunnel fire tests (2003) [18] and the Metro project [24]. Ingason and his co-workers Lönnemark and Li compiled this work and also reviewed state-of-the-art knowledge internationally in the book Tunnel fire dynamics [25]. This book summarizes and expand on the findings from a wide set of tunnel fire tests performed and put them in context with the science of "traditional" fire dynamics.

Ingason, Li and Lönnemark present the distinction between "open fires", "building fires" and "tunnel fires" in [25]. The main characteristic for tunnel fires is the interaction with tunnel ceiling and tunnel geometry overall, such as the size of cross section, gradient and length, ventilation conditions including metrological boundary conditions and the resulting HRR's.

2.1 Tunnel fire growth rate and maximum heat release rate

In 2001, before the Runehamar tunnel fire tests, Carvel, Beard, Jowitt and Drysdale, predicted the influence of longitudinal ventilation on HGV fire development and size (HRR) in tunnels using Bayesian methodology and an expert panel exposed to available test data [26]. The results show that the expected influence of longitudinal ventilation on FGR and HRR ranged from four to ten times depending on the velocity compared to no ventilation (only natural ventilation). This was an important encouragement to the fire safety community to perform full-scale tunnel fire tests which was rewarded in 2003.

Tunnel fire experiments performed in Runehamar tunnel in western Norway in 2003 show that tunnel fires including heavy goods vehicles (HGV's) can reach HRR's of above 200 MW [18]. According to Ingason et al, the maximum heat release rate is not determined by the ventilation (if not under ventilated of course), however, the ventilation velocity is crucial for the fire growth rate (FGR). The assumption that maximum HRR is not determined by the ventilation velocity is contradicted by Li, Mei, Li & Zhang [21], at least for smaller tunnel fires (< 30 MW). The article does not handle FGR since the tests are done with pool fires of Heptane and Acetone, which will quickly reach the maximum HRR. The FGR would only be subject to fire spread rate which is very fast in liquids compared to solid materials. The findings of Li et al. could however be interpreted as an effect of ventilation on maximum HRR in under ventilated fires, which is something else.

The maximum HRR and corresponding FGR varies a great deal in different sources. Table 1, from Annex A of NFPA 502 [6], summarizes typical tunnel fire data found from several experiments performed in the world. The values varies up to a factor of 10 for HGV's. This must be seen in conjunction with the different size of these vehicles and the wide variety of goods they can carry. One important aspect of today's requirements in tunnels, and an important distinction to make when assessing tunnel fire scenarios, is the difference between measured experimental data and the design fires given by different road authorities for tunnel design. At the time of writing the book on Tunnel fire dynamics (2014), Ingason et. al. compiled design fires to be used in road tunnels for different countries (see Table 1). The values are placed in the same table as the experimental data from NFPA together with Norwegian data at that time (not included in Ingasons summary). The data serves well as a reminder of what time it takes for the society to adsorb the information that was revealed about HRR for heavy goods vehicles in 2003

and earlier. It also shows that design fire scenarios are not the same as the expected fire scenario. In design fires given from authorities lie politics and what must be considered as a societal cost-benefit approach. However, in light of the data given in section 1.2, about HGV's being overrepresented in the fire statistics and the fact that "normal" goods, such as margarin (Mt. Blanc tunnel), furniture (Runehamar tunnel fire tests) etc. can give a HRR of up to and beyond 200 MW, this approach seems inadequate.

Table 1. Tunnel fire data for typical vehicles from NFPA 502 table A.11.4.1 of [6], table 6.1 of [25] and table 5.4 of [27].

Vehicles	**Experimental HRR** [6]		**Design fires for road tunnels per 2014**				
	Peak HRR (MW)	**Time to peak HRR (min)**	**PIARC* (MW)** [25]	**French (MW)** [25]	**Germany (MW)** [25]	**Norway (MW)** [27]	**NFPA 502 (MW)** [25]
Passenger car	5-10	0-54	2.5-5	2.5-5	5-10	20-100 (depending on length and annual average traffic, not vehicles)	5
Multiple passenger cars	10-20	10-55	8	8	5-10		15
Bus	25-34	7-14	20	20	20-30		30
HGV	20-200	7-48	20-30	30	20-30		150
Tanker (combustible liquid)	200-300	-	100	200	50-100		300

* PIARC is the World road association and recommendations given by them are used by several countries.

Recent investigations and experiments presented by Li and Ingason [13], show that the FGR are heavily dependent on the physical surroundings of the fire, and introduce an important distinction between shielded and non-shielded tunnel fires. In fact, FGR for HGV fires is found to have an approximately linear relationship with ventilation velocities for non-shielded fires. If a fire is shielded, however, a physical barrier (windbreak) exists directly upstream the fire source which limits the influence from the ventilation on the flame (deflection of flame that impose fire spread) and on the combustion process (not feeding sufficient oxygen). The latter can in some cases lead to local under ventilation, i.e. areas around the combustion zone with limited oxygen concentration which reduces the HRR.

2.2 Combustion toxicity in tunnel fires

The production of smoke and toxic gases are a well-known phenomenon and exposure to fire smoke represents a risk. The wide range of products and their share in the mix that normally is only referred to as smoke differ significantly depending on the fuel (what is combusted), ventilation, local geometry and the type of combustion (smouldering, open/free fire or under ventilated fire) (Gottuk & Lattimer, chapter 16 in [23]).

Mainly, the products from a fire affecting the ability to evacuate are divided in two main categories; irritants and asphyxiant gases. The former reduce the ability to evacuate because of e.g. irritated eyes (leading to tears and closing of the eyes) and the latter leading to unconsciousness or death, depending on the dose because of its accumulative effect (Purser & McAllister, chapter 63 in [23]). Typical asphyxiant gases from fire are HCN, CO, CO_2 and low oxygen concentrations.

The main toxic gas "tracer" for fatalities from smoke are carbon monoxide (CO) which is found to cause more than half of all fire fatalities (Gottuk & Lattimer, chapter 16 in [23]). CO in the smoke is a result of the incomplete combustion of pyrolized fuel, or reactants, containing carbon. CO are oxidized during the combustion process to form CO_2 and H_2O. However, seldom are fires able to combust all the reactants, resulting in a variable degree of CO and other un-combusted reactants in the smoke (Khan, Tewarson and Chaos, chapter 36 in [23]). For combustion to happen, sufficient oxygen is required and this is where the ventilation conditions come into the equation as an important factor. Even though subject to a variety of other variables, ventilation conditions seems to be the main parameter that determines the yield of CO in the resulting smoke. CO_2 concentration is bounded with CO, since an increased CO_2 concentration is a result of oxidized CO, so when the CO_2 concentration is high, the CO concentration is often low and vice-versa. In close to all cases they occur together in a variable degree. CO_2 is not only toxic in itself, as CO, it also has the characteristic that it increase the respiration of persons and so increase the total uptake of toxic gases which leads to a self-reinforcing toxic circle (Purser & McAllister, chapter 63 in [23]).

For tunnel fires, smoke is an even bigger problem than in building fires because evacuation happens in the same "compartment" as the fire. The evacuees and the smoke share the same path of travel, which in tunnels can be very long. Another important aspect for tunnel fires is the magnitude of the HRR, or mass loss rate of the fuel, which is considerably larger than that in building fires, as described in the previous section. Usually, larger fires results in higher production of smoke and toxic gases. On top of this, Ingason presents data for additional smoke gases from vehicles that show significant concentrations of a range of gases other than those normally considered for building fires, such as SO_2, volatile organic compounds, polycyclic aromatic hydrocarbons, polychlorinated dibenzo-p-dioxins and dibenzofurans [25]. This is probably because the materials used to fabricate vehicles differ from those in buildings.

As for building fires, CO and CO_2 are still the main gases to assess and the production of CO, or the CO/CO_2 ratio, is dependent on the ventilation conditions in a similar way as described above [25].

2.3 Tunnel ventilation as a measure to cope with fire

There are several different mechanical ventilation systems used for tunnels, the main systems are;

- Longitudinal system (Figure 1)
- Transverse system (Figure 2)
- Semi-transverse system (Figure 3)

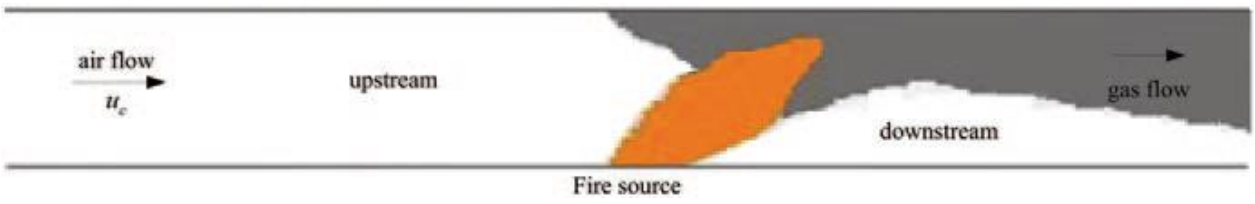

Figure 1. Illustration of longitudinal ventilation, normally induced by jet fans, forcing smoke to one tunnel portal. From figure 13.8 in [25].

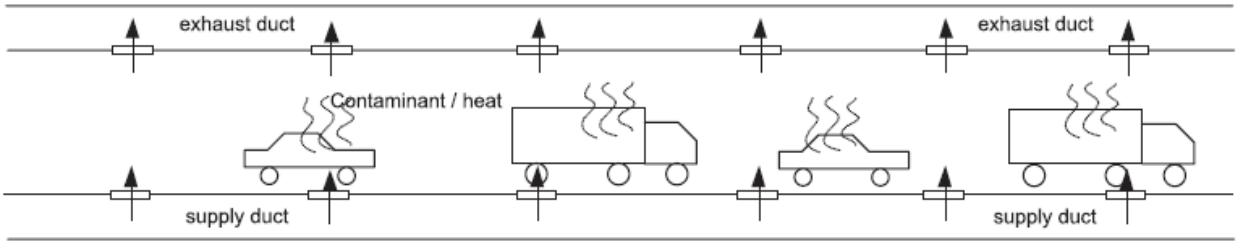

Figure 2. Illustration of transverse ventilation, smoke are transported out of the tunnel via ducts along the ceiling. Supply air can be supplied from the floor or the ceiling in separate ducts. From figure 13.4 in [25].

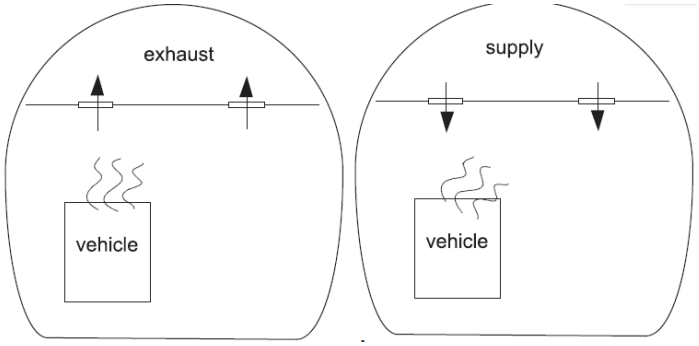

Figure 3. Semi-transverse ventilation system, only exhaust or supply air are used. From figure 13.6 in [25].

In Norway, the predominant ventilation design are longitudinal systems because transverse systems are difficult to design for tunnels deep underneath mountains or for subsea tunnels. The need for vertical shafts in densely populated areas (cities), which is one solution for the transverse systems, represent a great challenge, since these tunnels are primarily built to unburden the built landscape above. Shafts spreading polluted air are not wanted and occupy parts of valuable ground. Furthermore, transverse systems with ducts are more expensive since they demand a larger cross section area in the tunnel for the ducts leading to the vertical exhaust shaft or alternatively to the tunnel portals. Solutions with push-and-pull, i.e. using neighbouring vertical shafts for inlet air, sometimes accompanied by jet fans through the tunnel, to push smoke against the vertical exhaust shaft is also used.

The best ventilation system with respect to fire and life safety would obviously be transverse systems since they can effectively limit the smoke spread and mitigate the effect of fire and smoke in the tunnel. However, this has proven too costly and/or unwanted in most cases, as described above.

Longitudinal ventilation systems use jet fans to force smoke propagation in one direction, and by doing so create a smoke free environment upstream of the fire. The smoke can however to some extent travel against the ventilation direction (backlayering), depending on the ventilation velocity and HRR of the fire. The "critical ventilation velocity" is a thoroughly studied variable defined as the velocity needed to avoid backlayering for a specific fire scenario [25]. For effective firefighting and for people pinned or unable to evacuate upstream the fire, obtaining critical velocity can be crucial, but the impact on evacuees downstream the fire is less explored and something that will be investigated closer in this thesis.

As mentioned in section 1.3, there are several different ventilation strategies used for longitudinal ventilation systems during fire, and there is an ongoing debate in the tunnel building and operator industry regarding what strategy is best. The reason for this is that no clear and unimpeachable

recommendations have been given. Ingason and Li give recommendations in their report of 2016 [13], as far as possible, of lower ventilation velocities in the evacuation phase. But they also acknowledge that it is "*difficult to find out an optimal ventilation velocity as the ventilation has different effects at different locations and at different stages of the fire*" ([13], p. 28). Based on this it is obvious that further work to validate their findings and, if possible, give more input to this issue are needed.

The use of ventilation during evacuation in a tunnel fire can be looked upon as balancing on the egg of a knife because ventilation can worsen the conditions for the evacuees by increasing the fire growth rate, destroying smoke stratification or change what originally was a smoke free side of a fire to a smoke-filled part. This place a big responsibility on the shoulders of the one controlling the ventilation direction and velocity, and is one of the reasons for the ongoing debate.

Figure 4. Illustration of choosing the right ventilation strategy. Downloaded, changed and re-used according to terms given from [28].

The main challenge is of course the fact that longitudinal ventilation can worsen the situation for the evacuees. Smoke stratification and dilution of smoke, i.e. toxicity in the height of persons, is not fully understood and there are contradicting theories regarding these phenomena's which needs to be further investigated.

3 Methodology

There are conflicting information and uncertainties in the fire safety community, as well as in the industry, regarding the use of longitudinal ventilation during evacuation in tunnels. This is mainly related to how ventilation systems should be operated during the early phase of a fire, while evacuees can still be downstream the fire. The hypothesis that "*Increased longitudinal ventilation velocity will increase the probability of surviving an evacuation downstream a tunnel fire*" will be investigated by CFD simulations in FDS version 6.5.3 [20]. A literature study including results and findings from full scale tunnel fire tests and research on other fire dynamic aspects relevant for the input will form the basis for simulations, where different ventilation velocities will be applied. Jet fans in the centre of the tunnel ceiling will be used for ventilation, this will not give uniform airflows over the cross-section of the tunnel, but the target ventilation speeds for upper centre line of the tunnel investigated will be; 1.5 m/s, 3 m/s and 5 m/s.

End-results will consist of several simulations, with different variables, where visibility, temperature and concentration of CO, O_2 and CO_2 will be analysed for the downstream environment for different ventilation velocities.

To give a better perception of how the different ventilation scenarios affects evacuees, an evacuation analysis is performed in STEPS version 5.4 [22]. Results from the FDS simulations are imported to the STEPS-model to account for reduced walking speed in low visibility environment based on the light extinction coefficient and to enable calculations of FED values (toxic dose) for each individual.

The fire- and evacuation simulations performed here are used to assess the effect of different ventilation velocities on downstream evacuation conditions, i.e. it is not the intention of this report to give answers to how many will survive a tunnel fire. The main focus is to corroborate or to give new insight to how tunnel ventilation systems should be used during fire. This being said, input used in the simulations are based on as realistic data as possible.

Sensitivity analyses will be performed to investigate the influence of cell size and mesh split in FDS, as well as additional scenarios to investigate other parameters effect on the results other than ventilation velocity, such as FGR and HRR.

To set up the fire and evacuation analysis, a tunnel fire scenario is presented in chapter 4.

4 Tunnel fire scenario

For the purpose of the analysis, a tunnel fire scenario has been established for which the FDS and STEPS simulations are based upon. The scenario is typical for the challenges that are presented with respect to fire and life safety in tunnels in Norway.

The tunnel to be used in the simulations is 1000 m long and based on the geometry of a T 9.5 tunnel with no emergency exits other than the tunnel portals, according to [4]. Ventilation is applied by jet fans located in the centre top of the tunnel with a volume flow to achieve target longitudinal ventilation velocities of 1.5 m/s, 3 m/s and 5 m/s in the centre line of the tunnel. The difference between applying a uniform air flow over the cross section of the tunnel, which is often done in similar simulations, and using jet fans, which is the method used in real life, is central for the study of the conditions downstream a tunnel fire. The reason for this is shown in section 5.4 and in the results (chapter 8) for how the air flows inside the tunnel behave.

The fire consists of a heavy goods vehicle (HGV) loaded with furniture (70 % wood and 30 % PUR). The HGV is 20 m long, 2.6 m wide and 3.2 m high and are located 205 m from the closest tunnel portal.

Vehicles queuing up to 250 m downstream the HGV with passengers must evacuate on foot. The que consists of four buses with 30 passengers each and 30 cars with two passengers each. On the upstream part of the tunnel, 10 cars with two passengers each are assumed to evacuate on foot. In total this results in 200 passengers that needs to evacuate on foot to the tunnel portals, 180 downstream (maximum of 770 m) of the fire and 20 upstream (maximum 164 m). The only exits are the tunnel portals.

Tunnel geometry, jet fan characteristics and evacuation scenarios are further depicted in chapter 5 and 6. Figure 5 shows an overview of the tunnel scenario.

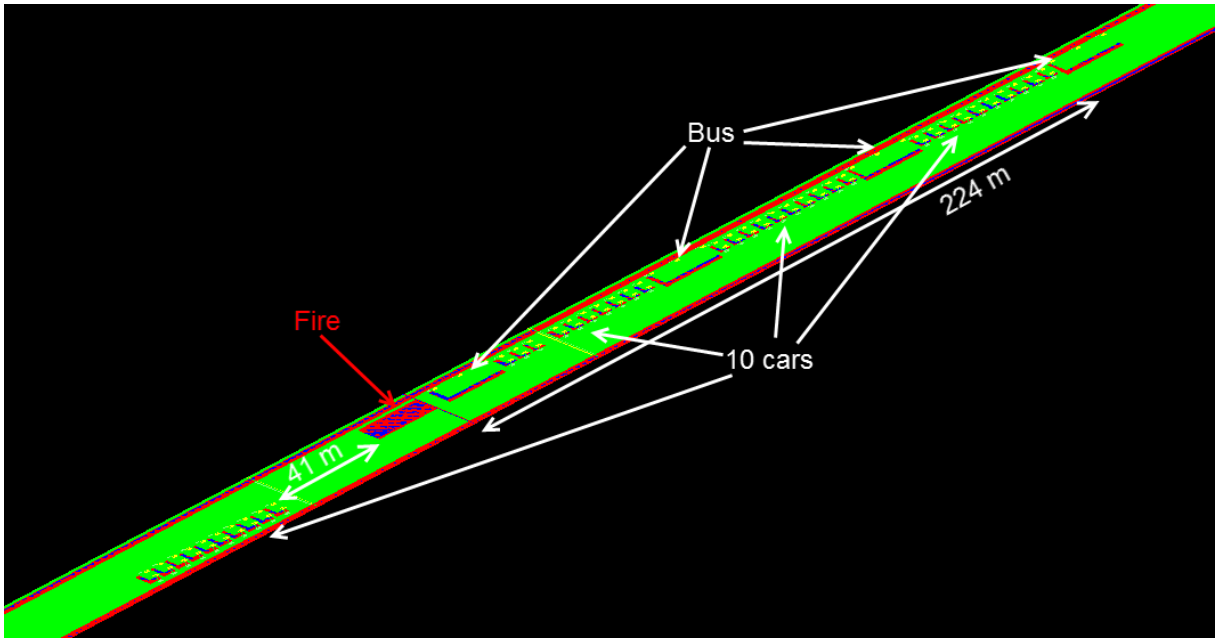

Figure 5. STEPS model showing the placement of buses and cars relative to the fire.

5 FDS input

The FDS model and input for the FDS simulations are presented in this chapter.

5.1 Tunnel geometry

The FDS model is based on a concrete T 9.5 tunnel cross-section given in Statens vegvesens handbook N500 [4]. This is one of the most used tunnel cross sections in existing bi-directional tunnels as well as new tunnels with low average traffic (yearly traffic). The T 9.5 are also used for new double/twin tube tunnels.

The geometrical values of T 9.5 are summarized in Table 2 and should be seen in conjunction with Figure 6.

Table 2. Geometrical values for T 9.5 tunnel profile given in table 3.3 and 3.4 of [4].

Total width (B_t)	Centre height wall radian (Y_v)	Wall radius (R_v)	Centre distance wall radians (x)	Centre height ceiling radian (Y_h)	Ceiling height (R_h)	Cross section area (inside)
9.5 m	1.57 m	4.79 m	0.45 m	1.213 m	5.212 m	53.61 m²

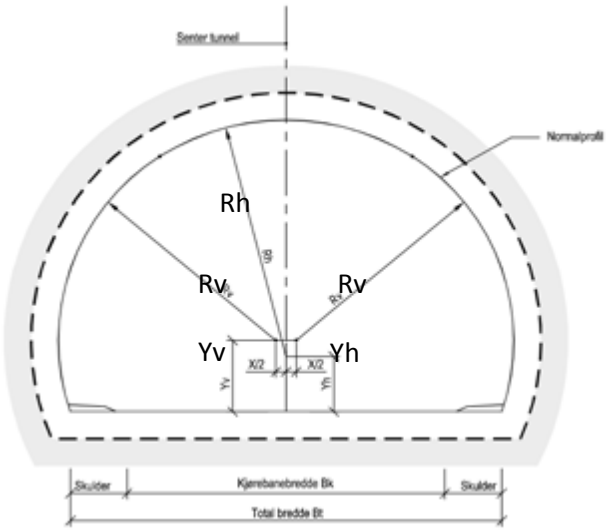

Figure 6. General tunnel tube with coded measures given in Table 2. From [4].

The modelled cross section is slightly smaller than the cross-section given for the T 9.5 tunnel in [4] due to the geometrical limitations in FDS (cubic) and cell size used in the model. The difference is however believed not to be significant.

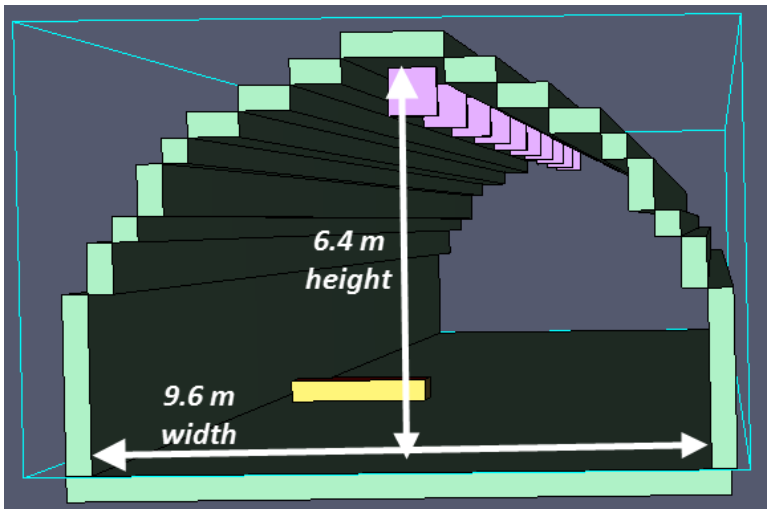

Figure 7. Modelled tunnel cross section (49.28 m²) from the FDS model in Pyrosim.

5.2 Jet fans

A total of 10 jet fans are placed centrally in the top of the tunnel, 50 m from each tunnel portal and continuously through the tunnel with 100 m internal distance. The jet fans are given an area of 0.64 m² and a perimeter of 3.2 m. Different volume flows has been considered to obtain target values of 1.5 m/s, 3 m/s and 5 m/s in the tunnel centre line. This is further explained in section 5.4.

Fire location, placement of jet fans and tunnel length of the model are presented in Figure 8.

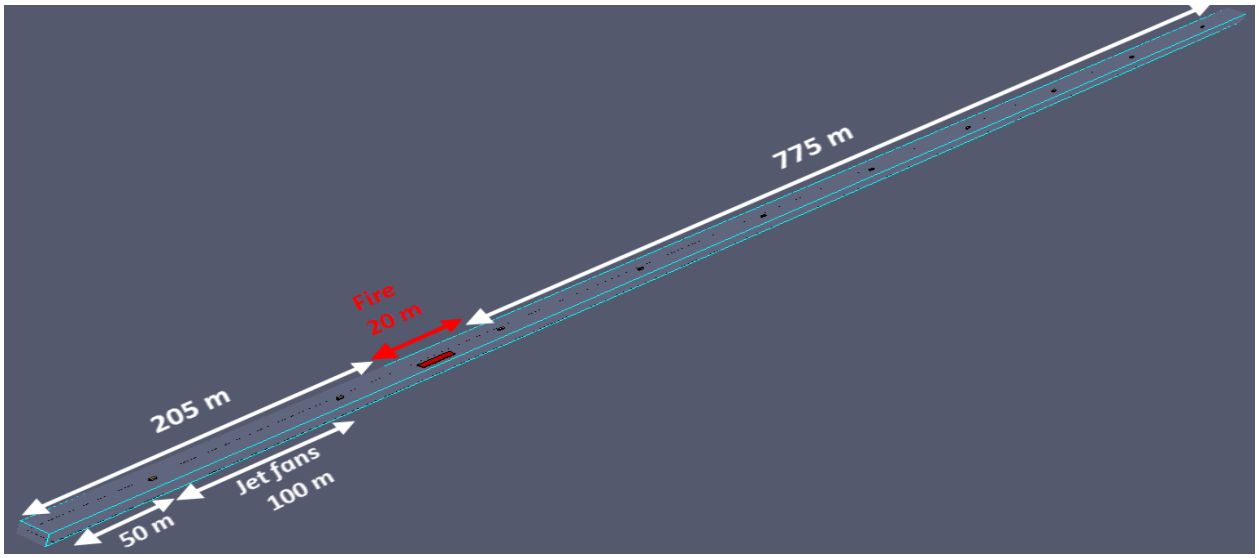

Figure 8. Model overview of tunnel from Pyrosim.

5.3 FDS combustion model

For the FDS simulations, a "simple chemistry model" is used in FDS, which means that the fire origins from a surface emitting "pyrolized" fuel consisting of a predefined mix of gases ready to combust when mixed with sufficient oxygen (air) to produce products [29]. In the case of locally under ventilated conditions, the combustion of the fuel will happen when and where sufficient oxygen meets the reactants. No pre-defined limits for auto ignition are set for the simulations, which, from FDS version 6 and onwards, means that the auto-ignition temperature is set to 0 °C by default, i.e. combustion will happen independently of temperature in the region where the fuel meets sufficient oxygen (air).

The heat of combustion, heat release per unit area, soot yield and CO yield are given as input to the FDS simulations. Since these parameters are results of the type of fuel used, fuel geometry, ventilation and tunnel geometry this is further described in section 5.5 after the simulated fire is presented in section 5.4.

5.4 Fire size and development

With reference to the distinction of shielded and non-shielded fires in section 2.1, the non-shielded HGV fire will be the main focus in this paper, but the shielded scenario (referred to as windbreak) will also be investigated. Non-shielded fires applies to HGV's where the vehicle cover consist only of tarpaulin which will quickly burn off or where the surrounding walls of the HGV are part of the fire or has been burnt away. The shielded fires, or fires with a windbreak, has a physical obstruction upstream of the fuel which reduce the oxygen supply to the fire. This is typically a back-end hatch of metal on HGV's.

When applying a heat release rate per unit area (HRRPUA) in FDS, using the experimental data from Ingason et al., one must consider the *exposed* fuel surface [25]. In FDS a simplification is made, treating the fuel area as a thin surface, whilst in reality, a HGV carrying furniture or similar products, would have a fuel area similar to a box, with 5 exposed surfaces (or even more depending on the porosity of the fuel). The tunnel fire scenario described in chapter 4 consists of a HGV which is 20 m long, 2.6 m wide and 3.2 m high, resulting in a exposed fuel surface of 196.64 m². The simulated fire, however, consists only of a surface of 52 m² due to the fire simulation model used.

The Runehamar test no. 3 having a HRR per square metre fuel of 500 kW resembles the fire scenario described here for a HGV loaded with furniture and are used as basis for the input HRRPUA. According to table 4.8 in [25] the HGV with furniture had a HRRPUA of 500 kw/m². To apply this HRRPUA in the simulations done here, an adjustment of the value is needed according to the ratio between the fuel area in the FDS model (52 m²) and the corresponding exposed area (196.64 m²), which is 3.78. This gives an input value for HRRPUA in the simulation of 1890 kW/m² and a maximum HRR of 98.28 MW. For convenience, this value is rounded up to, and referred to as 100 MW in the report.

Ingason present an expression for the FGR with respect to ventilation in [25] (eq. 5.26);

$$\frac{dQ}{dt} = 1.2 \times 10^{-3} U_0 \sum_{i=1}^{N} C_{f,i} W_{p,i}$$

where U_0 is the ventilation velocity impacting the fire, C_f is an material property given in table 5.1 of [25] and W_p is the "wet perimeter" (contact perimeter between fuel and air flow, here considered to be the surface area of 196.64 m²). Using material properties (C_f) for 30 % PUR and 70 % wood as fuel, will give the following fire growth rates for the three different ventilation velocities investigated;

1.5 m/s: 124.12 kw/s = 7.45 MW/min

3 m/s: 248.24 kw/s = 14.89 MW/min

5 m/s: 413.73 kw/s = 24.82 MW/min

However, the ventilation conditions in the initial stage of the fire will be low before fire alarm system (or detectors monitoring the pollution-level in the tunnel) start to ramp up the ventilation velocities. An iterative process with ventilation test simulations for each of the three target ventilation velocities are performed to obtain the set ventilation values that impact the fire (1.5, 3 and 5 m/s) and FGR for each scenario. I.e. the ventilation velocities referred to, are the ones "hitting" the fire and so it is not a uniform air velocity over the cross section of the tunnel.

The calculated theoretical HRR per time, based on Ingasons expression for FGR and fuel area given above, is illustrated in Figure 9. A description of HRR development for each scenario is found below the figure. It is noted that the fire decay stage, where fuel become consumed and HRR starts to decline, is not evaluated due to the fact that this thesis focuses on the evacuation phase.

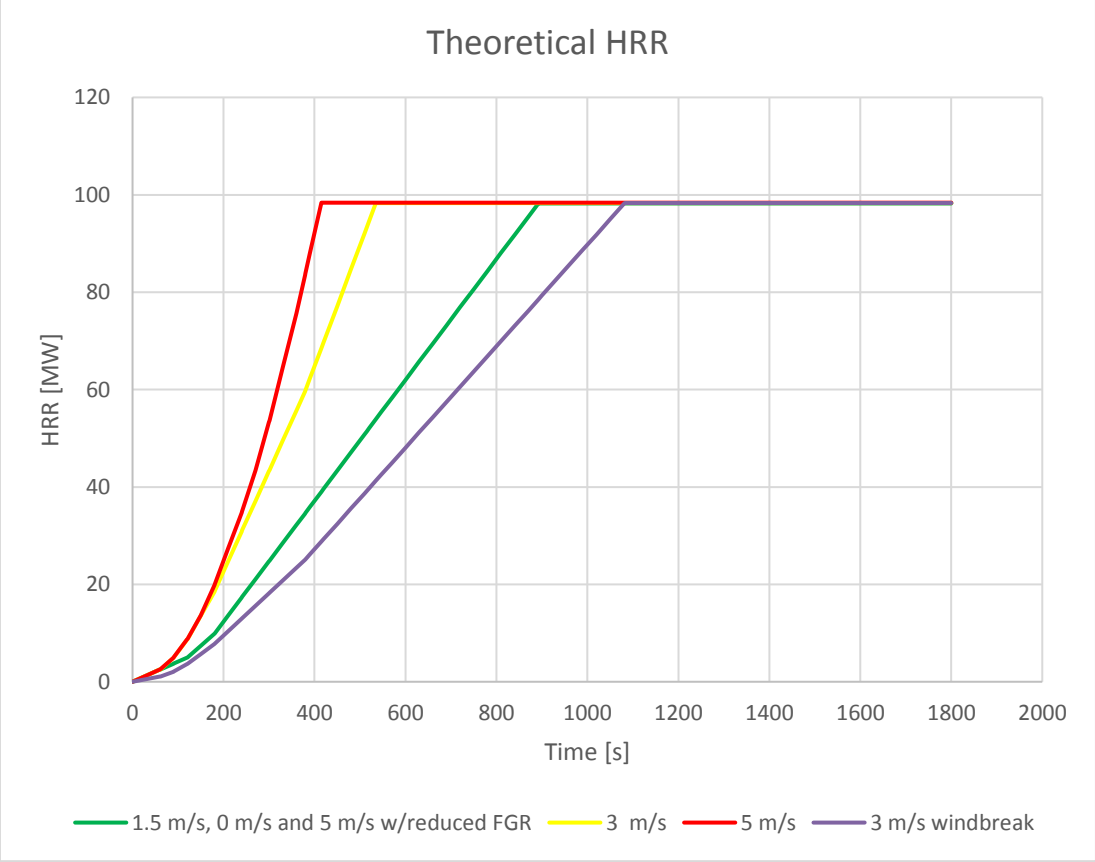

Figure 9. Theoretical HRR for different ventilations scenarios. Note that the FGR identified for the 1.5 m/s ventilation scenario is also used for the 0 m/s scenario, 5 m/s reduced FGR scenario and the 25 MW scenarios.

5.4.1 1.5 m/s ventilation

The model was set up with an initial fire following the FGR of 0.5 m/s ventilation velocity. Volume flow that gave 1.5 m/s to the fire was found to be 5.4 m³/s. Similar "test-simulations" was run for the 3 m/s and 5 m/s scenarios. A total of 10 jet fans and the given volume flow of 5.4 m³/s each indicate the following ramp-up for ventilation velocities and corresponding FGR in the simulation;

- A 0.5 m/s ventilation velocity is considered for the initial 2 minutes, corresponding to a FGR of 41,37 kW/s. This results in a HRR of 5 MW after 2 min.

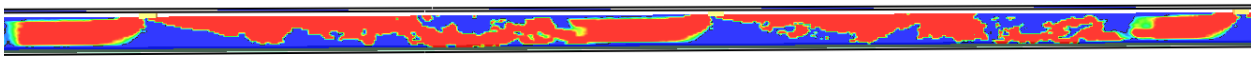

Figure 10. Longitudinal cross-section excerpt from FDS Smokeview after 120 sec of the ventilation test-simulation. Red areas indicate areas with velocity above 0.5 m/s.

- 1 m/s velocity for the next minute (FGR of 82.74 kW/s, resulting in a HRR of 10 MW after 3 min).
- Target velocity of 1.5 m/s is reached after 3 minutes giving a FGR of 124,12 kw/s until the maximum HRR of 100 MW is reached after approximately 15 minutes (892 seconds).

5.4.2 3 m/s ventilation

The corresponding scenario with 3 m/s ventilation velocity is set up with a volume flow of 10.8 m³/s for each jet fan and the following ramp-up for ventilation velocities and corresponding FGR in the simulation;

- A 0.5 m/s ventilation velocity is considered for the initial 60 seconds, corresponding to a FGR of 41.37 kW/s and resulting in a HRR of 2.5 MW after 1 min
- 1 m/s ventilation for the next 30 seconds
- 1.5 m/s between 90-120 seconds after fire start
- 2 m/s for the next minute
- 2.5 m/s after 180 seconds
- Target velocity of 3 m/s is impacting the fire after 380 seconds

Maximum HRR of 100 MW is reached after approximately 9 minutes (532 seconds).

5.4.3 5 m/s ventilation

For the 5 m/s ventilation scenario a volume flow of 18 m³/s is found to give 5 m/s air velocity "hitting" the fire. The FGR is set up based on findings from the test-simulations, showing a ramp-up speed of 0.5 m/s close to every 30 second after an initial velocity of 0.5 m/s for the first minute. The ramp-up is a result of hot gases pushing down the fresh air from the upstream jet fans, giving it less area (cross-section) and so the velocity "hitting" the fire is increased.

5 m/s air flow impacts the fire after 360 seconds and maximum HRR of 100 MW is reached after approximately 7 minutes (415 seconds).

5.4.4 0 m/s ventilation

For the 0 m /s ventilation scenario, no ventilation is included in the simulation, but the FGR from the 1.5 m/s scenario is used.

5.4.5 3 m/s ventilation w/windbreak

For the windbreak scenario the air flow from the 3 m/s ventilation scenario is used, but the FGR is reduced with 58 % according to [25], to account for the windbreak. Maximum HRR of 100 MW is reached after approximately 8 minutes.

For this scenario a windbreak is included upstream of the fire (2.4 m width and 3.2 m height).

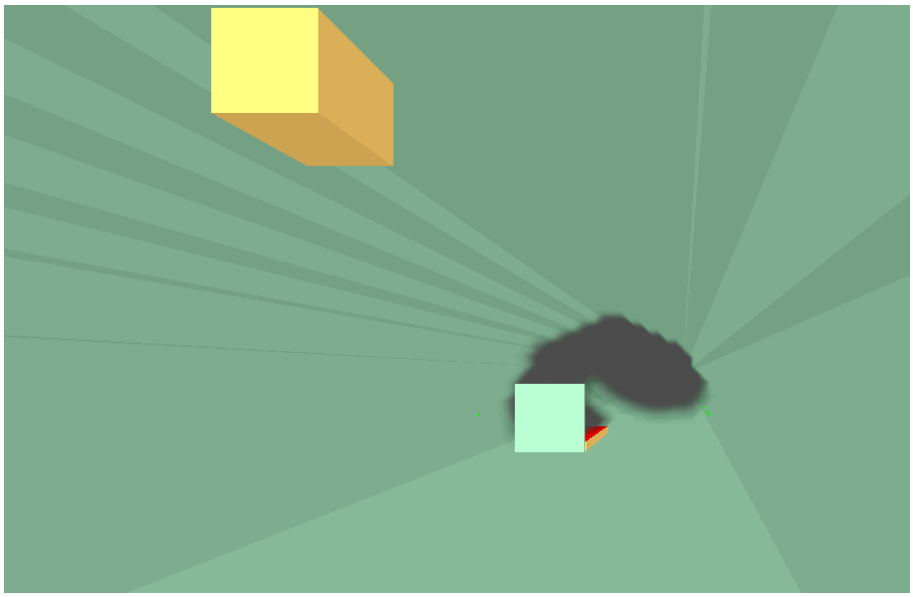

Figure 11. Illustration showing windbreak obstruction upstream the fire from the 3 m/s w/windbreak scenario.

5.4.6 5 m/s ventilation with reduced FGR

For the 5 m/s ventilation scenario with reduced FGR the same volume flow as for the 5 m/s scenario is used, but the FGR from the 1.5 m/s scenario is applied.

5.4.7 1.5 m/s ventilation and max 25 MW HRR

The same FGR as in the scenario for 1.5 m/s is applied, but the FGR is stopped when the HRR reaches 25 MW.

5.4.8 5 m/s ventilation and max 25 MW HRR with reduced FGR

The same FGR as in the scenario for 1.5 m/s is applied, but the FGR is stopped when the HRR reaches 25 MW.

5.5 Other FDS input parameters

Based on the input given for the tunnel fire scenario, other input parameters used for the simulations are summarized in Table 3. From section 2.2 on combustion toxicity it follows that setting specific input parameters for the production of different gases is challenging and dependent on a wide variety of parameters that is not necessarily accounted for in the FDS simulations. This is especially true when using the simple chemistry model for the reaction in FDS, which only accounts for carbon, oxygen, hydrogen and nitrogen as reactants that, in one step, transforms into the given yields of products consisting of soot and CO when mixed with air. It is therefore emphasized that the given values will never be the true ones and that arguments for both increased and decreased values will exist.

The amount (mass) of reactants that combust are dependent on the available oxygen (air). For every kg of reactants that combust, the given heat of combustion are released. This also applies to the production of soot and CO. However, since no auto ignition temperature limit are set (ref. section 5.3), all reactants will be transformed to products when reaching a location with sufficient oxygen. This means that the total production of CO and soot is equal in total, but that the combustion can happen at different locations.

Table 3. Input parameters for the FDS simulation.

Parameter	Value	Comment/Reference
Heat of combustion	20 MJ/kg	Based on 70 % wood with 16.7 MJ/kg and 30 % PUR with 25 MJ/kg from table 5.1 in [25] (rounded up)
Heat release per unit area	1890 kw/m²	Based on description given in section 5.4 of this report.
Fire reaction:		
Carbon	4,56	Composition of fuel (reactant) based on a mix of polyurethane and wood [30].
Hydrogen	6,56	
Oxygen	2,34	
Nitrogen	0,4	
Soot yield	0,09 g/g	Based on soot yield for 30 % PUR (GM23) and 70 % wood given in table A.39 of [23]. The value is increased 15 % to account for the values given being for well-ventilated conditions.
CO yield	0,1 g/g	Based on large-scale tests of yields for different materials and 70 % PUR and 30 % wood, from table 7.2 in [25].

For a full overview of the input to FDS, reference is made to Appendix B for the 1.5 m/s ventilation scenario. Changes done to the other simulations run in this thesis are limited to FGR (ramp up times), air flow of jet fans and HRR (for 25 MW sensitivity scenarios) as described for each scenario.

5.6 Cell size and mesh sensitivity analysis

The model is set up with a total of 5 meshes and used for all scenarios. It includes one fire-mesh, one mesh upstream and three mesh downstream the fire-mesh. Length of the different mesh within the tunnel are shown in Figure 12. Additional 4 m are added to mesh 1 and 5 outside the tunnel opening to capture smoke leaving the tunnel and to get the correct boundary conditions outside and at tunnel portals (open vents).

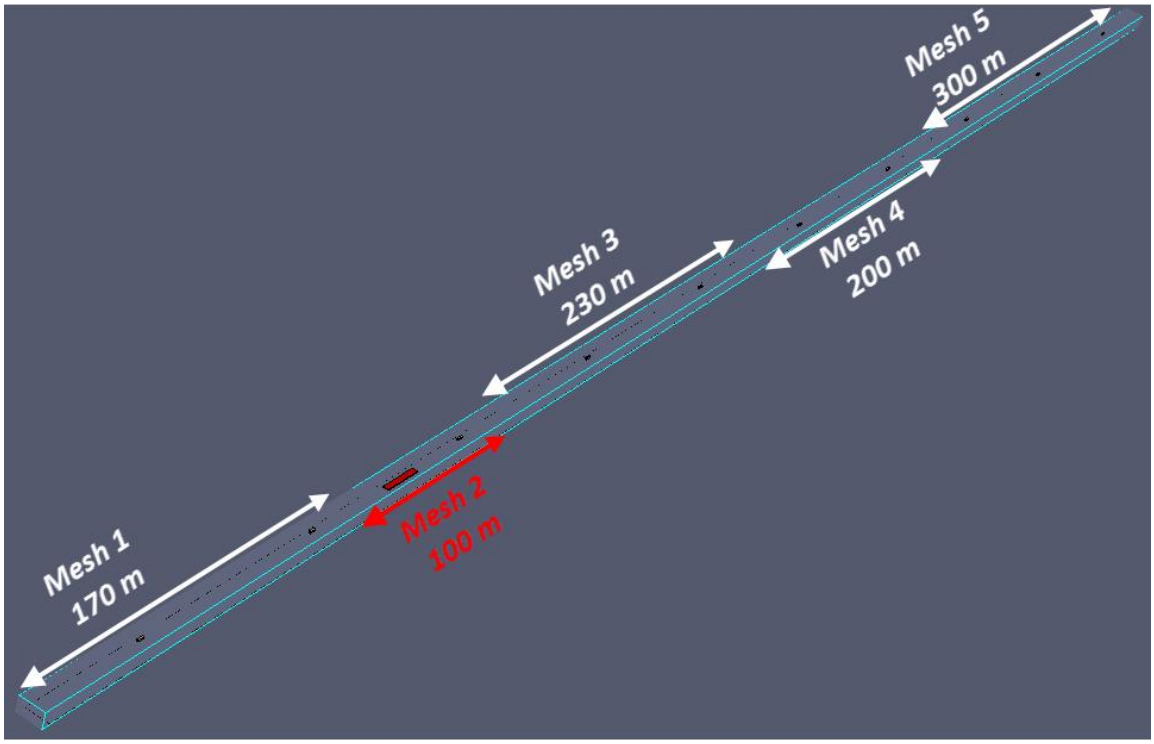

Figure 12. Overview of tunnel showing mesh configuration from Pyrosim.

The main reason to divide the simulation domain in different meshes is to enable use of parallel run of processors on the computer running the simulation, which reduces the total simulation time [29]. Furthermore, the division makes it possible to use different cell-sizes. The total number of cells is crucial for the computational time and quality of the results. A coarse grid (big cell size) gives less cells and shorter computational time, but it also reduces the quality of the results. This is mainly linked to FDS' ability to calculate turbulent flows, small turbulent structures requires smaller cells to "capture" them. Turbulent structures smaller than the cells in that area are not resolved (calculated), but modelled by FDS instead. If the ratio of modelled turbulence structures are big, this can affect the simulation results, not capturing the flows resulting from the given geometry and fire. This is further explained in Appendix A.

Two potential consequences of using too big cells are:

a) not capturing the mix of fuel and air, resulting in reduced HRR, and
b) wrong data output (results) as a consequence of not resolving the descending smoke layer sufficiently.

For the latter, it could have big consequences if a stratified smoke layer exists in the measured area, i.e. for the smaller cells the smoke layer could be situated in the cells just above the measured height, whilst for the bigger cells the smoke is included in the measured height, as illustrated in Figure 13.

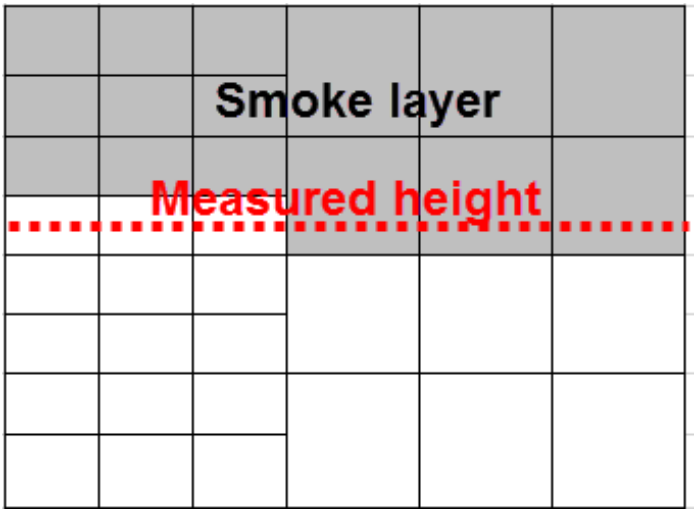

Figure 13. Illustration of how different cell sizes can affect results in FDS.

The same will be true, and even more relevant, for other parameters that has a vertical decrease or increasing value, e.g. temperature, concentrations of toxic gases, visibility etc.

The FDS user guide [29] gives a simplified method of finding cell size that "adequately" resolve the fire plume by the number of cells, of a specific cell size (δx), that will span over the characteristic fire diameter, D*. The FDS user guide emphasizes that this is not a universal solution to find the correct cell size, so additional sensitivity analysis for important parameters is needed for the simulation in question. This is done below, after first finding relevant cell sizes.

As it follows from above, a small cell size is desired to get the best results, but this will again affect computational time. To cope with this discrepancy, the method suggested is used to find a cell size that can both resolve the fire sufficiently and enable several simulations to be done within a reasonable period of time.

The FDS validation guide [31] refers to validation experiments where the $D^*/\delta x$ ratio varies between 5 and 20. The results show satisfying results for HRR and flame height within these limits. D* is found from the equation given below [20]:

$$D^* = \left(\frac{Q}{\rho_\infty \, c_p \, T_\infty \sqrt{g}}\right)^{\frac{2}{5}}$$

For a 100 MW fire the characteristic fire diameter, D*, will be 6.11, when assuming ρ_∞= 1.2 , c_p= 1.0 and T_∞=288 (15°C). A cell size of 0.4 m will result in $D^*/\delta x$=15, which indicate sufficient resolution of the flame. The use of the proposed method given in the FDS user guide and a $D^*/\delta x$ = 4-16 (FDS validation guide use 5-20 [31]) has shown to give sufficient turbulence resolution for small fires, as presented in Appendix A. This is not verified for tunnel fires with large HRR though.

In the early stages of the simulation, the HRR will be smaller and the number of cells spanning the fire will be lower. This is especially relevant for the 1.5 m/s ventilation velocity scenario. To mitigate this, the "fire mesh" in the 1.5 m/s scenario has 0.2 m cells (cubic). For the others, including the sensitivity scenarios, the 0.4 m cubic cells are used. This results in different amount of cells between the scenarios, 3 and 5 m/s having approximately 1.3 million cells and the 1.5 m/s scenario having 2.15 million cells.

Jet fans introduce turbulent flows, especially in the fire zone, where the air flow meets the buoyant hot gases. For this report, the main objective is to assess the conditions in a distance downstream of the fire and an additional refinement of the mesh to cope with this is not implemented. However, the potential consequence is investigated through the sensitivity simulations shown below.

Another possible error source is the mesh-to-mesh communication, i.e. the ability of FDS to correctly transfer information between different mesh. This can especially be a problem between meshes with different cell-size.

To investigate if the cell size and mesh division is affecting the results, a sensitivity analysis for a model with uniform meshes (all 0.4 m cells) and a model with a finer fire mesh (0.2 m cells in fire mesh and 0.4 m in the other) has been conducted. The same model as described in section 5.1 is used for a maximum 25 MW fire and 1.5 m/s ventilation velocity. HRR, temperature (2 m height) and CO concentrations (2 m height) within the fire mesh (45 m downstream the fire), the following mesh and the end mesh (200 m and 600 m downstream the fire) are measured.

The results for HRR, shown in Figure 14, indicate that there are no differences between the two cell sizes in the fire mesh. The sudden drop after 580 seconds of the 0.2 m cell size simulation is due to a restart of the simulation and is typical for simulation restarts in FDS, i.e. the drop is not connected to the cell size and should be disrespected.

The temperature and CO-concentrations in the neighbouring mesh downstream the fire mesh are close to identical for the different models, as shown in Figure 14 and Figure 16. A discrepancy for the temperature and CO concentration are identified in the fire mesh. The magnitude of the difference is 6 % on total average and about 13-14 % at maximum (420 sec). This is assessed to be acceptable, considering that interpolation are used to obtain the values to account for differences between central parts and towards the walls of the tunnel and that methodological errors because of this may partially contribute to the discrepancy. Furthermore, it is observed that this difference is not continued to the next mesh, where values are identical and which are the areas of particular interest for this report. This indicate that no vital information for the parameters investigated here are lost between the meshes and that the fire mesh cell size does not significantly influence the results. It is, based on this, concluded that the model set-up with respect to cell size and mesh are acceptable.

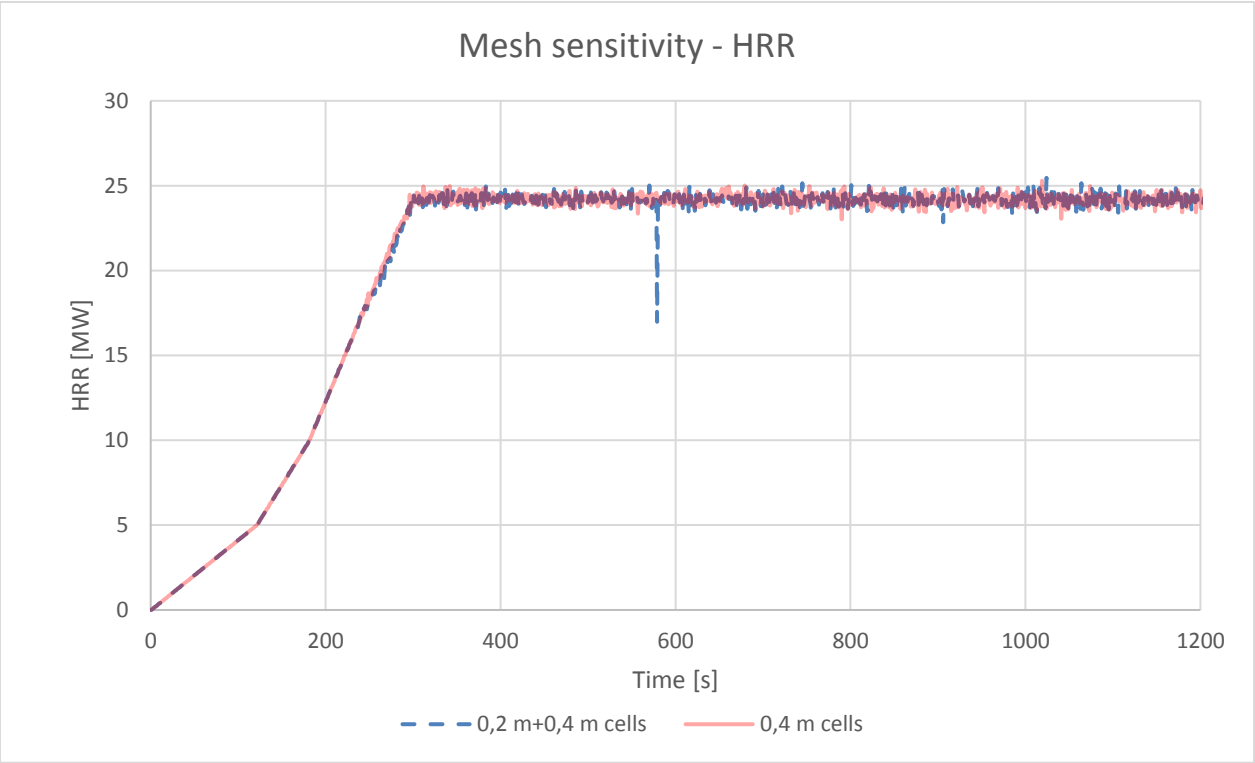

Figure 14. Cell size sensitivity analysis with respect to heat release rate (HRR).

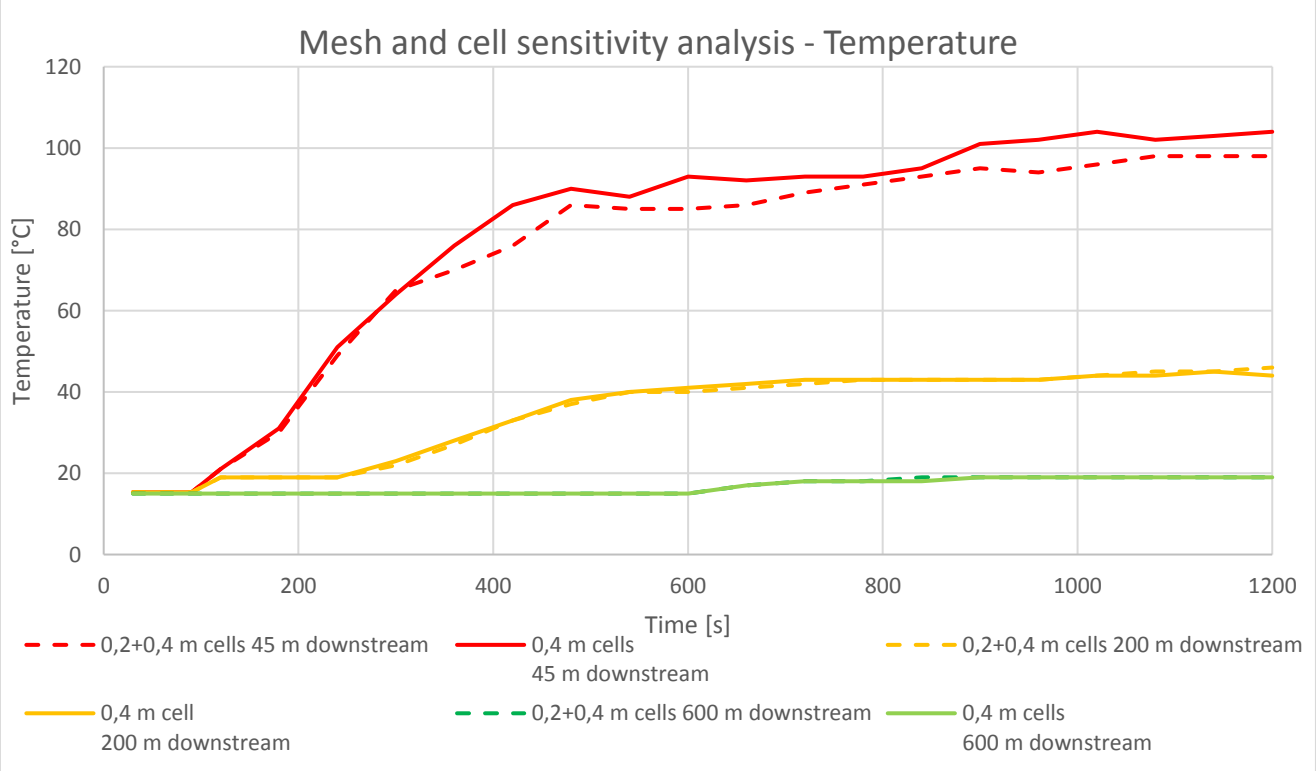

Figure 15. Mesh and cell size sensitivity analysis with respect to temperature.

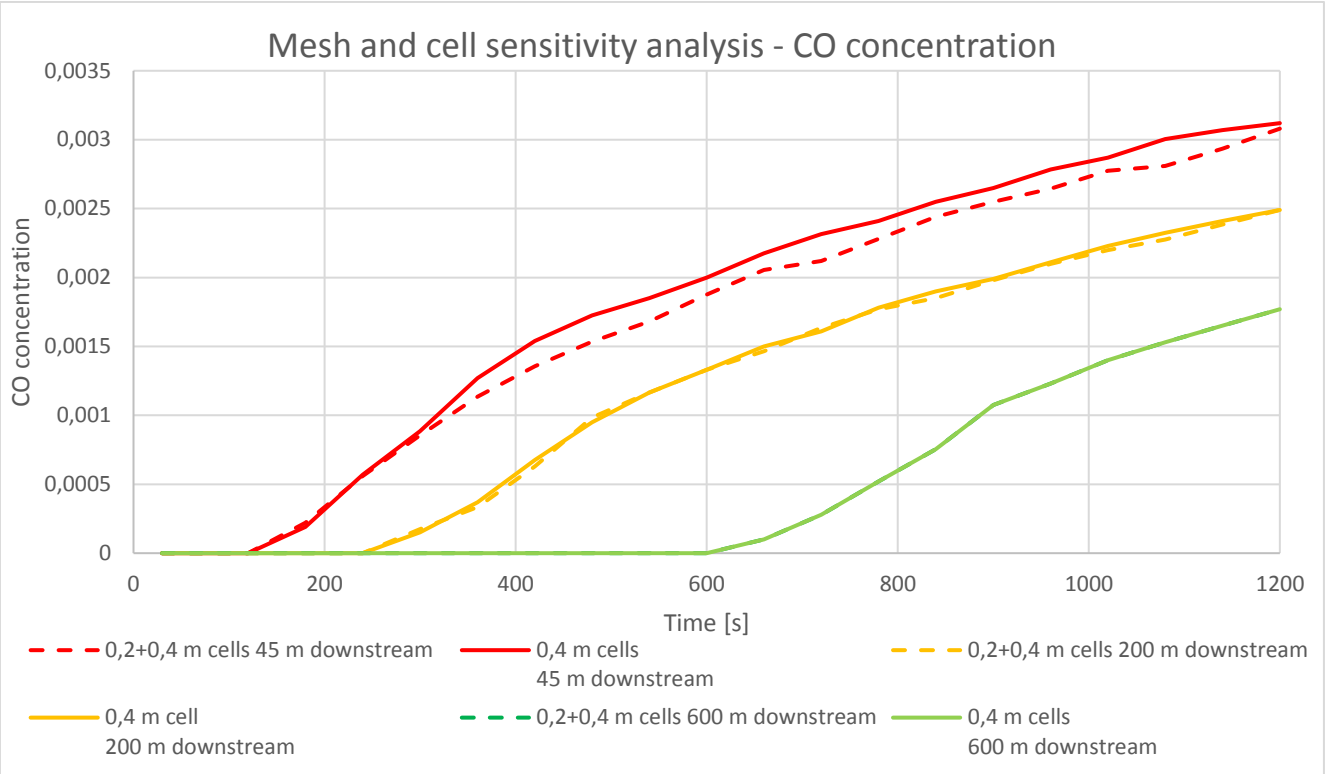

Figure 16. Mesh and cell size sensitivity analysis with respect to CO concentration.

5.7 Simulation scenarios

The fire scenarios to be investigated is divided in two parts; main FDS scenarios including the target ventilation velocities and additional scenarios to investigate different correlations. The scenarios are summarized in Table 4. The FGR for each scenario is described in section 5.4.

Table 4. Summary of FDS simulation scenarios.

Scenario	Explanation
1.5 m/s	1.5 m/s target ventilation and maximum HRR of 100 MW
3 m/s	3 m/s target ventilation and maximum HRR of 100 MW
5 m/s	5 m/s target ventilation and maximum HRR of 100 MW
Additional scenarios:	
0 m/s	0 m/s target ventilation to assess situation without ventilation
3 m/s w/windbreak	3 m/s target ventilation with windbreak applied to the upstream part of the fire
5 m/s w/reduced FGR	5 m/s target ventilation, but reduced FGR (same as 1.5 m/s) to assess difference in downstream conditions when FGR is not changed.
1.5 m/s max 25 MW	Used to assess the impact of reduced HRR
5 m/s max 25 MW and reduced FGR	Used to assess the impact of reduced HRR

6 STEPS input

Evacuation simulations are made in STEPS ver. 5.4 to give a better perception of how the tunnel environment in each scenario affects evacuees in a possible evacuation situation. STEPS is a 3-D simulation program for analysis of people movement and are used both to study evacuation and normal people flows. The program is developed and validated by Mott MacDonald [22].

The fire simulation results are linked to the evacuation simulations by importing slice files for the light extinction coefficient (visibility), CO and CO_2. This makes it possible to evaluate FED values for each individual when also considering the effect that visibility has on walking speeds. The geometry of the tunnel is imported from the FDS file as well.

The results of the STEPS simulations (FED calculations and egress times) performed here will serve as a visualization of the difference between ventilation velocities since no detailed evacuation analysis is performed accounting for family relations, different fire alarm and warning systems etc.

For this analysis, only one directional evacuation is considered, i.e. persons downstream are considered not to bypass the fire and will evacuate to the tunnel portal downstream by foot. The same applies for persons upstream the fire, whom will use the tunnel portal upstream. This is considered realistic considering the FGR used in the simulations will prevent anyone passing the fire. The FGR also affects the reaction time set for the evacuation simulation and the fact that people are forced to leave their vehicles and evacuate on foot.

No differentiation has been done for the evacuees on an individual level, so they are uniform with respect to walking speed and other attributes. No relationship is considered between the persons. Since only one evacuation route is available, depending on which side of the fire they are placed, the patience-level is not relevant for these scenarios.

6.1 Model

A total of 200 persons are included in the model; 180 downstream (4 buses á 30 people and 30 cars á 2 people) and 20 upstream (10 cars á 2 people). The distance between each vehicle is 1 m and the closest car upstream the fire is located 41 m from the fire. The closest vehicle on the downstream side, which is a bus, is located 5 m from the fire. Each car is assumed to be 4 m long and 2 m wide whilst the bus is 20 m long and 3 m wide.

This set-up results in a maximum walking distance of 770 m and applies to the bus closest to the fire on the downstream side of the fire, as can be seen from Figure 5.

6.2 Walking speed

A 1.2 m/s uniform walking speed is assumed for the evacuees when not affected by smoke (visibility). This is within the region what normally is used for evacuation simulations on a flat surface (Gwynne & Boyce, chapter 64 in [23]). The walking speed is affected by visibility through results for the light extinction coefficient (K) from FDS according to the following points (based on [32] findings from Frantzich and Nilsson (2003) for light emitting signage presented in table 14.2 and referred to in [25]);

K=0.8 (10 m visibility): 1.2 m/s

K=1.6 (6 m visibility): 1.0 m/s

K=2.67 (3 m visibility): 0.5 m/s

K=8 (1 m visibility): 0.3 m/s

As one can see, the visibility does not affect the walking speed before it goes below 10 m. A linear relationship is applied between the given points of extinction coefficient (visibility).

Walking speeds (visibility) below 0.3 m/s are not considered so 0.3 m/s is the minimum walking speed that can be obtained in the simulations. This is to avoid never-ending simulations with evacuees standing still. It is assessed that the FED calculations will account for the evacuees exposed to such low visibilities since they will then obtain high FED-values and can be considered as fatalities. Test simulations also show that the CO concentration in areas with visibility of below 1 m is close to 2000 ppm, which is the instant tenability criteria of [33].

6.3 Pre-movement time

The pre-movement time in the evacuation simulations are somewhat simplified, since an analysis of alarm/warning systems and psychological aspects are not performed. The chosen pre-movement time is mainly based on an assessment of the visual perspective of the fire and smoke situation that persons in the vehicles have. The reaction time is assumed to be heavily affected by the relatively fast fire development for all the scenarios and are therefore quite small compared to what is used for buildings where most people will not see smoke or flames because of compartmentation, but also for what has been seen in actual tunnel fire incidents.

Below a scene from a HGV fire in Oslofjordtunnelen is described with focus on behaviour during fire.

Figure 17. From a HGV fire in Oslofjordtunnelen 2017. First visible flame/smoke happens at 17:50:30, and the trailer is still driving. From Statens vegvesens uploaded video on youtube [34].

After about 2 minutes the HGV stops and the chauffeur exits the truck and tries to extinguish the fire with a hand held extinguisher. No other cars are seen passing the location of the fire after this time, but a second person in a car also stops in front of the truck. Even though heavy smoke are produced and flames are growing rapidly, the chauffeur and the second person is not seen to start evacuation before the film ends, 6:20 after the first flames are seen from the truck.

Figure 18. From a HGV fire in Oslofjordtunnelen 2017. 6 minutes after the first flames are seen from under the truck a second person are approaching the chauffeur. From Statens vegvesens uploaded video on youtube [34].

The FGR of this fire in Oslofjordtunnelen resembles the exponential curve many design fires follow for buildings based on the observations of the footage, with a slow initial phase. The design fire used for the simulations here are more linear. After 6 minutes the theoretical HRR is above 20 MW for all simulation scenarios, which can be compared to a fully developed bus fire as described in section 2.1. The first persons to start evacuation, located close to the fire, will therefore have a relatively short pre-movement time.

No relation between the evacuees, such as family groups etc. are included, but an offset reaction time is considered to be influenced by both seeing other evacuees closer to the fire start evacuation (and passing by) and the fact that smoke and severity of the situation will gradually increase by time for those further away from the fire.

Based on this, the following distribution of pre-movement times, with an offset for evacuees further away from the fire, are applied in the simulations;

- Upstream cars; 1:30 min
- First bus downstream fire; 1:00 min
- First 10 cars and second bus downstream fire; 1:10 min
- Second bus and next 10 cars downstream fire; 1:20 min
- Third bus and next 10 cars downstream fire; 1:30 min
- Fourth bus and next 10 cars downstream fire; 1:40 min

For the sensitivity analysis a 30 second reduction to this pre-movement time and maximum 1.0 m/s walking speed is applied. An additional 2 minute pre-movement time compared to the original is also investigated for the 1.5 m/s and 5 m/s w/reduced FGR scenarios (minimum of 3 min pre-movement time).

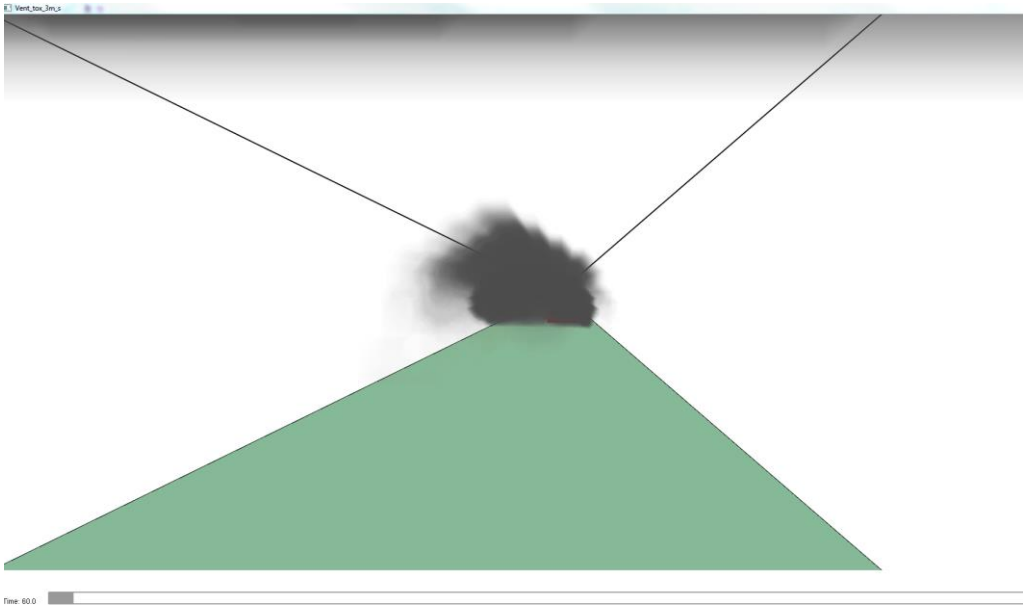

Figure 19. Fire situation seen from 100 m downstream the tunnel in the 3 m/s ventilation scenario after 60 seconds.

6.4 STEPS simulation scenarios

All the FDS simulation scenarios are run with two different pre-movement times; a minimum of 1 minute (and maximum walking speed of 1.2 m/s) and a minimum of 30 seconds pre-movement time (maximum walking speed of 1.0 m/s). The offset pre-movement times follows the description given in section 6.3. In addition, simulations for the 1.5 m/s and 5 m/s ventilation w/reduced FGR are run with a minimum of 3 minute pre-movement time (maximum walking speed of 1.2 m/s).

Reference simulations for the 1 minute and 30 sec pre-movement times are run without smoke impacting the walking speed.

Table 5. Summary of STEPS simulation scenarios

Scenario	Explanation
Ref.sim 1 min	Reference simulation with no smoke - minimum 1 min pre-movement time and max walking speed of 1.2 m/s
Ref.sim 30 sec	Reference simulation with no smoke - minimum 30 sec pre-movement time and max walking speed of 1 m/s
1.5 m/s ventilation 1 min	1.5 m/s ventilation – minimum 1 min pre-movement time and max walking speed of 1.2 m/s
1.5 m/s ventilation 30 sec	1.5 m/s ventilation – minimum 30 sec pre-movement time and max walking speed of 1 m/s
1.5 m/s ventilation 3 min	1.5 m/s ventilation – minimum 3 min pre-movement time and max walking speed of 1.2 m/s

Scenario	Explanation
3 m/s ventilation 1 min	3 m/s ventilation – minimum 1 min pre-movement time and max walking speed of 1.2 m/s
3 m/s ventilation 30 sec	3 m/s ventilation – minimum 30 sec pre-movement time and max walking speed of 1 m/s
5 m/s ventilation 1 min	5 m/s ventilation – minimum 1 min pre-movement time and max walking speed of 1.2 m/s
5 m/s ventilation 30 sec	5 m/s ventilation – minimum 30 sec pre-movement time and max walking speed of 1 m/s
0 m/s ventilation 1 min	0 m/s ventilation – minimum 1 min pre-movement time and max walking speed of 1.2 m/s
0 m/s ventilation 30 sec	0 m/s ventilation – minimum 30 sec pre-movement time and max walking speed of 1 m/s
3 m/s w/windbreak 1 min	3 m/s ventilation w/windbreak – minimum 1 min pre-movement time and max walking speed of 1.2 m/s
3 m/s w/windbreak 30 sec	3 m/s ventilation w/windbreak – minimum 30 sec pre-movement time and max walking speed of 1 m/s
5 m/s w/reduced FGR 1 min	5 m/s ventilation w/reduced FGR – minimum 1 min pre-movement time and max walking speed of 1.2 m/s
5 m/s w/reduced FGR 30 sec	5 m/s ventilation w/reduced FGR – minimum 30 sec pre-movement time and max walking speed of 1 m/s
5 m/s w/reduced FGR 3 min	5 m/s ventilation w/reduced FGR - minimum 3 min pre-movement time and max walking speed of 1.2 m/s
1.5 m/s 25 MW 1 min	1.5 m/s ventilation max 25 MW – minimum 1 min pre-movement time and max walking speed of 1.2 m/s
1.5 m/s 25 MW 30 sec	1.5 m/s ventilation max 25 MW – minimum 30 sec pre-movement time and max walking speed of 1 m/s
5 m/s 25 MW 1 min	5 m/s ventilation max 25 MW and reduced FGR – minimum 1 min pre-movement time and max walking speed of 1.2 m/s
5 m/s 25 MW 30 sec	5 m/s ventilation max 25 MW and reduced FGR – minimum 30 sec pre-movement time and max walking speed of 1 m/s

7 Measurements

To investigate how the different ventilation velocities affects the toxicity in the tunnel, CO is used as an indicator. CO is, together with HCN, believed to be the main reason for fire related deaths (McGrattan & Miles, chapter 32 in [23]). The tenability limits and effects of HCN is however less explored compared to CO [35]. This is why FED CO, also accounting for CO_2 which enhance the intake of other toxic gases due to its effect on respiration, will be assed for the STEPS analysis.

FED CO will be calculated based on the following equation given in ISO 13571: 2012 [35]:

$$FED_{CO} = \frac{\overline{C_{CO}}}{35000} \times \Delta t \times 10^{\frac{\overline{C_{CO_2}}}{5}}$$

The HCN part of the equation is not included, as described above. This will result in underestimated FED values, since the HCN part, if included, is added to the FED CO values in the original equation. Furthermore ISO 13571 gives an uncertainty of +/- 35 % for the FED calculation with respect to human tenability. This serves well as a reminder that the results of these simulations and FED calculations are meant for comparison of different ventilation scenarios. However, to put the calculated FED values in perspective, it is noted that for FED values of 0.3, about 11 % of the population are expected to be incapacitated, whilst 50 % are incapacitated when the FED value reaches 1.0 [35].

Since STEPS log the accumulated dose of CO and CO_2 for each evacuee, the average concentrations, referred to above as $\overline{C_{CO}}$ and $\overline{C_{CO2}}$, are calculated based on the accumulated value and divided on time of exposure (time from start to end of CO exposure).

Temperature, heat flux and oxygen are also important tenability criteria's, and will be shortly addressed based on instant values. Tenability criteria's for these "instant" values, together with corresponding limits for CO and CO_2 are given in INSTA TS 950 [33], presented in Table 6.

Table 6. Proposed tenability criteria's in INSTA TS 950 for building fire safety [33].

Parameter	Value (tenability limit)	Comment
Visibility	10 m in areas > 100 m² 3 m in area < 100 m² Smoke free height of 1.6 m + 0.1 m x H	Visibility is not a threat in itself, but low visibility indicates thick smoke and high toxicity. Here, reduced visibility is used to limit walking speed, so that time spent in the toxic environment will increase with decreasing visibility.
Thermal	Continuous radiation intensity of maximum 2,5 kW/m². Short duration of maximum 10 kW/m² in combination with maximum dose of 60 kJ/m².	Radiation is not included here since only evacuees in a distance from the fire are assessed. As long as the temperature criteria is met, radiation from the smoke layer is assumed not to represent a problem.
Temperature	Maximum 80°C	
Toxicity:		
Carbon monoxide	< 2000 PPM	
Carbon Dioxide	< 5 %	
Oxygen	>15 %	

8 Results

The main FDS scenarios was run for at least 2100 seconds (35 minutes). The results are presented in graphs and tables in this chapter. The results are discussed further in chapter 9, therefore only a brief explanation for each figure/table is given.

8.1 Heat release rate

As can be seen from the resulting HRR in Figure 20, only the 5 m/s ventilation velocity scenario is able to maintain the theoretical HRR set for the simulations, shown in Figure 9. However, all the main scenarios obtain the theoretical maximum HRR at the set time.

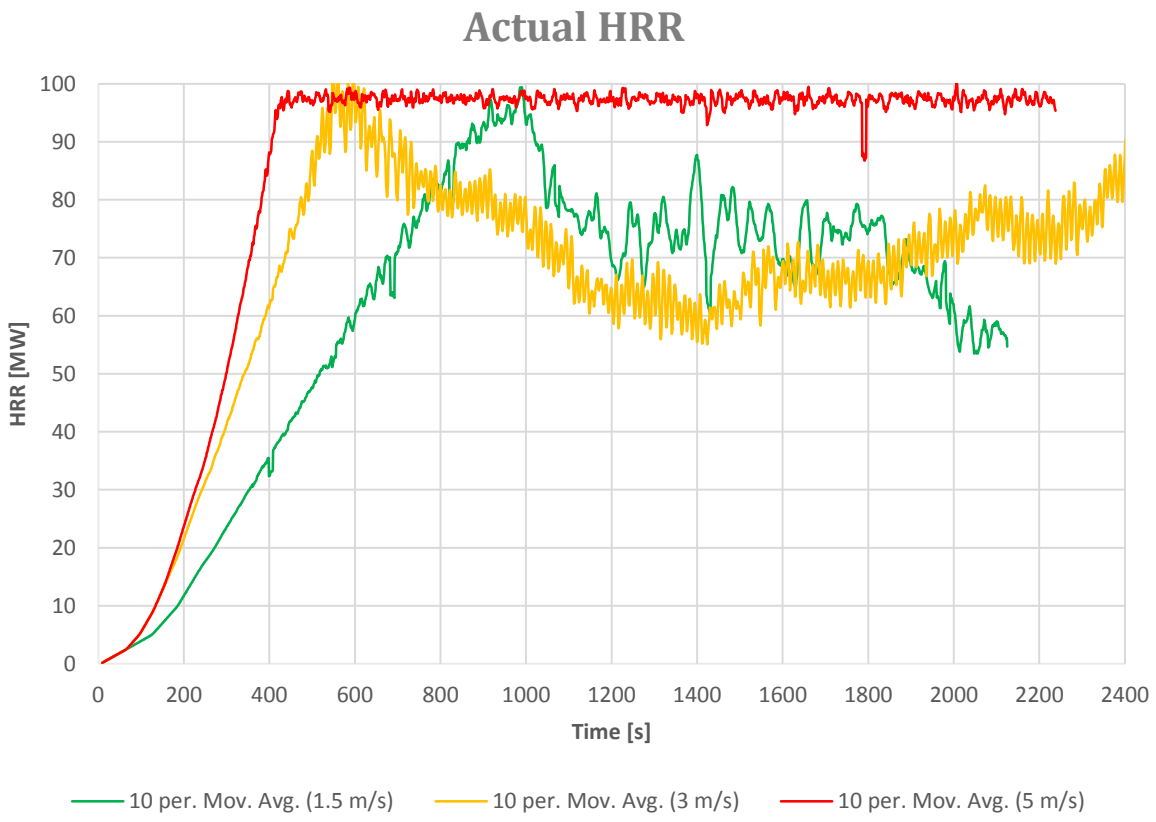

Figure 20. HRR obtained for the different ventilation scenarios in FDS. Due to massive fluctuations a 10 sec. average are used to present the HRR curves.

Additional FDS scenarios are shown in Figure 21.

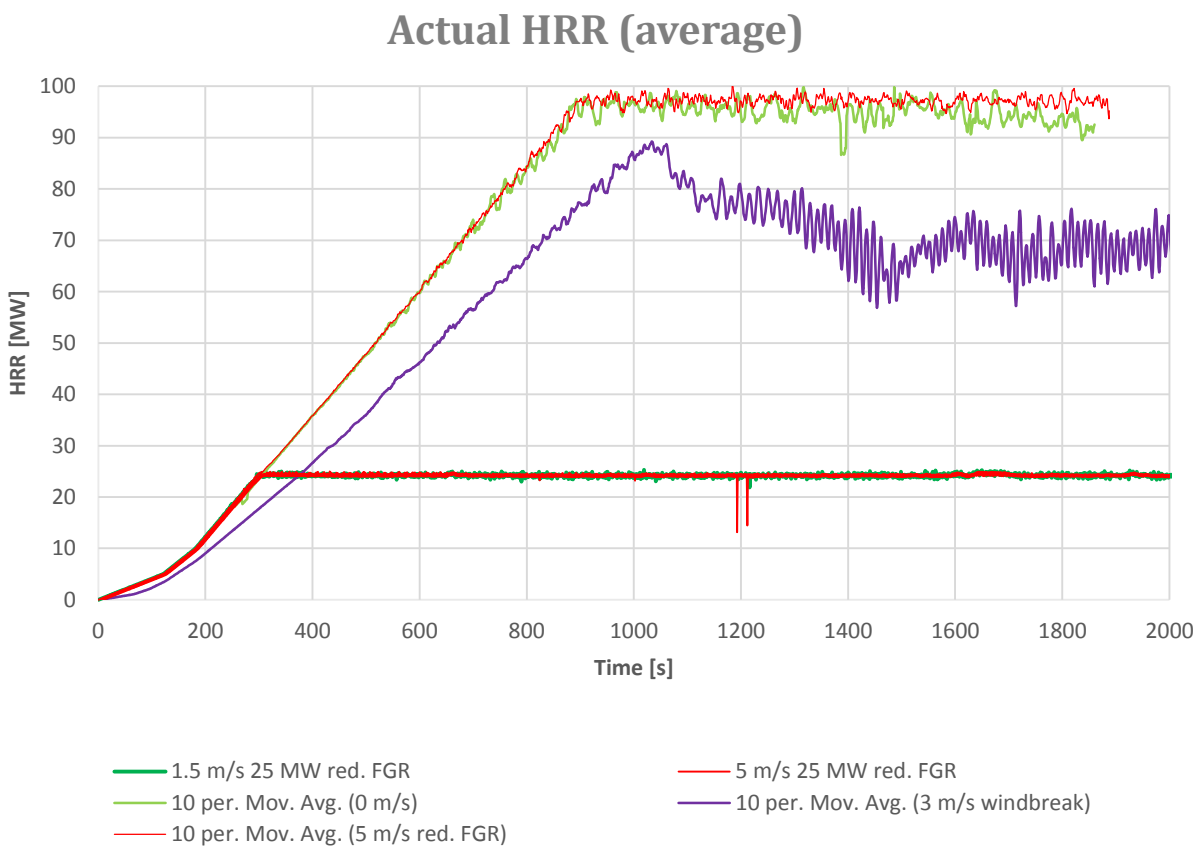

Figure 21. Actual HRR for additional scenarios.

Some of the additional scenarios are run with the same FGR as the 1.5 m/s scenario (0 m/s and 5 m/s w/reduced FGR). These are shown together in Figure 22, for comparison. It is noted that the 0 m/s scenario is the only one other than the 5 m/s ventilation scenarios, able to maintain the predefined HRR.

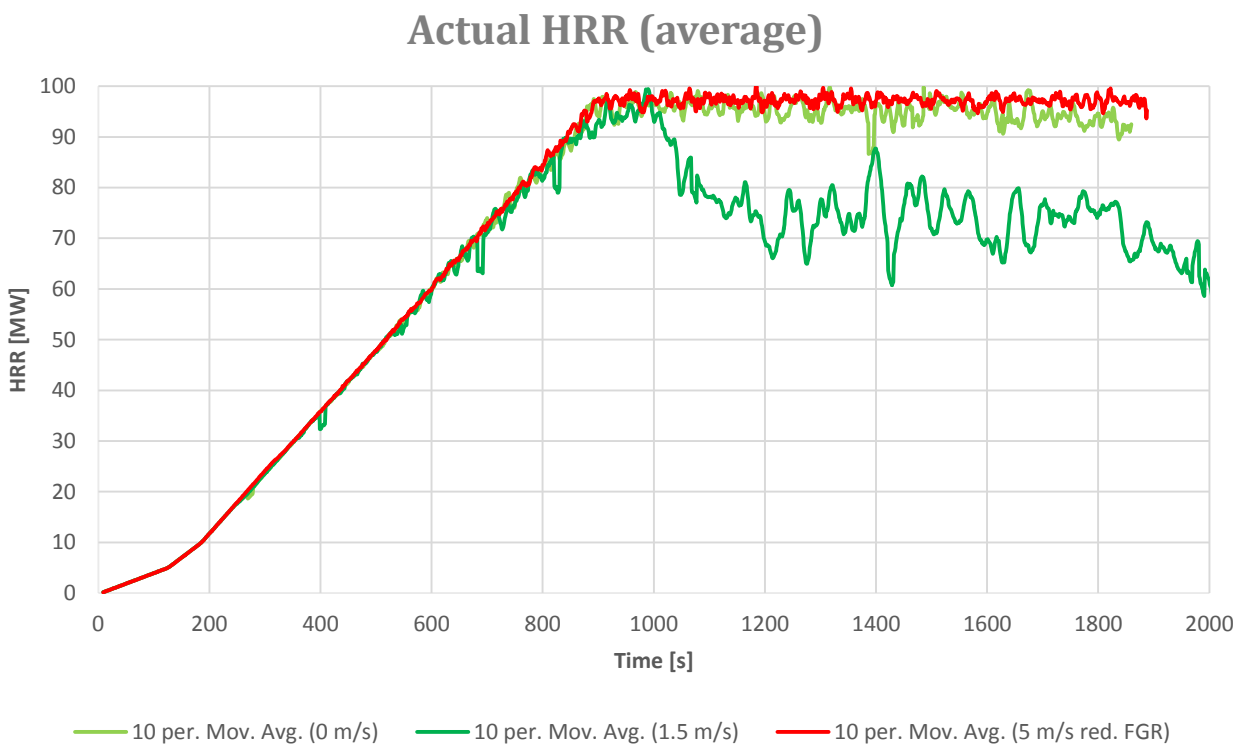

Figure 22. Actual HRR for scenarios with the same predefined FGR.

8.2 Airflows and backlayering

8.2.1 1.5 m/s ventilation scenario

Shortly after simulation start, the airflow from the closest upstream jet fan to the fire (55 m) is pushed towards the floor due to the fire induced flow of hot gases. In the 1.5 m/s scenario, this jet fan is "overrun" by the fire gases after about 2.5 minutes and opposite flow (to the left) continues all the way to the tunnel opening after 6 minutes (200 m upstream the fire). The airflow movement is illustrated in Figure 23.

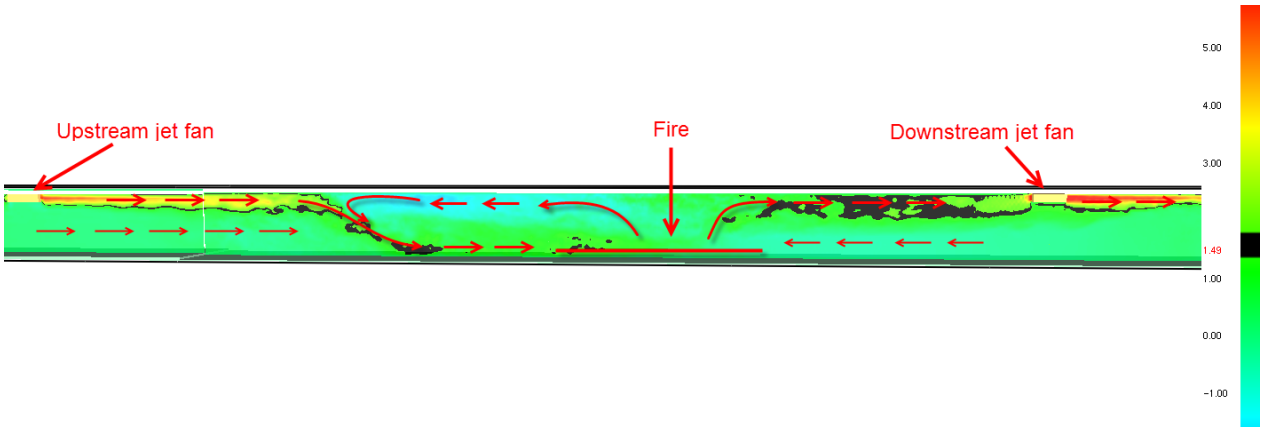

Figure 23. Velocity slice (m/s) in the middle of the tunnel (longitudinal cross-section) after 60 seconds in the 1.5 m/s ventilation scenario.

For the rest of the simulation time, a steady ingoing and outgoing flow is observed around the fire; ingoing air along the floor and outgoing at the top.

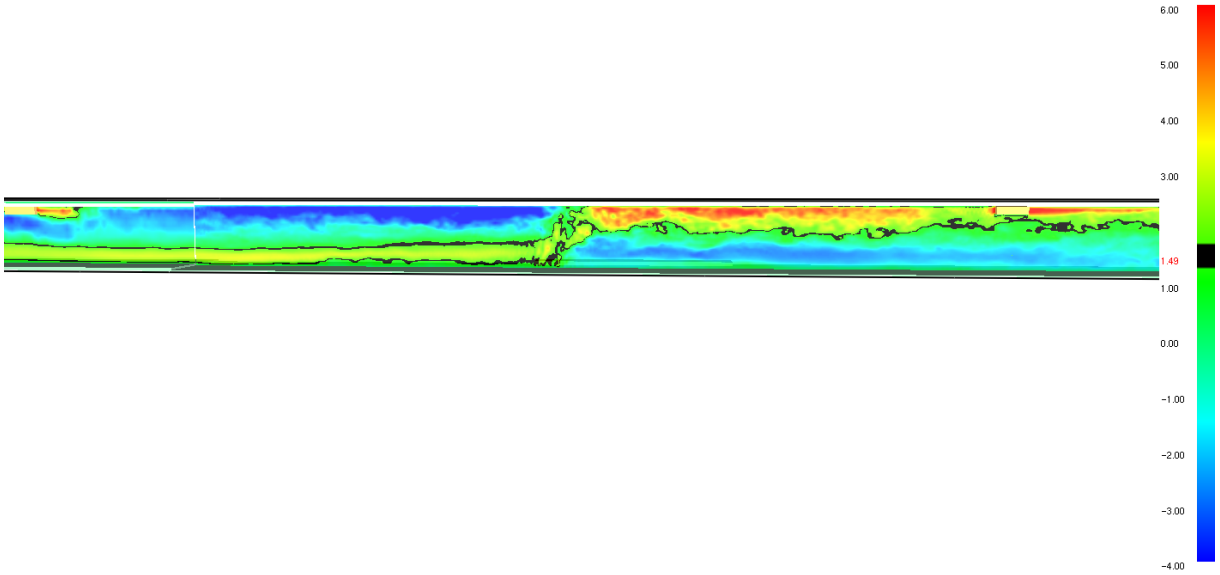

Figure 24. 1.5 m/s scenario airflow (m/s) after 25 minutes (longitudinal cross-section). Blue colours indicate air moving opposite of the ventilation direction, yellow and red indicate flow along with the ventilation direction.

The airflow from the jet fans located upstream of the fire is pushed towards the floor along with the ramp-up of HRR. Figure 25 to Figure 28 illustrates how the backlayering propagates upstream the fire located in the centre of the figures. In contrast to Figure 23 and Figure 24, the colour map is here changed to better illustrate the opposite airflows. Red areas represent a positive airflow (same as ventilation direction to the right), whilst the blue areas represent airflow induced by the fire towards the ventilation direction in the upstream part of the tunnel. On the downstream part (to the right of the fire) fresh air are being sucked into the fire along the floor.

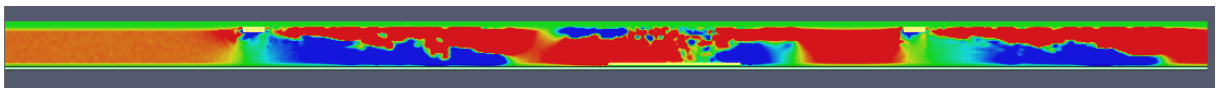

Figure 25. Airflow (m/s) after 30 sec for the 1.5 m/s scenario (longitudinal cross-section). Fire located in the middle of the figure.

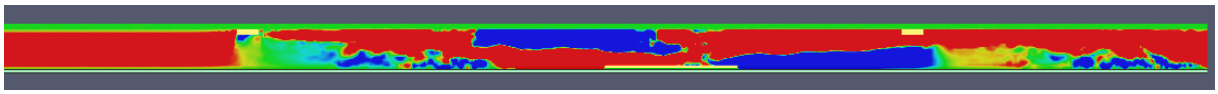

Figure 26. Airflow (m/s) after 60 sec for the 1.5 m/s scenario (longitudinal cross-section). Notice how the blue area in the ceiling above the fire grows (airflow opposite of the ventilation direction) and push the fresh airflow to the ground. On the right side of the fire, fresh air is sucked into the fire along the floor.

Figure 27. Airflow (m/s) after 90 sec for the 1.5 m/s scenario (longitudinal cross-section).

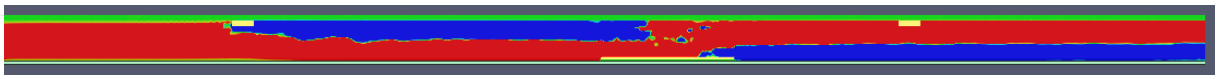

Figure 28. Airflow (m/s) after 150 sec for the 1.5 m/s scenario (longitudinal cross-section). The backlayering has reached the first jet fan 55 m upstream of the fire.

8.2.2 3 m/s ventilation scenario

The first jet fan is overrun by the hot gases from the fire after 3.5 minutes for the 3 m/s scenario. The backlayering reaches 50 m from the upstream tunnel portal at a maximum, corresponding to a backlayering of 155 m, after 8.5 minutes. Before the hot airflow reaches this area, a pulsating phenomenon occurs affecting the airflow in the whole tunnel. This is most dominant on the upstream side of the fire. The phenomena starts after about 7 minutes and continues throughout the simulation time. The "wavelength" of this pulse seems to keep steady at about 12-13 seconds, i.e. the fire inhales/exhales every 12-13 second for the rest of the simulation. Figure 29 illustrates the pulsation observed.

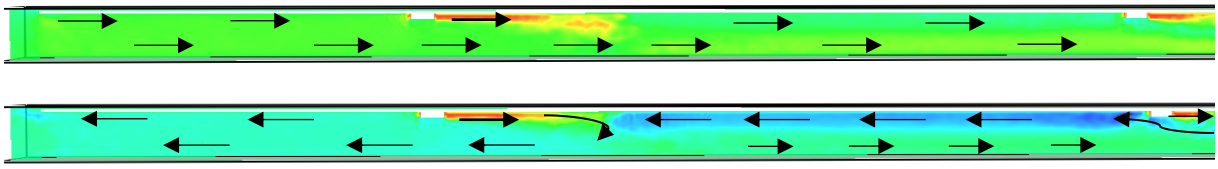

Figure 29. Longitudinal cross-section showing airflow (m/s) for the 150 first meters of the tunnel upstream the fire in 3 m/s scenario after 503 seconds (top figure) and 509 seconds (bottom figure). Green colour indicates airflow to the right and blue indicates airflow opposite of the ventilation direction.

The longitudinal airflow in the centre of the tunnel varies between 5 m/s to minus 5 m/s (opposite of the ventilation direction) as a result of the pulsation throughout the simulation on the upstream part. On the downstream part, the speed varies between 3 m/s and minus 2.5 m/s. Generally, there is a clear distinction between ingoing air in the bottom and outgoing smoke in the top downstream of the fire, even though smoke covers the whole tunnel.

8.2.3 5 m/s ventilation scenario

For the 5 m/s scenario the same pulsation is observed. It starts about 6 minutes into the simulation, 1 minute before the hot airflow from the fire reaches the first upstream jet fan at 7 minutes. This is also the maximum backlayering for this scenario, corresponding to a length of 55 m. The "wavelength", or frequency, of the pulsation is shorter in this simulation compared to the 3 m/s scenario, only 7 seconds. The smoke-front upstream the fire, where the pulsation is most prominent, also extends and retracts a shorter distance compared to the 3 m/s scenario. Generally the pulsation is less distinct in this scenario, especially downstream the fire. The airflow varies greatly between the upper and lower part of the tunnel, from 5 m/s in the upper part (ceiling) to minus 1 m/s on the lower part (floor).

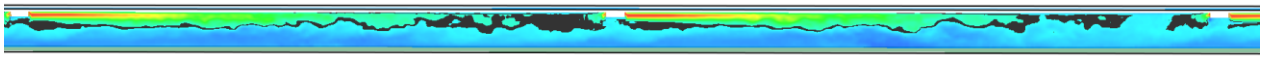

Figure 30. Longitudinal airflow (m/s) 425 to 625 m downstream the fire 29.5 minutes into the 5 m/s ventilation scenario illustrating the opposite upper and lower airflows in the tunnel. Black areas indicate airflow of 2 m/s, green and red areas have higher airflow to the right and blue indicate air moving to the left (towards the fire).

8.2.4 Additional scenarios

The 5 m/s scenario with reduced FGR follows the same flow pattern as the 5 m/s scenario, but reaches the first upstream jet fan after about 10 minutes, i.e. 4 minutes later than the original scenario. This is believed to be because of the delayed ramp-up of HRR (FGR). The pulsation behaviour upstream the fire starts first after about 16 minutes.

For the 0 m/s scenario, a well-defined upper (outgoing hot gases) and lower (ingoing air) airflow layers are established early and kept throughout the simulation. The maximum airflow velocities in the 0 m/s scenario are close to 5 m/s adjacent to the fire and decrease smoothly the further away from the fire one gets. No pulsation was observed for this scenario.

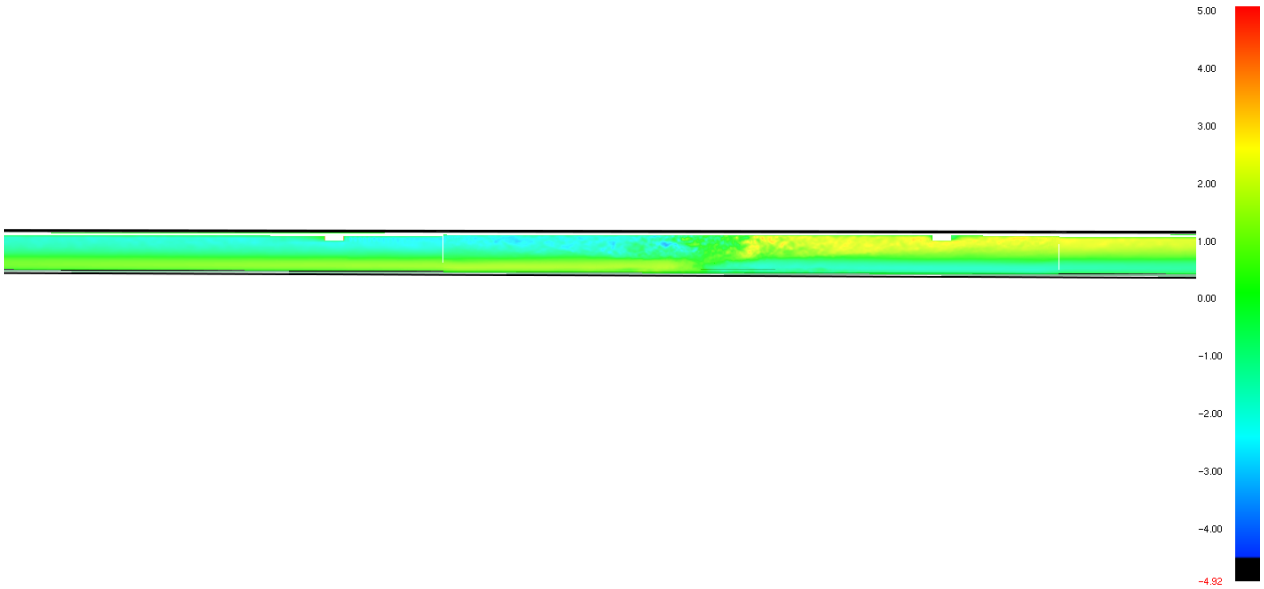

Figure 31. Airflows (m/s) in the 0 m/s scenario after 4 minutes (longitudinal cross-section).

For the 3 m/s scenario with windbreak, airflow behaves a little bit different than that from the 3 m/s. In contrast to the latter, the backlayering spreads all the way to the upstream tunnel portal for a short period, between 1080-1300 seconds, before it goes back again to the same length as for the 3 m/s scenario, 155 m upstream the fire. The pulsation effect, seen for the 3 m/s, 5 m/s and 5 m/s w/reduced FGR, starts at the same time as the smoke reach the upstream tunnel portal after 16 minutes, in contrast to the others where the pulsation started when smoke reached the downstream tunnel portal .

For the 25 MW scenarios with 1.5 m/s and 5 m/s with reduced FGR, the former scenario gets backlayering all the way to the upstream portal after 6.5 minutes. The 5 m/s ventilation scenario is able to hold the smoke downstream the fire, and by doing so achieving the critical velocity and a smoke-free path upstream of the fire.

8.3 Toxic gases

The concentration of CO is measured every minute based on slice files in 2 m height for different distances downstream the fire. Where significant differences between central and outer areas of the tunnel section exists (towards the tunnel wall), values are interpolated. This is more prominent for measurements done 200 m and closer to the fire compared to measurements 600 m downstream the fire. The instant tenability criteria of 2000 ppm described in chapter 7 corresponds to the first horizontal axis in the graphs of 0.002.

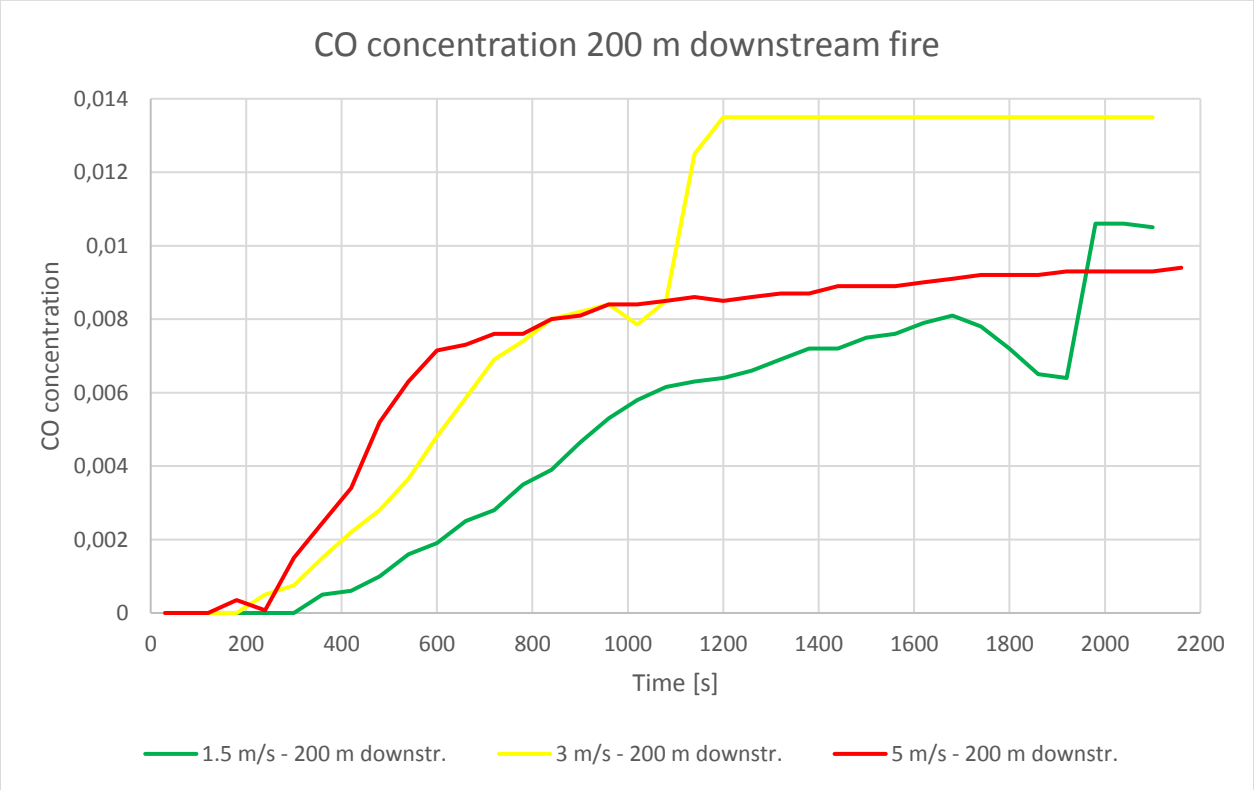

Figure 32. CO concentration measured 200 m downstream the fire for the main FDS scenarios.

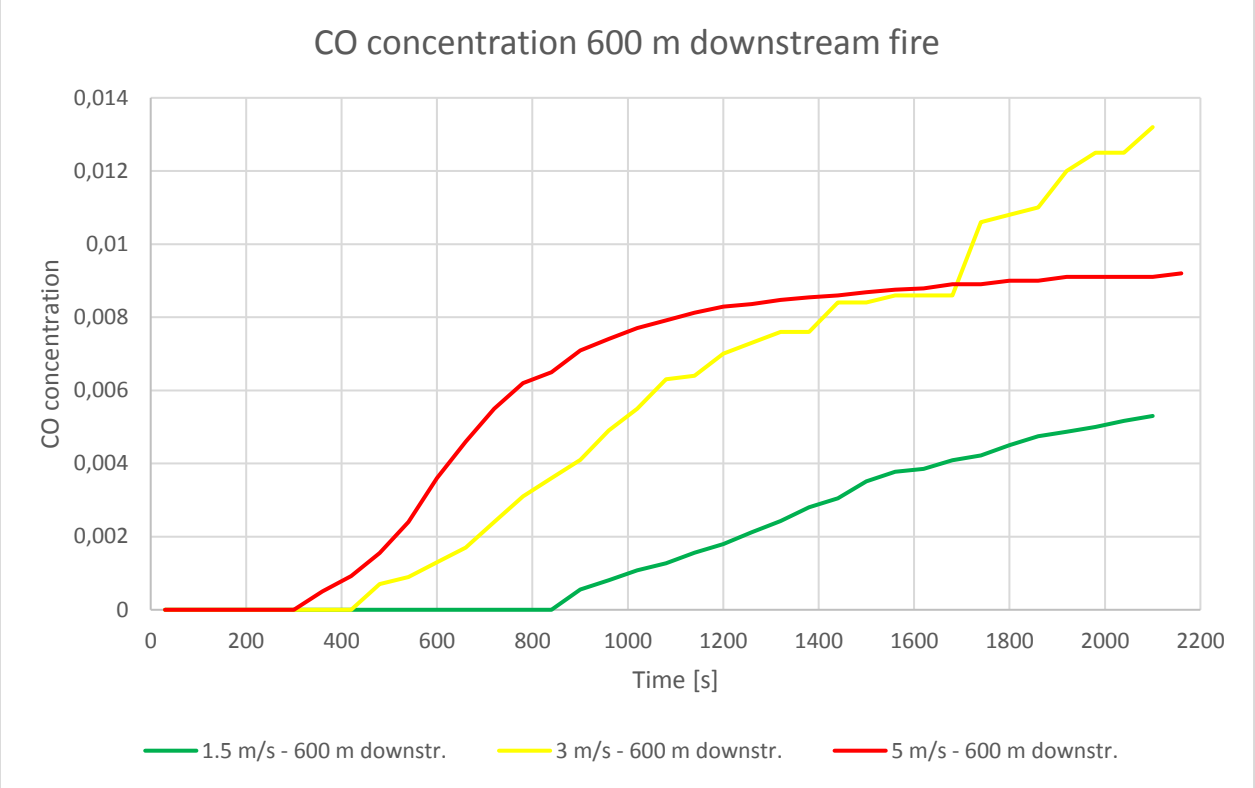

Figure 33. CO concentration measured 600 m downstream the fire for the main FDS scenarios.

The sudden rise in CO concentration 200 m downstream the fire for the 1.5 m/s scenario observed in the graph of Figure 32 is illustrated in Figure 34. Notice that there are two CO concentration "fronts", one yellow with CO concentration of about 0.0105 and a tail that includes the 200 m measuring point and one orange "plug" with CO concentration of about 0.0130. The latter never reaches the measuring point 200 m downstream the fire during the simulation time of 35 minutes.

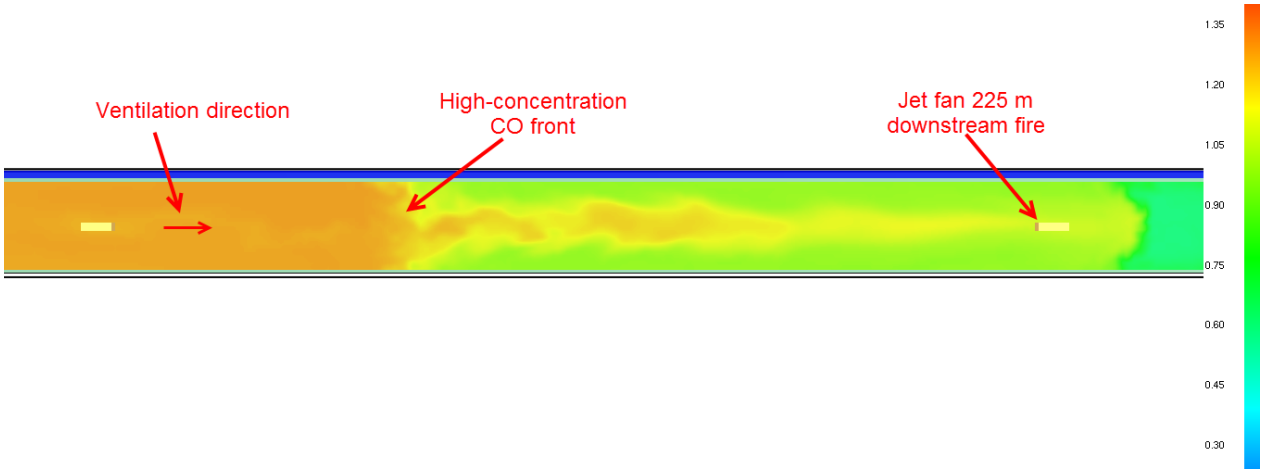

Figure 34. Plane view from smokeview-file for 1.5 m/s ventilation scenario after 2100 seconds showing CO-concentraion in 2 m height (legend given in 10^{-2}). Note how the "plug" of high concentration CO propagates downstream the fire.

In the 3 m/s scenario, after about 10 minutes, the same "plug" of high concentration of CO starts to wander downstream the tunnel. For this scenario, the "plug" travels faster and reaches the same downstream area as the 1.5 m/s scenario after about 17 minutes, i.e. 18 minutes earlier, as seen in Figure 35. After about 38 minutes, the CO concentration for the whole downstream part of the tunnel is above 0.0125 in the 3 m/s scenario. For the 1.5 m/s scenario this concentration is only observed 150 m downstream the fire after 35 minutes (end of simulation time).

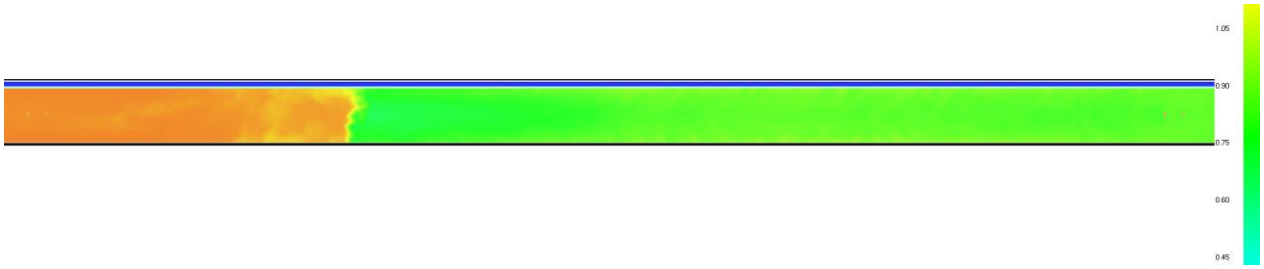

Figure 35. CO concentration (legend shows concentration in 10^{-2}) from the smokeview-file for 3 m/s ventilation after 1020 seconds 100-250 m downstream fire (plane view).

The "plug" of CO is identical with the propagation of O_2 concentration falling below about 5 %. Oxygen concentration does not fall below 8 % downstream the fire in the 5 m/s scenario and nor is such high CO concentrations observed (maximum of 0.0094).

The instant tenability criteria of 2000 ppm (0.002) are breached 200 m downstream the fire after 360 second for the 5 m/s scenario, 420 seconds for the 3 m/s scenario and 600 seconds for the 1.5 m/s scenario.

The additional scenarios follows the same trend as the main scenarios; the highest ventilation velocities gives the highest CO concentrations in the early phase (20 minutes) 200 m downstream. 5 m/s scenario with reduced FGR and 3 m/s with a windbreak have a "delayed" CO concentration curve of 400 seconds compared to the original scenarios with same ventilation velocities having a higher FGR. The delay of 400 seconds coincided with the delayed HRR peak for these scenarios.

The "plug" of high CO concentration is not observed during the simulation time of 30 minutes for the 0 m/s scenario. The maximum CO concentration is observed to be 0.0106 for the 0 m/s scenario 200 m downstream the fire, but exceeds the 5 m/s scenario with reduced FGR with respect to CO concentration after 25 minutes. Keeping in mind that the HRR curves of the 0 m/s and the 5 m/s scenario with reduced FGR are close to identical (see Figure 22), it is interesting to compare the CO concentrations for these two scenarios.

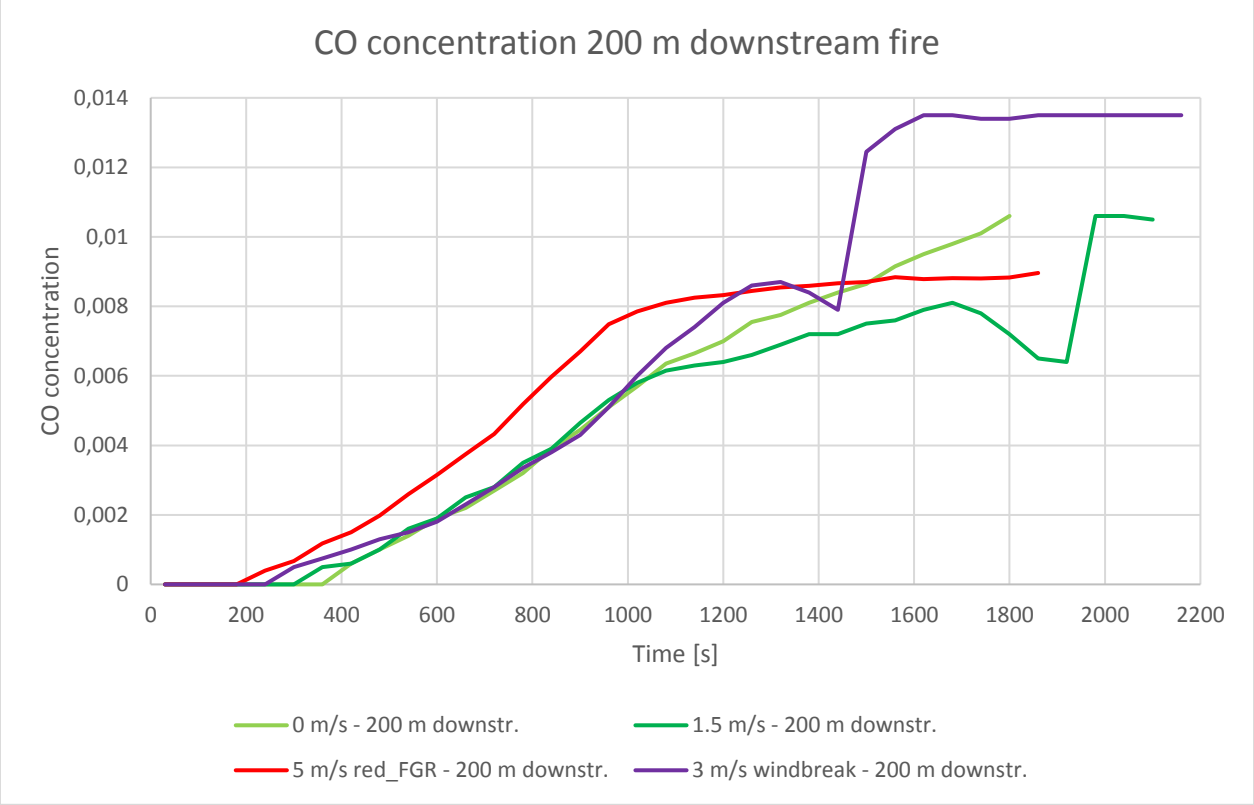

Figure 36. The CO concentration measured 200 m downstream of the fire for additional scenarios. 1.5 m/s scenario included for comparison with 0 m/s and 5 m/s w/reduced FGR scenarios, since these have the same predefined FGR.

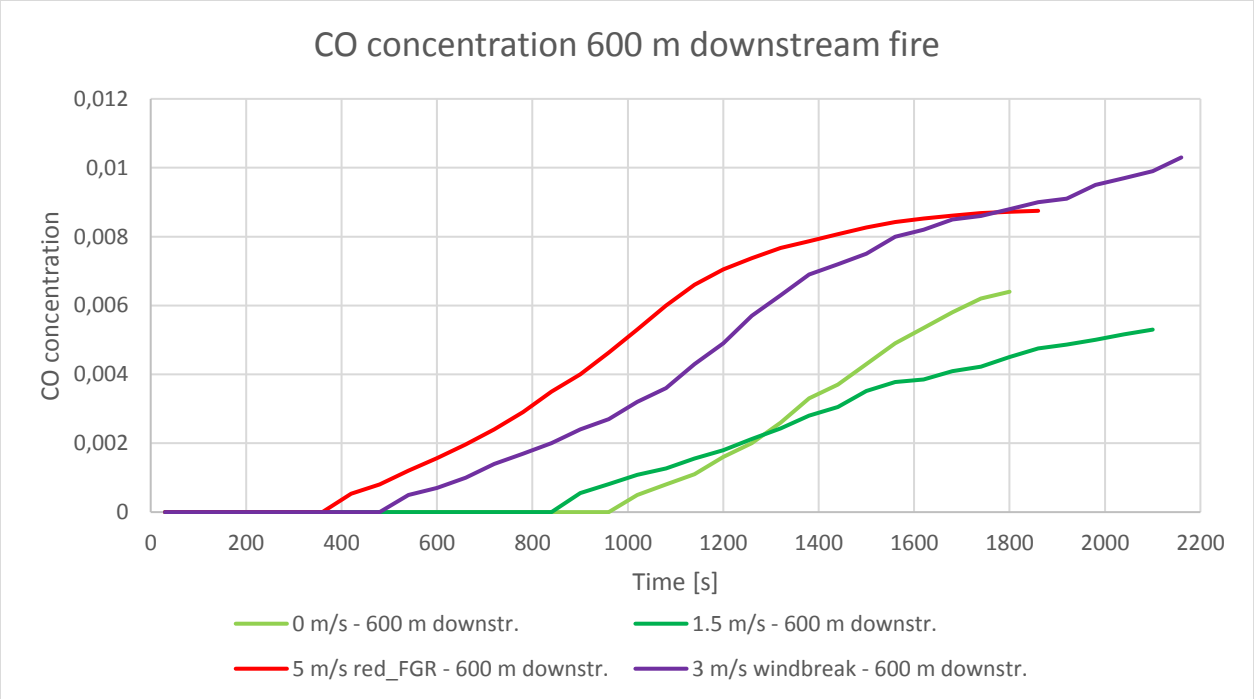

Figure 37. The CO concentration measured 600 m downstream of the fire for additional scenarios. 1.5 m/s scenario included for comparison with 0 m/s and 5 m/s w/reduced FGR scenarios, since these have the same predefined FGR.

The 25 MW scenarios resembles the corresponding 100 MW scenarios with respect to the CO development; lower ventilation velocities giving lower CO concentrations in the beginning. Note that the same FGR are applied to both 25 MW simulations.

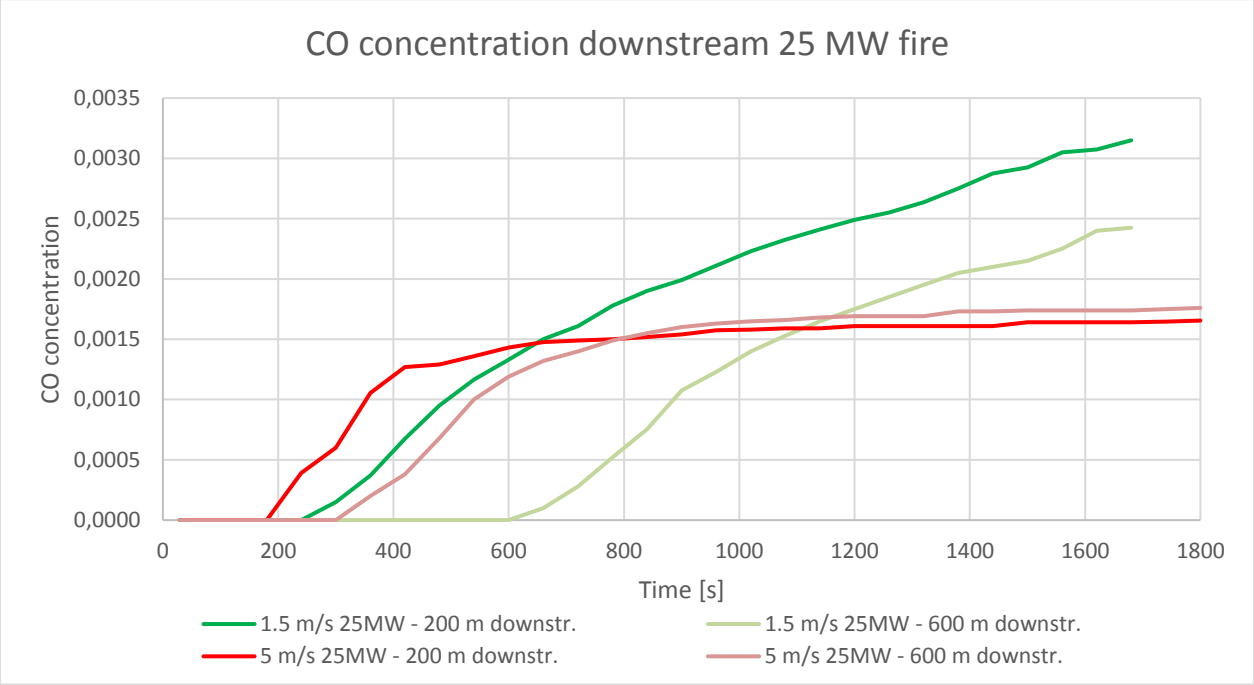

Figure 38. The CO concentrations 200 m and 600 m downstream the fire for the 25 MW scenarios.

8.4 Visibility

Visibility are measured every minute based on slice files at 200 m and 600 m downstream the fire. The results show a sudden drop in visibility which comes later for the lower ventilation velocities. Since the 0 m/s, 5 m/s w/reduced FGR and 25 MW scenarios does as well, neither visibility or the differences seen between ventilation velocities seem to be correlated to the HRR.

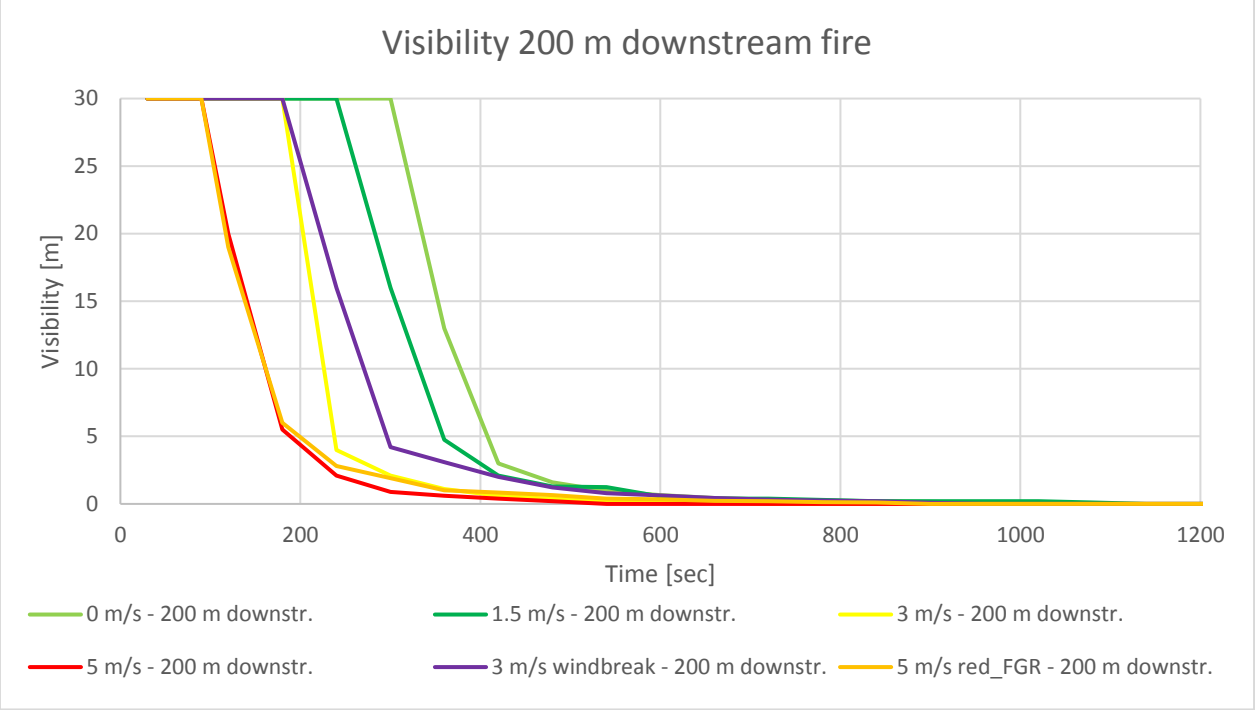

Figure 39. Graph showing visibility 200 m downstream of the fire in 2 m height for all 100 MW scenarios.

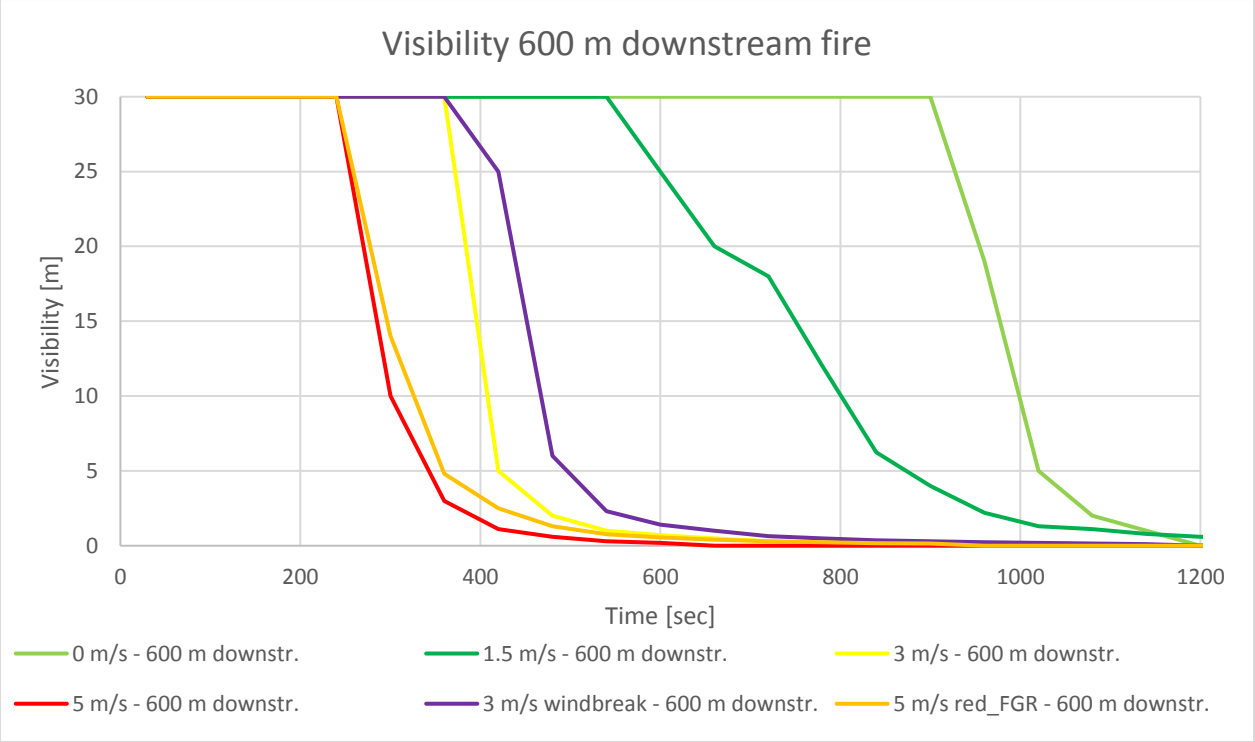

Figure 40. Graph showing visibility 600 m downstream of the fire in 2 m height for all 100 MW scenarios.

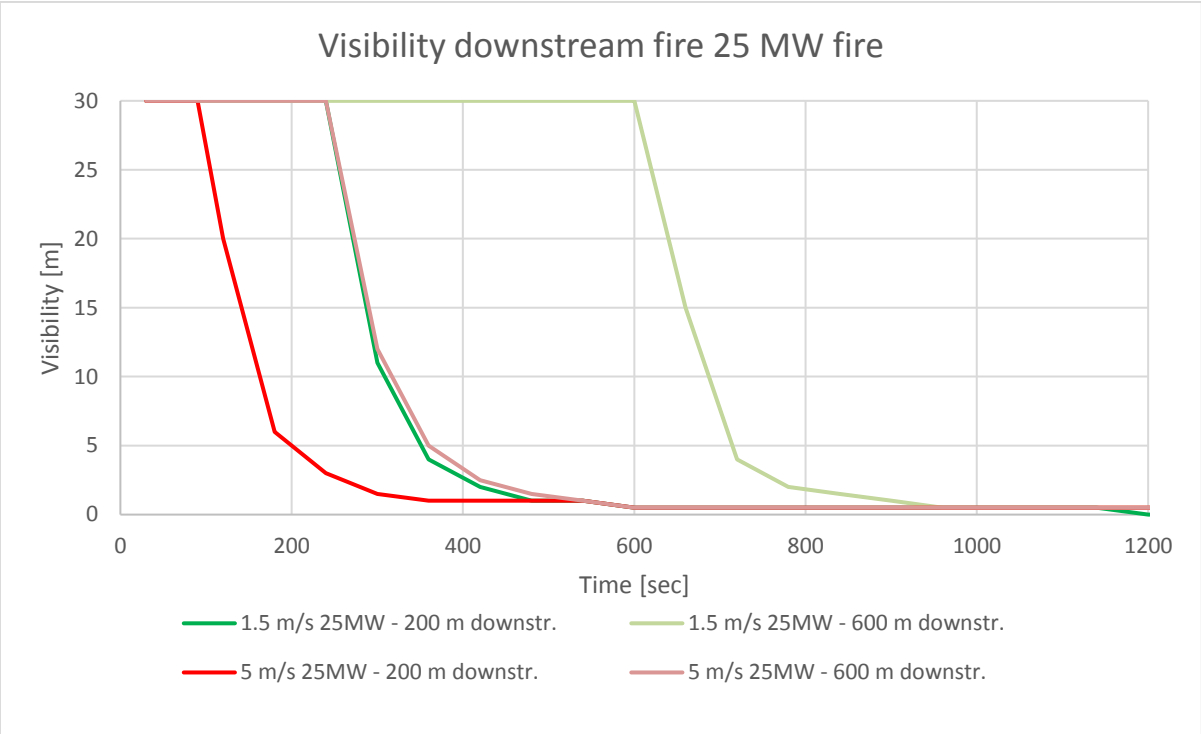

Figure 41. Graph showing visibility 200 m and 600 m downstream of the fire in 2 m height for 25 MW scenarios.

8.5 Temperature

Temperature has been logged every minute in 2 m height for all scenarios 45 m and 200 m downstream the fire, see Figure 42 and Figure 43. Results show that the temperature does not reach the tenability criteria of 80 ˚C before the tenability criteria of CO is breached for the 1.5 m/s and 3 m/s scenarios at 200 m downstream the fire. For the 5 m/s ventilation scenario, the temperature reaches 80 ˚C after about 290 seconds 200 m downstream the fire, whilst a CO concentration of 0.002 (2000 ppm) is reached after about 360 seconds.

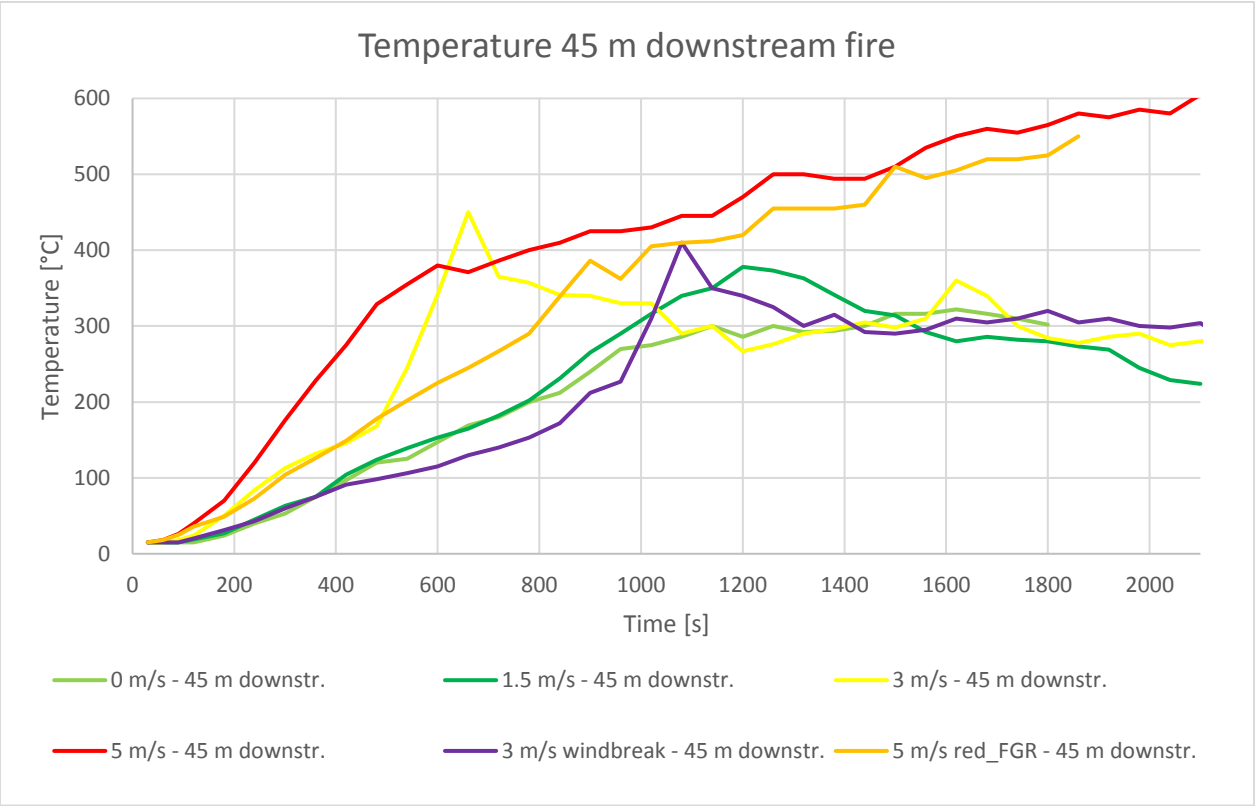

Figure 42. Temperature results 45 m downstream the fire in 2 m height.

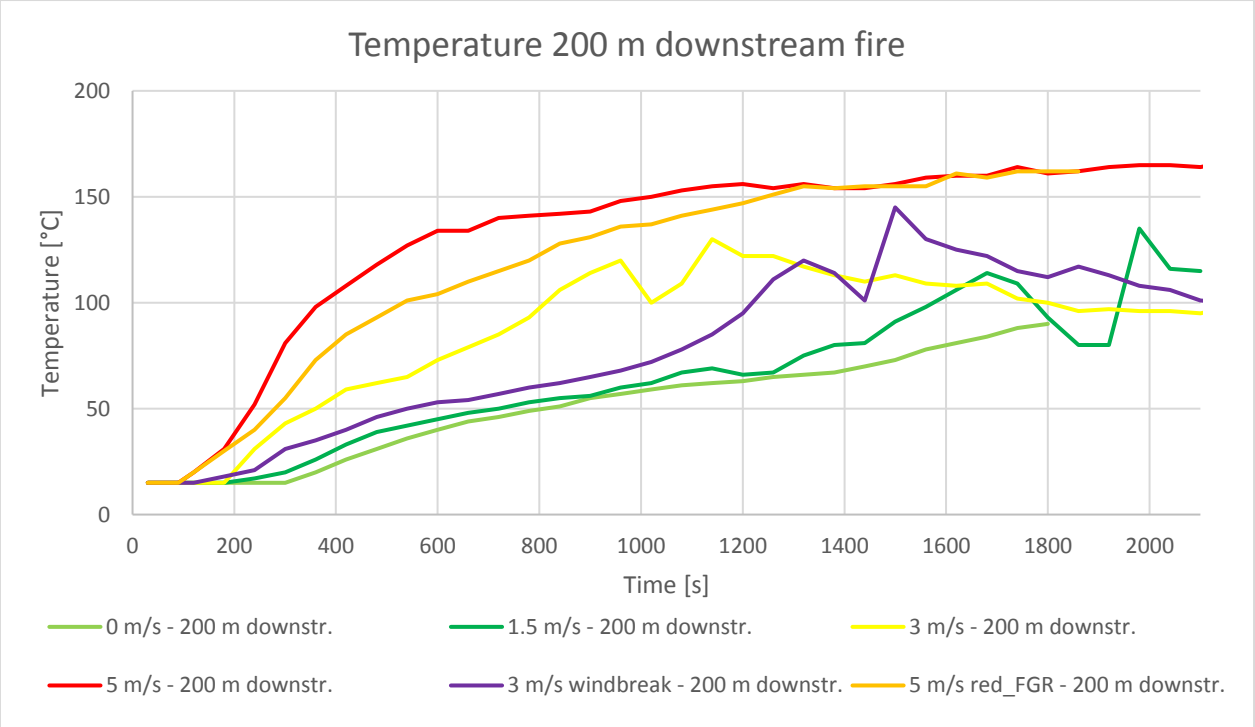

Figure 43. Temperature results 200 m downstream the fire in 2 m height.

8.6 Evacuation and FED results

The evacuation times (from start of fire to the last person has left the tunnel) are given in Table 7, whilst the number of evacuees inside the tunnel at any given time are shown in Figure 44. Note that 0 m/s and both 1.5 m/s scenarios (100 MW and 25 MW) have the same evacuation time and progress as the reference simulation without smoke.

For the 5 m/s, 5 m/s with reduced FGR and 25 MW with 5 m/s ventilation simulations the FDS simulations was terminated at 37 min, 31 min and 30 min respectively, whilst the evacuation time for the corresponding scenarios are 41 min, 39 min and 39 min. This gives a discrepancy of 4 min, 8 min and 9 min. When this happens, STEPS freeze the values for visibility and concentration of gases that are imported from FDS so the values stay as they were at the end of the FDS simulation for the different areas. Considering the results for HRR, CO and visibility, close to steady state conditions are achieved at this time for all these scenarios and it will not have a significant effect on the results.

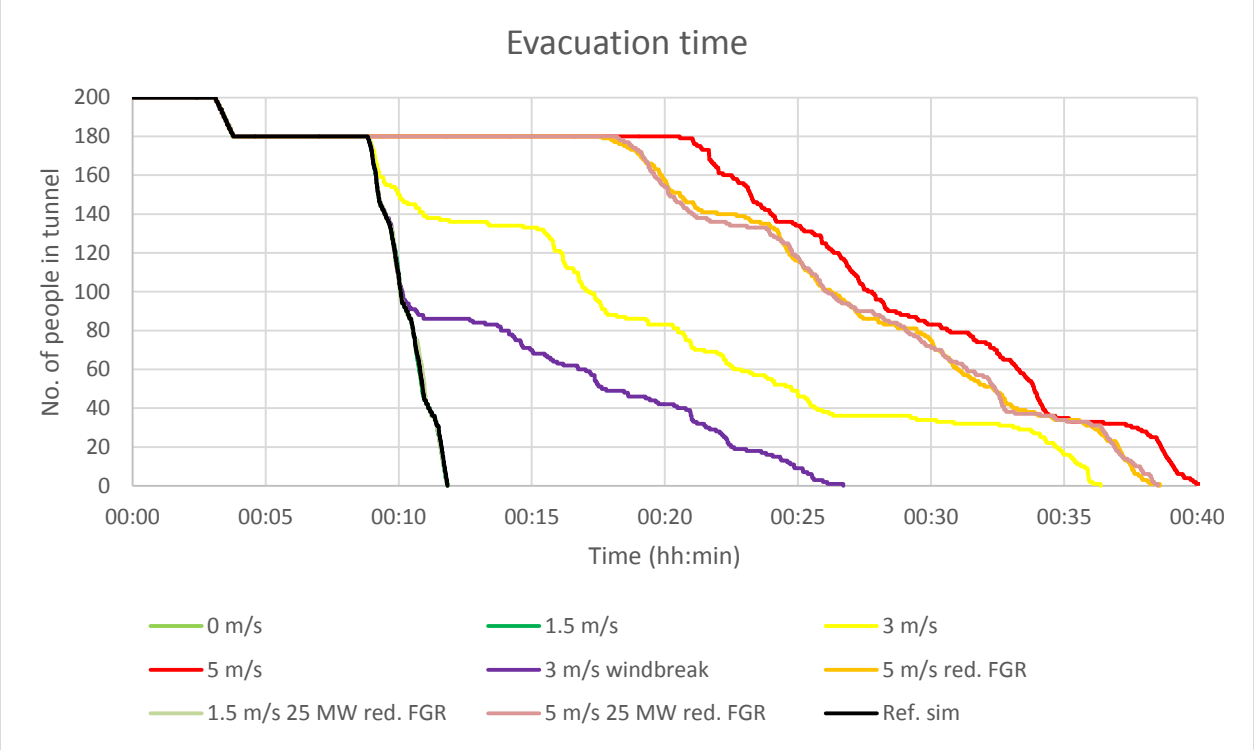

Figure 44. Evacuation time for all scenarios. Evacuees caught by smoke experience low visibility and reduced walking speed, resulting in long evacuation time for some of the scenarios.

Additional scenarios was also run for the egress simulations to investigate increased pre-movement time (minimum of 3 min) and reduced pre-movement time and walking speed (minimum 1 min pre-movement time and 1 m/s walking speed). Table 7 includes evacuation times for all scenarios. The values given in the first parenthesis is the result for the simulations with reduced pre-movement time and the second parenthesis include the results from the simulations run with increased pre-movement time. As can be seen, the increased pre-movement time has significant impact on the total evacuation time for the 1.5 m/s scenario. Results indicate that 42 of the evacuees are caught by smoke, since 158 persons does not experience FED values above 0.3, whilst 42 persons get FED values above 1.0.

Table 7. Summary of STEPS-simulation results. Results for 30 sec pre-movement time and 1 m/s walking speed is given in parenthesis. The additional scenario run for 1.5 m/s ventilation and 5 m/s w/reduced FGR with 3 min pre-movement time is shown in a second parenthesis.

Scenario	Evacuation time (min:sec)	No. of people with FED<0.3	No. of people with 0.3<FED<1.0	No. of people with FED>1.0	Comments and FED distribution
Ref. sim (no smoke)	11:56 (13:36)	-	-	-	No smoke included.
0 m/s ventilation	11:56 (13:35)	200 (200)	0 (0)	0 (0)	No ventilation. No evacuees exposed to CO in any of the two simulations.
1.5 m/s ventilation	11:56 (13:37) (44:47)	200 (200) (158)	0 (0) (0)	0 (0) (42)	No evacuees exposed to CO in main scenario. Max FED value of 0.0345 for 30 sec pre-movement time and 43.2 for 3 min pre-movement time.
3 m/s ventilation	36:40 (36:12)	80 (63)	36 (20)	84 (117)	FED>10=44 (71)
5 m/s ventilation	40:49 (38:48)	20 (20)	0 (0)	180 (180)	FED>10= 171 (177)
5 m/s ventilation w/reduced FGR	38:54 (36:55) (45:41)	20 (20) (20)	0 (0) (0)	180 (180) (180)	FED>10=104 (96) (180)
3 m/s ventilation w/windbreak	26:55 (30:43)	151 (113)	19 (36)	30 (51)	FED>10=0 (9)
1.5 m/s max HRR 25 MW	11:56 (13:36)	200 (200)	0 (0)	0 (0)	No evacuees exposed to CO. Max FED value of 0.0287 in sensitivity simulation.
5 m/s max HRR 25 MW and reduced FGR (same FGR as 1.5 m/s scenario)	38:50 (37:12)	20 (20)	42 (43)	138 (137)	FED>10= (0) Max FED=3.13 (2.86)

Figure 45 illustrates how evacuees are able to stay in front of the smoke in the 1.5 m/s scenario. From the results it is evident that they are all able to keep the smoke behind them all the way to the tunnel portal (exit).

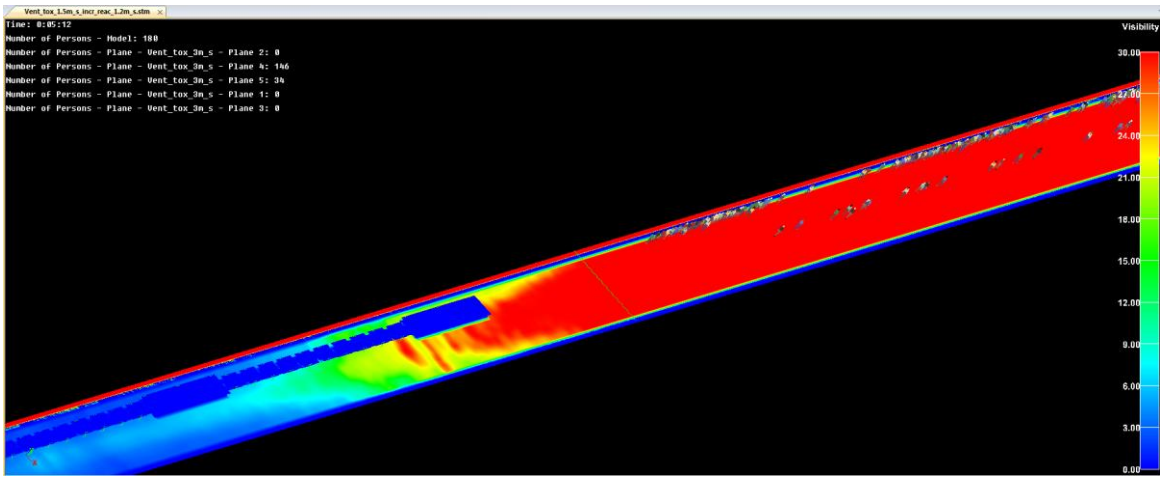

Figure 45. 1.5 m/s scenario after 05:12 showing evacuees "out running" the smoke front towards the downstream tunnel portal. The colour map shows the visibility in 2 m height, red colour indicates visibility of over 30 m and blue is below 6 m.

An extra evacuation simulation was run to investigate the effect of placing an emergency exit in the tunnel based on requirements in NFPA502 [6], which gives a distance of 300 m between exits. The exit was placed about 250 m downstream of the fire, "simulating" a fire 50 m from the neighbouring exit upstream this exit. This will be close to the worst possible location of the fire when having emergency exits every 300 m. The exit was given a capacity of 1.33 pers/sec, corresponding to a door of between 1.2 and 1.5 m width (Gwynne & Rosenbaum, chapter 59 in [23]). The scenario used for this simulation was the 5 m/s ventilation scenario, which had a total evacuation time of 40:49 minutes and 180 persons obtaining FED values above 1.0. The only change that was done to the STEPS-model was inserting the exit.

The results show an evacuation time of 11:16 minutes and 40 persons obtaining FED values above 0.3, of which 35 had a FED value above 1.0.

8.7 Instant tenability criterias

The instant tenability criteria's are described in Table 6. Time of reaching these values 200 m downstream the fire are given for the different scenarios in Table 8.

Table 8. Time for breaching instant tenability criteria's proposed in INSTA TS 950 [33] 200 m downstream the fire in 2 m height.

Scenario	> 10 m visibility	> 5 m visibility	Temperature < 80 °C	CO < 2000 ppm	CO_2 < 5 %	Oxygen > 15 %
0 m/s ventilation	380 sec	410 sec	1600 sec	630 sec	990 sec	950 sec
1.5 m/s ventilation	330 sec	360 sec	1380 sec	630 sec	980 sec	940 sec
3 m/s ventilation w/windbreak	270 sec	290 sec	1100 sec	630 sec	1000 sec	960 sec
3 m/s ventilation	220 sec	230 sec	670 sec	430 sec	630 sec	610 sec

Scenario	> 10 m visibility	> 5 m visibility	Temperature < 80 °C	CO < 2000 ppm	CO_2 < 5 %	Oxygen > 15 %
5 m/s ventilation w/reduced FGR	170 sec	200 sec	390 sec	480 sec	800 sec	730 sec
5 m/s ventilation	170 sec	190 sec	290 sec	340 sec	490 sec	450 sec
25 MW scenarios:						
1.5 m/s max HRR 25 MW	310 sec	340 sec	Not breached	900 sec	Not breached	Not breached
5 m/s max HRR 25 MW and reduced FGR (same FGR as 1.5 m/s scenario)	170 sec	210 sec	420 sec	Not breached	Not breached	Not breached

9 Discussion

A number of fire and egress simulations has been performed to investigate the effect of different ventilation velocities on the downstream tunnel environment. The three main simulations, 1.5 m/s, 3 m/s and 5 m/s, are set up with different fire growth rates (FGR) based on findings from full scale tunnel fire tests which show that ventilation increase fire spread and enhance the combustion process. To further examine the ventiltaion effect on the evacuation conditions without varying the FGR, simulations with different ventilation velocities and the same FGR as found for the 1.5 m/s scenario has been assessed as well (0 m/s and 5 m/s). In addition, a 3 m/s ventilation scenario with a windbreak (shielded fire) and 58 % reduced FGR compared to the normal 3 m/s scenario has been investigated. Furthermore, two 25 MW scenarios with 1.5 m/s ventilation and 5 m/s ventilation has also been assessed, both with the same FGR as for the original 1.5 m/s scenario.

9.1 Heat release rate

The simulation results show that the HRR is sensitive to different ventilation velocities, and that only the 5 m/s (two scenarios) and 0 m/s (!) scenarios are able to maintain the predefined HRR of 100 MW. This could be a result of the uniform airflow established for the 0 m/s with a distinct upper (outgoing) and lower (ingoing) airflow on both sides of the fire. The airflow seems to find a natural balance that gives sufficient oxygen to the fire via the lower layer in contrast contrast to the scenarios with ventilation. This is believed to be caused by the jet fans located in the ceiling introducing contradicting airflows in the upper level of the tunnel upstream the fire. This leads to smoke with low oxygen level being pushed down and recirculated into the fire. This seems to be the case for the 1.5 m/s and 3 m/s scenarios. In the 5 m/s scenarios the mechanical driven airflows are big enough to overcome the opposite airflows sufficiently to feed the fire with enough oxygen despite the fact that smoke is recirculated here as well. However, the airflow is not sufficient to obtain critical velocity.

The heavy HRR fluctations and the fact that maximum HRR is not maintained in the 1.5 and 3 m/s scenarios indicate that the fire is underventilated. For the other additional scenarios, including 0 m/s and the 5 m/s with reduced FGR (same FGR as for the 1.5 m/s), HRR is maintained. For the windbreak scenario (3 m/s), theoretical maximum HRR is not reached. Peak HRR for this scneario is about 90 MW. Due to this, and to further examine the effect of ventilation on toxicity without the results being biased by different HRR's, additional scenarios with a maximum HRR of 25 MW are analyzed. One with 1.5 m/s ventilation and one with 5 m/s. Both the 25 MW scenarios follow the FGR of the original 1,5 m/s scenario, reaching 25 MW after 305 seconds as can be seen in Figure 21.

The 3 m/s scenario with a windbreak (shielded fire) illustrates the importance of an unobstructed air supply to the fire to be able to achieve and maintain the relatively high HRR's which is typical for HGV tunnel fires.

9.2 Airflow and backlayering

The two additional simulations (1.5 m/s and 5 m/s ventilation velocities) with a predefined maximum HRR of 25 MW and identical FGR show that the 5 m/s ventilation scenario is the only simulation achieving critical velocity.

A general observation is that the smoke and toxicity is significantly higher towards the walls of the tunnel downstream the fire. This represents a big challenge, since this is where walkways are located and will be the preferred evacuation route to avoid to be hit by driving cars. The phenomena is more prominent close to the fire, whilst the conditions are more uniform further down the tunnel (600 m). The reason for this is believed to be the fact that the walls cool the smoke and so it descends faster. The geometry of the tunnel together with the mechanical ventilation could also contribute to this, since the smoke is also pushed towards the walls which is "curved". As a natural effect of obstructions (jet fans), friction from the walls etc., the smoke is not only pushed in the longitudinal direction. When hitting the curved walls, the the smoke travels downwards.

For the upstream part of the tunnel, smoke propagating towards the ventilation direction is severely delayed compared to the downstream part for all scenarios with ventilation. FED calculations for the upstream evacuees shows that they are not affected by smoke in any of the scenarios. Considering that none of the 100 MW fire scenarios are set up with a ventilation system (airflows) which achieve critical velocity, this design value for the ventilation system (critical velocity) has no major effect in the self-evacuation phase. In fact, since conditions downstream the fire are significantly worsened with higher ventilation velocities, using critical velocity during evacuation is not seen to have any positive effect in the scenarios investigated here. Of course, a clear distinction between self-evacuation phase and rescue phase is needed, since response personnel are reliant on critical velocity to be able to reach the accident area.

The pulsating phenomenon observed in the 3 m/s and 5 m/s scenarios was also seen in the Runehamar tunnel fire tests in 2003 for fires with a HRR of above 125 MW. Lönnemark, Bror and Ingason [36] concludes that the phenomenon is a result of the tunnel system as a whole, such as distances between different objects in the tunnel and outside conditions. Furthermore, they suggest that disturbance at the (tunnel) outlet can be a trigger that sets off the oscillations. This is interesting, since the start of the pulsation in the simulations performed here coincides perfectly with the time for smoke reaching the downstream tunnel portal, supporting the suggested trigger proposed by Lönnemark et al.

9.3 Toxic gases

Based on the fact that only the 5 m/s simulation of the main scenarios was able to maintain a 100 MW HRR, it may not be surprising that the corresponding CO values downstream the fire are bigger for this scenario. However, comparing the 5 m/s scenario with reduced FGR and the 0 m/s scenario, which has the same FGR and are also able to maintain the same HRR in the simulation as the 5 m/s scenario, shows that the difference in downstream CO concentration during the evacuation phase is not only correlated to the FGR or HRR alone. The maximum CO concentration measured 200 m downstream the fire on a level of 2 m in height is higher for the 0 m/s scenario, but it is lower during the first 25 minutes and 600 m downstream it does not exceed the 5 m/s scenario with reduced FGR during the simulation time of 30 minutes. After 30 minutes, the CO concentration 600 m downstream the fire is almost 40 % higher in the

5 m/s scenario with reduced FGR compared to the 0 m/s scenario. Both simulations reach the maximum HRR of 100 MW after about 14.5 minutes.

The difference in CO concentration for the main scenarios of 5 m/ and 3 m/s are very distinct for the first 12-13 minutes 200 m downstream the fire and up until 20 minutes 600 m downstream the fire. At these times the CO concentration in the 5 m/s scenario starts to flatten out and the CO concentration in the 3 m/s scenario surpass that of the 5 m/s scenario. The 1.5 m/s scenario exceeds the CO concentrations of the 5 m/s scenario after about 33 minutes, 200 m downstream of the fire. 600 m downstream the fire, the CO concentration in the 5 m/s scenario is twice as high as the 1.5 m/s scenario after 30 minutes.

Both the 1.5 m/s and 3 m/s scenarios has a sudden rise in CO concentration after 17 minutes and 32 minutes, respectively. This is assessed to be caused by the under ventilated conditions resulting in reduced HRR since no such sudden rise are observed for the 5 m/s or 0 m/s scenarios.

Measurements downstream the fire for the 25 MW scenarios further supports the findings from the 100 MW scenarios, that CO concentrations are higher for the high ventilation velocities in the early phase of the fire, but the difference is not as big as in the 100 MW scenarios. CO concentration for the 1.5 m/s scenario surpasses the 5 m/s scenario after 11 min 200 m downstream and after 19 minutes 600 m downstream the fire.

The maximum CO concentrations downstream the fire are significantly lower in the 25 MW scenarios compared to the corresponding 100 MW scenarios. The difference is close to a factor of five for the 5 m/s scenarios (25 MW with reduced FGR and 100 MW with reduced FGR) 200 m downstream the fire after about 16 minutes. For the 1.5 m/s scenario, the 100 MW fire has a CO concentration which is 2.5 times that of the 25 MW fire after 16 minutes and 200 m downstream the fire.

600 m downstream the fire, the 100 MW scenario has 4 times as high CO concentration as the 25 MW fire after 20 minutes, whilst the difference between the two 1.5 m/s scenarios are zero at the same time, but the 100 MW increase its CO concentration to about 1.6 times that of the 25 MW after 30 minutes.

The 5 m/s 25 MW scenario showed non-lethal toxic concentrations, but even so, the accumulated dose for the evacuees (FED) show that fatalities are likely anyways. This is an important perspective to the findings of Nilsen and Lindvik in 2001, referenced in [19], and are directly linked to visibility and its effect on walking speed and subsequently the exposure time.

9.4 Visibility

Visibility is a major parameter of any evacuation analysis and even more important in tunnels since the travel distances are normally long. Visibility determines both the total evacuation time and exposure time for evacuees, i.e. the resulting FED values. For the scenarios investigated here, visibility is quickly decreased when smoke first reach the measuring point 200 m downstream the fire, but there is a big difference with respect to when this starts. The 0 m/s ventilation scenario gives twice as much time before visibility falls below 5 m at 2 m height 200 m downstream the fire compared to the 5 m/s scenarios (including the 5 m/s scenario with the same FGR as the 0 m/s scenario). The time to breach the tenability criteria's for visibility is decreasing successively with increased ventilation velocity.

Not surprisingly, 600 m downstream the fire the differences for when visibility starts to drop are further increased between the 0/1.5 m/s scenarios and the 3/5 m/s scenarios. Here, both the 0 m/s and 1.5 m/s scenarios use more than twice the time to obtain visibility below 5 m compared to the others.

The visibility results shows that 200 m downstream the fire, the tenability criteria (both 10 m and 5 m) is breached well before the instant tenability criteria of CO is breached. Considering the steep drop in visibility, this is an important observation since the visibility will significantly reduce the walking speed and the evacuees are trapped and will be exposed to the high CO concentrations that will come. Without FED calculations and accounting for the effect of visibility on walking speed, this correlation would not have been captured, e.g. if one only look at instant tenability criteria's and calculate the egress independently.

It is concluded that visibility measurements show a similar development between the the different ventilation velocities as the CO concentration; downstream visibility is severly reduced earlier for the higher ventilation velocity scenarios compared to scenarios with lower ventilation velocity.

9.5 Evacuation and FED values

The STEPS simulations show big variation in egress time for the different scenarios. As can be seen from Figure 44. If or not evacuees are caught by smoke is vital for the total egress time.

The egress times are "clustered" for the scenarios where no one experience FED values of any significance (0 m/s and both 1.5 m/s scenarios), others are ranged by the order of ventilation velocity, as can be seen in Figure 44. The egress time for the 25 MW scenario with 5 m/s ventilation velocity and reduced FGR are close to the same time as for the corresponding 100 MW scenarios. This indicates that maximum HRR does not influence the egress time, but the number of people experiencing FED values above 1.0 are lower for the 25 MW scenario.

The 3 m/s scenarios (one without windbreak and one with windbreak and 58 % reduced FGR) seems to be more sensitive to the FGR than the others. This could be due to the fact that smoke only catch up with parts of the evacuees and at a later stage, whilst in the 5 m/s ventilation scenarios, all are caught by the smoke and in the 0/1.5 m/s scenarios, no one is caught up by the smoke.

Figure 46 compile egress times and FED values already given in the results chapter for all the scenarios investigated.

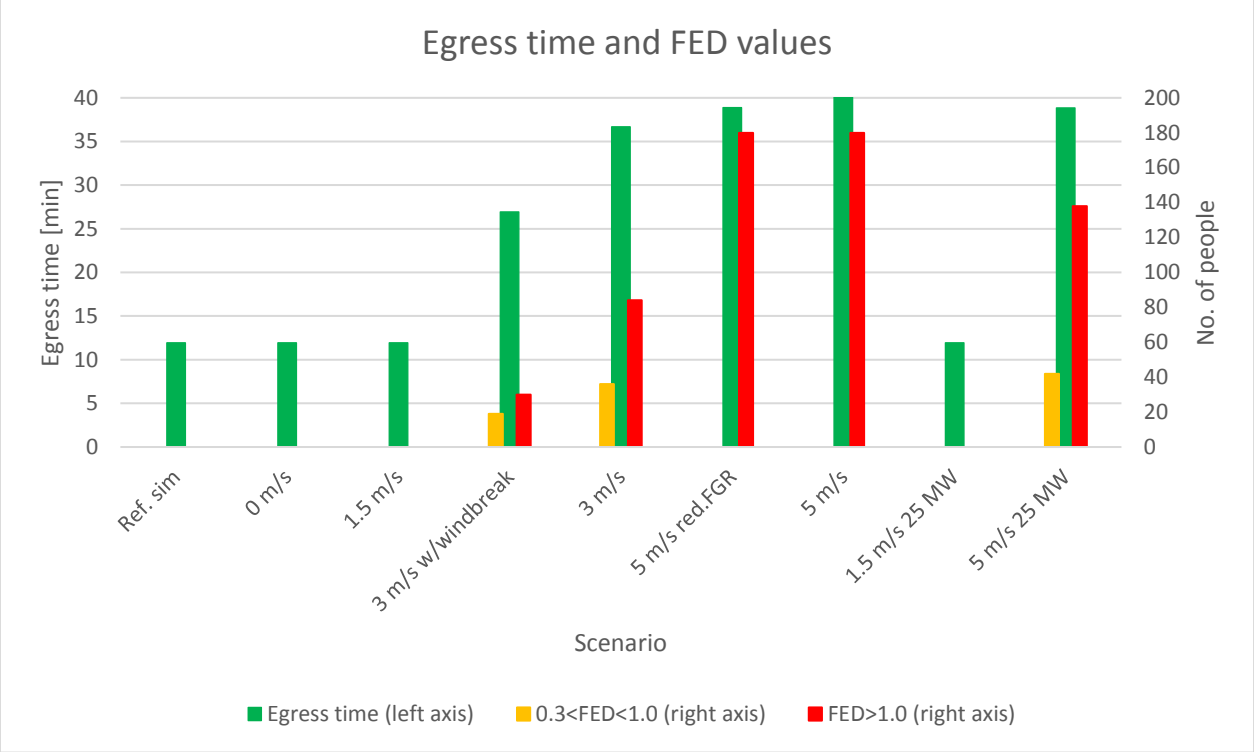

Figure 46. Graph showing egress times and FED values for all scenarios.

The results differ significantly from those obtained by Caliendo, Ciambelli, De Guglielmo, Meo and Russo in their study of 50 MW tunnel fire in 2012 [37], which gave evacuation times of up to 12 minutes for a 50 MW HGV fire and a maximum evacuation route of 590 m. They also used STEPS simulations and input from CFX (also a CFD software) to account for reduced walking speed based on visibility. However, several differences exists as well, and the main parameter can be the CO-yield used, which was based on design fire scenarios described by FIT [38] according to their separate CFD report [39]. FIT describes an average CO-yield of 0.05, half of what is used here. Egress times also indicate that the soot-yield, which affects the walking speed, probably is lower than what is used here. Caliendo et. al refers to FIT [38] for the soot yield, but this is not explicitly given there so the soot yield is unknown.

The underventilated fires in the 1.5 m/s and 3 m/s scenarios results in heavy HRR fluctations, as a result of a "breathing" fire, typical for under ventilated fires. As a result, a "plug" of thick smoke with high CO-concentration that propagates downstream the tunnel is produced. An important observartion from the 1.5 m/s scenario is that the evacuees are able to outrun this plug (see Table 7), and are apparantly unaffacted by the smoke. When increasing the pre-movement time (minimum of 3 min), evacuees in this scenario is also affected. It is natural to think that the more you increase the pre-movement time, the more people will be affected. However, the results show that the situation still gets worse for the 5 m/s scenario with the same FGR, so the lower ventilation scenario would still be the preferred solution.

Time is a universally important variable when talking about fire and evacuation. The fact that lower ventilation velocities significantly increases the time before the tenability criteria's are breached downstream a tunnel fire, even if the CO concentration is higher when the smoke first reach the different measuring-points, indicate that low ventilation velocities are preferred. Pre-movement time is however critical for the result. This is clearly illustrated by the 1.5 m/s ventilation scenario with a

minimum pre-movement time of 3 minutes (successively increased for persons further away from the fire). Total evacuation time is decided by the last person leaving the tunnel, and for this scenario the time is close to quadrupled compared to the same scenario with a minimum of 1 min pre-movement time. However, the number of evacuees caught by smoke are limited compared to the 5 m/s ventilation scenario. Only 42 persons are exposed to smoke in the former and 180 in the latter (corresponding to all evacuees downstream the fire).

The results indicate a "ceiling effect" [40], i.e. if anyone in the simulation are caught by smoke this automatically gives close to maximum evacuation time from the tunnel. The maximum evacuation time are 43 minutes, based on the lowest possible walking speed of 0.3 m/s and the maximum travel distance of 770 m. This is further supported by the steep fall in visibility. On the other hand, both evacuation time, the number of occupants obtaining FED values above 0.3 and the actual FED values resulting from the 3 m/s scenarios lies between those from the 1.5 m/s and 5 m/s ventilation scenarios, contradicting the suspicion that the ceiling effect also applies to FED values.

As mentioned in section 9.3, the CO concentration is greater towards the tunnel walls, which is where the preferred evacuation route is. In the STEPS-simulations, a majority of the evacuees follows this route since the buses have exits towards the same tunnel wall and half of the persons evacuating from cars will exit at the same side. This could be a possible distinction between different research simulations. Here, it is believed that the main path of travel will be along the tunnel walls, since this is where the walkways, normally equipped with lighting, are placed.

Essentially, the results of the increased pre-movement time underpin the importance of starting evacuation early in the fire development. This can be achieved by fire detection and alarm systems with different technical installations to communicate the alarm, such as communication via radio, variable signage, PA-system etc. The extra simulation with an exit placed in the tunnel, simulating exits every 300 m as described in NFPA502 [6], shows a major difference in number of people being exposed to smoke. This fortify the belief that emergency exits, and the distance between them, are the main measure that can effectively reduce the consequences of a tunnel fire on human lives.

9.6 Uncertainties

The use of simulations to interpret real life can be dangerous if not used in the correct way and will never eliminate the need for full-scale testing. Simulation tools does not give us anything we do not put in to the model, it simply calculate and, for this case, visualize the results for us to better understand them. But, it saves a great amount of time, categorize the output and helps us with the math, since others has done the work for us. The equations, algorithms and graphics are all there because someone put them in the software. These equations and algorithms are results of several centuries of research on physics (modern) and chemistry. For fire dynamics simulations, the fundamental theory is the laws of conservation (mass, energy and momentum) on which the algorithms is based upon. Considering this, and the validation performed for the FDS software [31], it is really all up to the user to input the correct data and interpret the results the right way. The human error is difficult to measure and often difficult to disclose, and this is why verifiability is so important and the reason why a lot of technical input is a big part of the report.

A vast majority of the input data used for this report is based on the work of Ingason and his co-workers. This could have a negative effect on the findings, even though Ingason also review others work, so where it has been possible, other independent sources of information has been used or checked against the input data this thesis is based on. The reason for the narrow list of referenced tunnel fire tests is the fact that tunnel fire dynamics is a young discipline and that there is a limited amount of full scale fire tests performed in tunnels with the level of documentation that Mr Ingason and his associates has provided. This is of course a result of the costs related to such testing and because commercial testing is kept undisclosed. The European community has acknowledged this, and has put together several international projects, funded by the member countries. Projects such as UPTUN [41], EUREKA [42], SOLIT [43] are finished or ongoing tunnel fire test programs. It should be noted though that the Runehamar tests performed by Ingason et al. was part of the UPTUN program and that it is still running. Of course, the mentioned research programmes has given invaluable input and paved the way for later findings. Both UPTUN and EUREKA significantly raised the awareness and subsequent safety level of European tunnels.

Another possible error source is, although thought to be minor, the method used to measure CO concentrations. CO is measured "manually" from slice files in 2 m height and interpolated for the cross-section. The interpolation is needed because there are higher concentrations towards the wall in early stages and close to the fire due to the smoke descending faster and are pushed down by the tunnel geometry. The walls also cools down the smoke, giving colder smoke towards the walls and so it descends faster. Since the same method is used for all simulations and the main objective is to compare the different simulations against each other, the impact of this uncertainty is believed to be limited.

The use of the simple chemistry model for combustion in FDS is identified as a possible source of error affecting the resulting HRR for the different scenarios. This is something that should be investigated closer, e.g. by testing and comparing the results from other combustion models.

A sensitivity analysis has been performed to investigate cell sizes and mesh communication, the analysis shows that the cell size give some discrepancy in the fire mesh, but that information are passed on to the next mesh correctly. Considering the objective of this report, studying conditions downstream the fire, this is assessed to be negligible. However, there can still be hidden sources of error that are not captured in the analysis, this will be part of the residual uncertainty that most analysis will suffer from.

The critical ventilation velocity was not reached for any of the main simulation scenarios. However, in the 25 MW scenario with 5 m/s ventilation it was. The results from the 25 MW scenario show similar results as the main scenarios, and obtaining critical velocity will based on this, not affect the results.

Vehicles queuing in the tunnel is not included in the simulation. Such obstructions can influence the turbulence and possibly the results. However, it is natural to think that this would worsen the conditions for the higher ventilation velocities and thus only enhance the tendency shown that higher velocities gives shorter available safe egress time.

10 Conclusions

Effect of different longitudinal ventilation velocities on downstream evacuation conditions during tunnel fires has been investigated with a number of fire and egress simulations. The literature study and results from the simulations show that ventilation has a great effect on the FGR and HRR due to inert conditions for high HRR's without adequate oxygen supply rate. This phenomena is enhanced for shielded fires. This affect the smoke production, which is linked to the HRR. On the other hand, under ventilated fire produces more CO and other toxic gases, resulting in a thick smoke plug propagating downstream the fire. The downstream smoke spread (speed) is again linked to the ventilation velocity. For longer distances, this can have a significant effect. Low ventilation velocities makes it possible to escape the thick smoke, even when considering relatively low walking speeds (maximum of 1 m/s). Pre-movement time is however critical for the result and the report underpin the importance of low pre-movement times for successful evacuation. Another important aspect is the major effect observed for reduced distance between emergency exits. Using the recommended distance between exits given in NFPA502 of 300 m can reduce the number of persons obtaining FED values above 0.3 with more than 75 %.

The conclusive scenarios for deciding if increased ventilation velocity will increase probability of surviving downstream a tunnel fire in the simulations performed here are the 0 m/s and 5 m/s scenarios with reduced FGR. These two simulations have the same FGR and obtain the same HRR curves during the simulation time. Even when not accounting for the fact that increased ventilation will increase the FGR, and the rate of smoke production in the early phase, these simulations show that during the first 23 minutes of a relatively severe HGV fire, no ventilation is better than high ventilation velocities. The other scenarios further supports this conclusion, even though reduced HRR obscures the results to a certain degree.

As for the dilution effect of high ventilation velocities, this is seen as a more smooth increase and stabilization of the CO concentration on a lower level for the 5 m/s scenarios compared to the 1.5 m/s and 3 m/s scenarios. The 1.5 m/s and 3 m/s gave a "plug" of thick smoke with high CO concentration which exceeded the CO concentration of the 5 m/s scenario, but at a late stage in the simulations.

The 25 MW scenarios illustrate the importance of visibility. CO concentrations are kept relatively low, below the tenability limit of 0.002 in both the 25 MW scenarios, but due to low visibility, evacuees obtain long exposure time in the 25 MW 5 m/s ventilation scenario, resulting in a high number of evacuees with high FED values.

The overall results, taking all scenarios investigated into consideration, give and indisputable indication that low ventilation velocities, or no ventilation at all, will give far better chances of surviving an evacuation downstream a tunnel fire. The hypothesis presented in section 1.3 is therefore not supported by the findings in this report. The results are relatively unambiguous and should be investigated further to confirm them and possible give better recommendations on tunnel ventilation strategies.

11 Further work

In line with increased complexity, height and size of buildings, technical safety installations has become more and more important. The commercial demand for such systems has ensured innovation and improvements which has increased the overall safety, or kept the safety level constant when put to the test by more complex building design. Reliability of the systems and the possibilities they represent enable realization of new projects and improvements to existing constructions in a cost effective way. As for buildings, it is important that the tunnel community push for such innovation when it comes to the special environment that long, deep and highly trafficked tunnels represent.

The results of this report indicate that further analysis and, optimally, full scale tunnel fire tests with focus on effects of ventilation velocities on toxicity, to validate the findings is needed. Several uncertainties has been identified, which can be further investigated by "desktop" analysis, but only full scale fire tests which further supports the findings can give the necessary confidence so that a clear recommendation for tunnel ventilation strategies can be given.

References

[1] K. Melby, E. Øvstedal, F. H. Amundsen and G. Ranes, "Subsea road tunnels in Norway," Norwegian Public Roads Authorities, Oslo, 2002.

[2] F. H. Amundsen, «De fem store tunnelbrannene i Norge - Statens vegvesnes rapporter nr. 340,» Statens vegvesen (Norwegian Public Roads Administration), Oslo, 2017.

[3] *Byggteknisk forskrift (TEK17),* Direktoratet for byggkvalitet, 2017.

[4] Håndbok N500, Vegtunneler, Statens vegvesen - Vegdirektoratet, 2016.

[5] Samferdselsdepartementet, *Forskrift om minimum sikkerhetskrav til visse vegtunneler (tunnelsikkerhetsforskriften), FOR-2007-05-15-517,,* Lovdata; https://lovdata.no/dokument/SF/forskrift/2007-05-15-517, 2007.

[6] N. F. P. Association, *NFPA 502 - Standard for Road Tunnels, Bridges, and Other Limited Access Highways,* National Fire Protection Association, 2017.

[7] P.-K. (. Foss, «Dokument 3:16 (2015–2016), Riksrevisjonens undersøking av arbeidet til styresmaktene med å styrkje tryggleiken i vegtunnelar,» Samferdselsdepartementet, 2016.

[8] D. f. s. o. beredskap, "Direktoratet for sikkerhet og beredskap (DSB) homepage," Direktoratet for sikkerhet og beredskap (DSB), [Online]. Available: https://www.dsb.no/menyartikler/statistikk/branner/. [Accessed April 2018].

[9] "Statistisk sentralbyrå homepage," Statistisk sentralbyrå, 24 February 2016. [Online]. Available: https://www.ssb.no/bygg-bolig-og-eiendom/statistikker/bygningsmasse/aar/2016-02-24. [Accessed April 2018].

[10] E. Jersin, «Storulykker i Norge 1970 - 2001,» SINTEF Teknologiledelse, Sikkerhet og pålitelighet, Trondheim, 2003.

[11] Håndbok 021 - Vegtunneler, Statens vegvesen, 2002.

[12] Håndbok 021 - Vegtunneler, Statens vegvesen, 2006.

[13] Y. Z. Li og H. Ingason, «Influence of ventilation on road tunnel fires with and without water-based suppression systems,» SP Technical Research Institute of Sweden, Borås, 2016.

[14] T.-O. Nævestad, K. Ranestad, B. Elvebakk og S. Meyer, «Kartlegging av kjøretøybranner i norske vegtunneler 2008-2015,» Transportøkonomisk Institutt, Oslo, 2016.

[15] R. Carvel, «A review of tunnel fire research from Edinburgh,» *Fire Safety Journal,* 9 May 2016.

[16] H. Hejny, «The European project UpTun – improving the level of fire safety in existing tunnels,» *Safety and Security Engineering Vol 82,* pp. 519-529, 2005.

[17] T.-O. Nævestad og S. Meyer, «Kartlegging av kjøretøybranner i norske vegtunneler 2008-2011,» Transportøkonomisk institutt, Oslo, 2012.

[18] H. Ingason, Y. Z. Li og A. Lönnemark, «Runehamar tunnel fire tests,» *Fire safety journal,* vol. 71, pp. 134-149, 2015.

[19] A. Lönnemark, «On the characteristics of Fires in Tunnels (Doctorla thesis),» Lund Institute of Technology, Lund, 2005.

[20] K. McGrattan, S. Hostikka, R. McDermott, J. Floyd, M. Vanella, C. Weinschenk og K. Overholt, *Fire Dynamics Simulator Technical Reference Guide Volume 1: Mathematical Model,* National Institute of Standards and Technology, 2017.

[21] L. Li, P. Mei, S. Li og H. Zhang, «Effect of longitudinal ventilation on heat release rate of tunnel fires,» *Fire safety journal,* vol. 30, pp. 230-232, 2012.

[22] M. MacDonald, «Mott McDonald homepage,» Mott MacDonald, 2018. [Internett]. Available: https://www.stepsmottmac.com/validation.

[23] M. J. (. i. c. Hurley, SFPE Handbook of Fire Protection Engineering, fifth edition, 5 red., New York Heidelberg Dordrecht London: Springer, 2016.

[24] A. Lönnemark, A. Claesson, J. Lindström, Y. Z. Li, M. Kumm og H. Ingason, «Full-scale fire tests with a commuter train in a tunnel,» SP Technical Research Institute of Sweden, Borås, 2012.

[25] H. Ingason, Y. Z. Li og A. Lönnemark, Tunnel fire dynamics, New York Heidelberg Dordrecht London: Springer, 2014.

[26] R. O. Carvel, A. N. Beard, P. W. Jowitt og D. D. Drysdale, «Variation of heat release rate with forced longitudinal ventilation for vehicle fires in tunnels,» *Fire Safety Journal,* vol. 36, pp. 569-596, 2001.

[27] Statens vegvesen, Håndbok 021 - Vegtunneler, Statens vegvesen, 2010.

[28] H. Braxmeier, S. Steinberger, I. Melnicenco, A. Thiemermann og A. Dominic, «Pixabay,» Hans Braxmeier & Simon Steinberger GbR, April 2018. [Internett]. Available: https://pixabay.com/en/knife-sharp-blade-cut-metal-2228114/ and https://pixabay.com/en/arms-fly-balancing-idea-like-2938764/. [Funnet April 2018].

[29] K. McGrattan, S. Hostikka, R. McDermott, J. Floyd, M. Vanella, C. Weinschenk og K. Overholt, Fire dynamics simulator - User's guide, sixth edition, Various: National Institute of Standards and Technology, 2017.

[30] A. Back, T. Bergström, T. Dittmer, M. Hjohlman, F. Magnusson, J. Norén, D. Rosberg og J. Wahlqvist, «Stöd för tillämning av CFD-modeller,» Föreningen för brandteknisk ingenjörsvetenskap, Stockholm, 2013.

[31] K. McGrattan, S. Hostikka, R. McDermott, J. Floyd, M. Vanella, C. Weinschenk og K. Overholt, «Fire Dynamics Simulator Technical Reference Guide Volume 3: Validation,» National Institute of Standards and Technology, Various, 2017.

[32] G. W. Mulholland, «Smoke production and properties,» i *SFPE Handbook of Fire Protection Engineering*, 3rd red., National Fire Protection Association, 2002, pp. 2_258-2_268.

[33] C. I. F. S. Design, *SN-INSTA/TS 950 Fire safety engineering - Comparative method to verify fire safety design in buildings,* Standard Norge, 2014.

[34] S. vegvesen, «Youtube,» Statens vegvesen, 5 May 2017 [video]. [Internett]. Available: https://www.youtube.com/watch?v=zqX4-oOhWzk. [Funnet April 2018].

[35] *ISO 13571: Life-threatening components of fire - Guidelines for the estimation of time to compromised tenability in fires,* Geneva: International Organization for Standardization, 2012.

[36] A. Lönnemark, B. Persson og H. Ingason, «Pulsations during large-scale fire tests in the Runehamar tunnel,» *Fire safety journal,* vol. 41, pp. 377-389, 2006.

[37] C. Caliendo, P. Ciambelli, M. L. De Guglielmo, M. Grazia Meo og P. Russo, «Simulation of People Evacuation in the Event of a Road Tunnel Fire,» *Procedia - Social and Behavioral Sciences,* vol. 53, pp. 178-188, 2012.

[38] E. T. N. F. i. Tunnels, «Fire in tunnels, Technical report part 1: Design fire scenarios,» Thematic Network Fire in Tunnels, Brussels, 2005.

[39] C. Caliendo, P. Ciambelli, M. L. De Guglielmo, M. M. Grazia og P. Russo, «Numerical simulation of different HGV fire scenarios in curved bi-directional road tunnels and safety evaluation,» *Tunnelling and Underground Space Technology,* vol. 31, pp. 33-50, 2012.

[40] T. H. Taylor, «Ceiling effect,» SAGE Publications, 2010.

[41] K. Bergmeister, «Innovative Technologies to Upgrade Fire Safety of Existing Tunnels,» *Beton- und Stahlbetonbau,* nr. 103, pp. 1-9, 2008.

[42] A. Haack, «Fire Protection in Traffic Tunnels: General Aspects and Results of the EUREKA Project,» *Tunnelling and Underground Space Technology,* vol. 13, nr. 4, pp. 377-381, 1998.

[43] S. Kratzmeir, «New approaches in fire protection for tunnels - The SOLIT project,» *Tunnelling and Underground Space Technology,* vol. 21, pp. 283-284, 2006.

Western Norway University of Applied Sciences

Appendices

Western Norway University of Applied Sciences

Appendix A. Turbulence – Intensity and resolution of turbulence using FDS

Turbulence

Intensity and resolution of turbulence using FDS

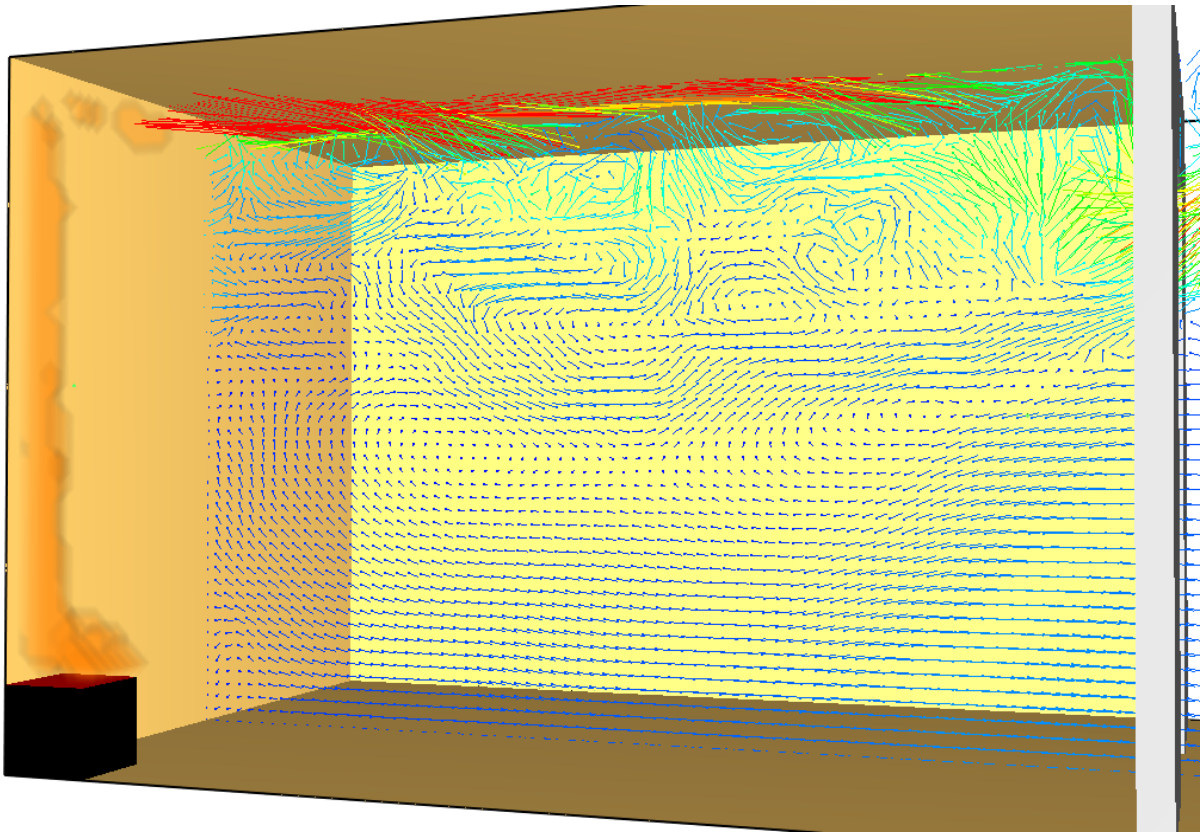

ING4006 – Advanced fire and egress modelling

Assignment 3

JOHAN KR MØLLER (127667)

HØGSKOLEN STORD/HAUGESUND 2016

Turbulence

Turbulence can be defined as a temporary and chaotic situation [1]. In fluid dynamics, it is related to the characterization of flows. While laminar flows is relatively uniform, i.e. smooth velocity changes and mainly one-directional, turbulent flow is characterized by swift changes both in direction and velocity. Turbulence can be said to be somewhat self-reinforced. This is best illustrated by a flows tendency to obtain turbulent behaviour when it meets obstructions if the initial velocity is high enough; at first the liquid flows in a laminar manner, i.e. uniform flow in one direction. When the flow, or parts of it, meets an obstruction, the uniformity is broken and parts of it collides with the laminar flow before (upstream) and outside the obstruction. This again changes the flow around the obstruction. How far this "interruption" is reaching in the opposite direction of the laminar flow or outside the obstruction, is determined by the viscosity and velocity of the laminar flow. Downstream the obstruction, the turbulence can sustain for a longer distance. This is further underlined by the fact that when a flow has very high velocity, the "obstruction" could merely be represented by friction, e.g. a pipe wall, or simply the forces acting on a smoke flow from the relatively still-standing surrounding air.

These characteristics of turbulence makes it an important phenomena to understand and handle in many contexts, e.g. when considering flow in pipes, the transition from deflagration to detonation, entrainment in fire plumes and the mixing of combustible gases and oxygen to obtain combustion when temperature is high enough or an ignition source is available. Diffusion is strongly driven by turbulence, and is important for the movement of smoke, for instance in a fire compartment.

Turbulence is characterized by fluctuations (changes), as indicated above, which varies with time and length [2]. The fluctuations are destroyed by natures desire for balance. This is something best described in the law of conservation of energy, implying that the change in internal energy of a control volume (CV) is equal to energy going in to it minus that going out. Turbulence in fluids are characterized by high fluid velocities, i.e. relatively high levels of energy. In buoyant fires, the energy going into the CV is a result of energy (heat) released in the combustion process. The same way no one will be able to find an everlasting machine, or *perpetuum mobile* as the greeks called it, turbulence is dependent on the supply of energy because of friction/gravity.

The loss of energy in turbulent structures (eddies), happens through a transformation of energy from large eddies, referred to as the integral scale, to smaller eddies. At the end, energy dissipates from the smallest eddies, at the Kolomogorov scale, to the internal energy of the fluid [3]. The scales handle length, time and velocity. The Kolomogorov scale is given by $(v^3 / E)^{1/4}$ [3], where "v" refers to viscosity and "E" refers to rate of dissipation. This relationship is directly linked to the Reynolds number of the fluid at hand. In other words will high viscosity and low rate of dissipation lay the ground for large eddies and are the reason for some fluids to obtain and sustain turbulent behaviour more easy than others. The predominant factor, as shown above, is viscosity, i.e. oil will obtain "balance" faster than water. The smallest eddies in the Kolomogorov scale is found to be 0,1-1 mm. At this scale one is considering viscosity and dissipation, i.e. the very basic chemical reactions that is fundamental for fire dynamics.

Turbulence intensity

The turbulence intensity, I, is calculated based on simulation results for the given scenario based on average velocities for u, v and w directions and the variance between 20-30 seconds according to the following equation;

Equation 1

$$I = \frac{\sqrt{\frac{1}{3}(Var(u) + Var(v) + Var(w))}}{\bar{u}}$$

In addition to the given simulation set-ups (two different grid-sizes) given in [7], a third simulation was performed to investigate the consequence of a finer "fire-mesh", i.e. two meshes were used in the simulation. This is not a recommended way to investigate turbulent flows, but since mesh-splitting is extensively being done in the industry it can be interesting to compare the results with the uniform mesh simulations. The fire-mesh was defined for the first 0,8 m of the room (X=0.0,0.8) and the cell-size was set to 0.025 m in all directions, while the other mesh, accounting for the rest of the computational domain, had 0.05 m cells.

Results from the calculations of turbulence intensity are given in *Table 9*.

Table 9. Turbulence intensity in different parts of the room calculated on basis of FDS simulations with different cell sizes.

Cell size	**0.1 m**	**0.05 m**	**0.025/0.05 m**
Fire	0,2414	0,3580	0,3929
Room	0,3941	0,4938	0,3052
Door upper	0,2965	0,2694	0,2540
Door lower	0,1333	0,1278	0,1040

The results show that the turbulence intensity is largest in the midst of the room, where it is close to 50 % in the 0.05 m simulation. One would expect more turbulence above the fire or in the top of the door, but from the visual observation of the airflow in the room through the smokeview-file, it is clear that the high turbulence intensity is a result of the conflicting in- and outflow (see Figure 47 and Figure 48 below). The device measuring the room velocity is placed close to where the neutral plane seems to be located in large parts of the sample-time used for the calculations (20-30 seconds). This area has relatively small velocities and at the same time big variations (fluctuations) because the flow will change direction, depending on the height of the neutral plane. Both for the "fire-device" and the "upper door-device", the flow will be more one-directional, i.e. going upwards (positive w-velocity) above the fire and out (positive u-velocity) in the top of the door, and have relatively large velocities, which reduces the intensity.

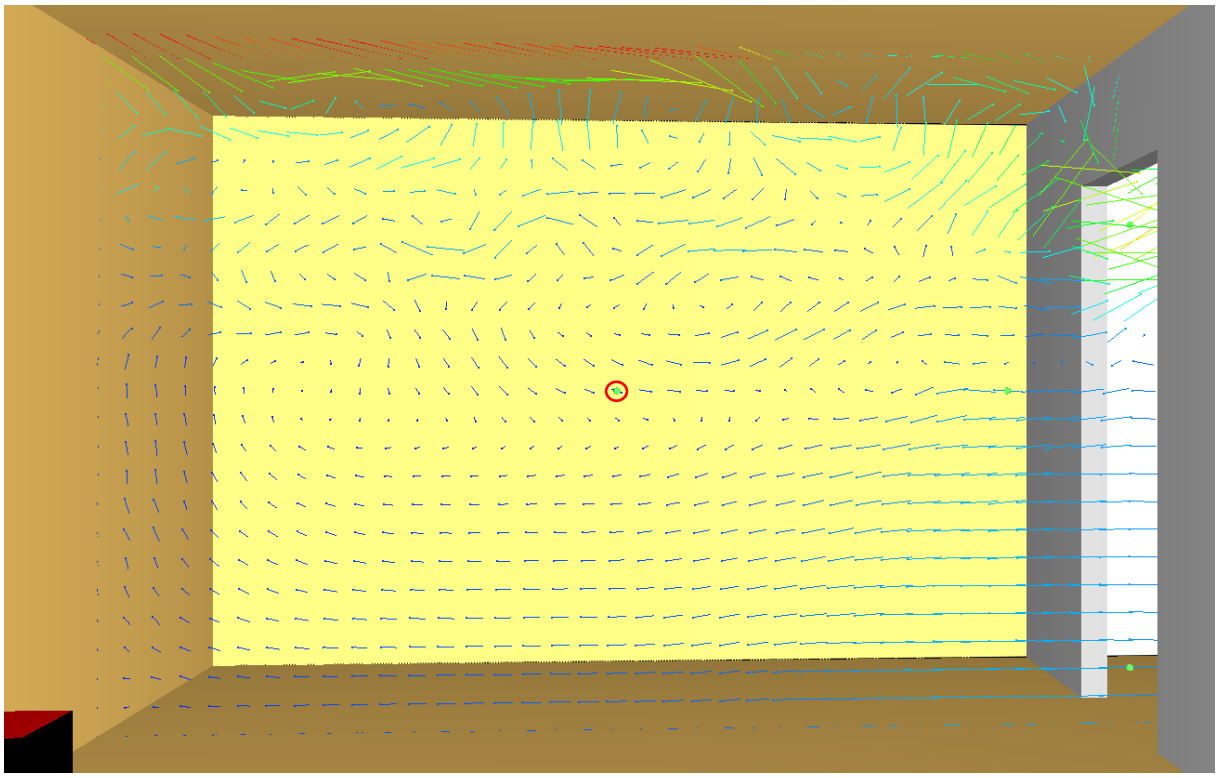

Figure 47. Vector slice of the velocity inside the room after 24 seconds for the simulation with 0.1 m grid-size.

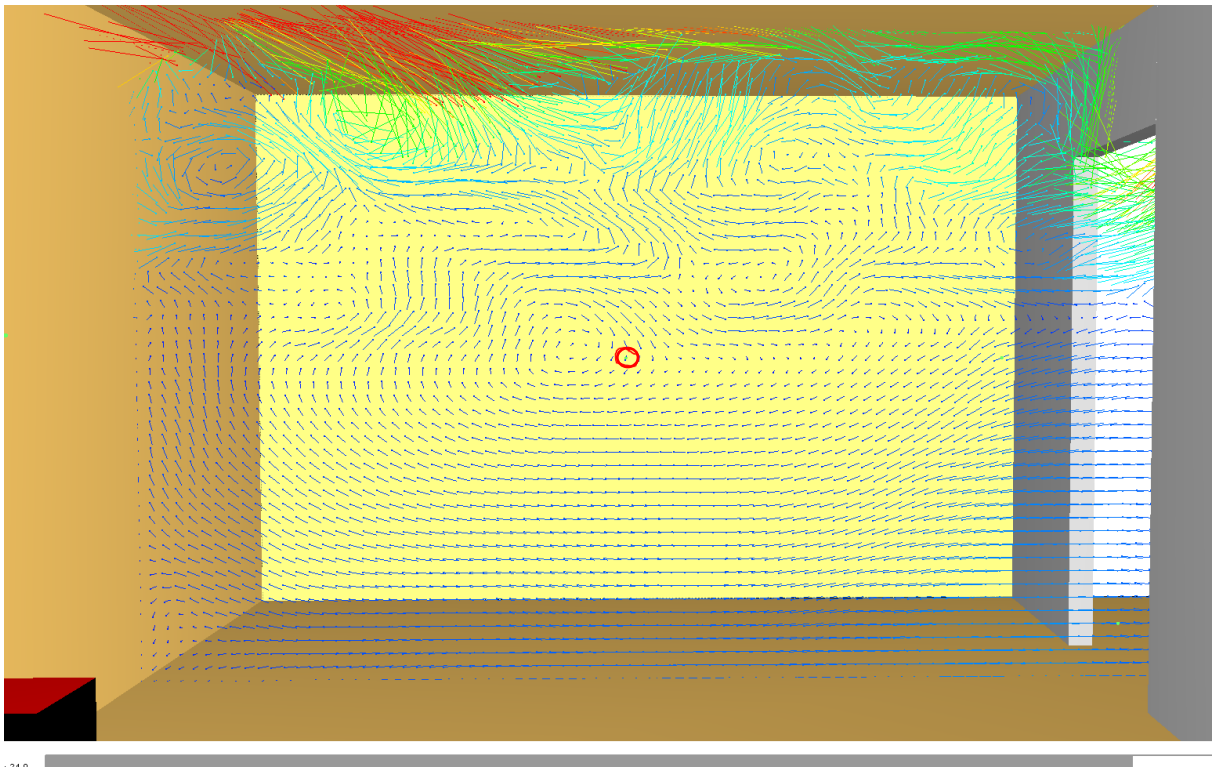

Figure 48. Vector slice of the velocity inside the room after 24 seconds for the simulation with 0.05 m grid-size.

The different cell-size simulations show that the turbulence intensity becomes larger with smaller cell-size for the fire and the room, which was expected since the smaller cell-size would capture more of the turbulence, or fluctations. However, for the door, this theory does not seem to be true, since the intensity is smaller for the smaller cell-sizes. The results show that the fluctuations, or variance, is much larger for the 0.1 m cell simulation compared to the simulation with 0.05 m cells. In fact, the variance is 2 times bigger for the 0.1 m simulation whilst the mean velocity is only 1,29 times bigger, resulting in greater intensities for the 0.1 m simulation. This is also illustrated in Figure 49, where we see that the fluctuations are greater for the 0.01 m grid-size simulation, whilst the average velocity is just a little higher than the 0.05 m grid-size simulation. This indicates that the larger grid seems to overestimate the fluctuations at these locations.

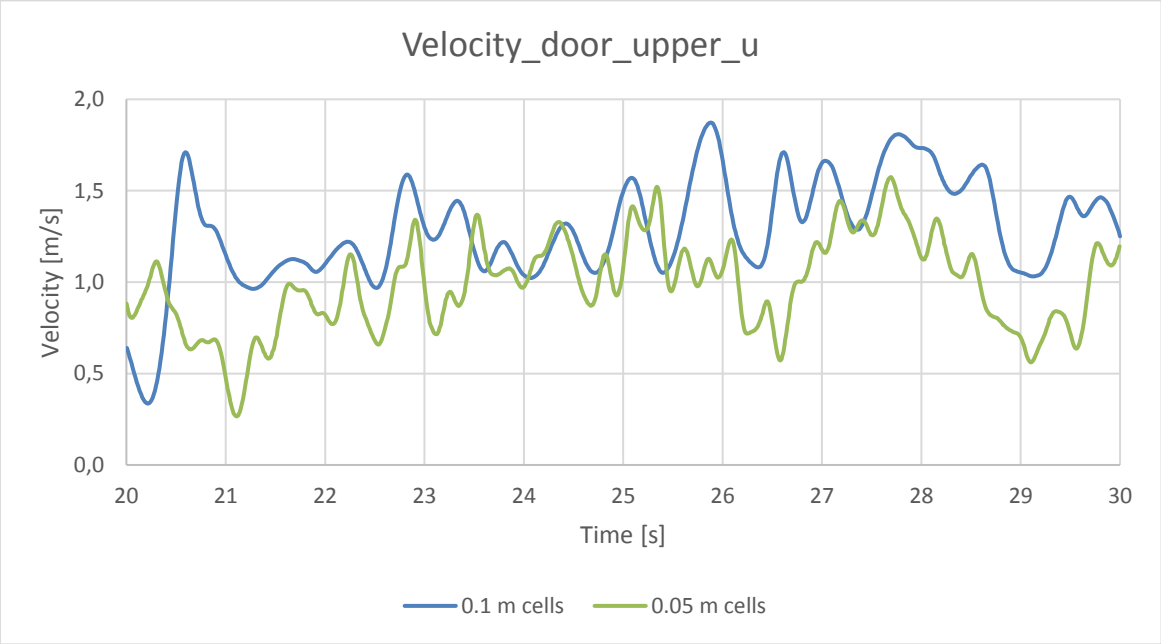

Figure 49. U-velocity in the upper part of the door for 0.1 m and 0.05 m cell simulations.

The results from the split-mesh simulation indicate that the turbulence doesn't seem to be transferred correctly from the finer to the coarser mesh, and that information might have been lost between the two meshes. This conclusion is based on the fact that while the fire grid seems to further resolve the turbulence, a sudden drop is seen for the turbulence in the room compared to the other simulations. This indicates that for this simulation, the splitting of the mesh inside the room does not give reliable results and that great consideration should be made when splitting meshes.

Turbulence resolution

The "average" turbulence resolution (TR) is calculated based on the resolved kinetic energy ($k_{resolved}$) and the subgrid kinetic energy (k_{sgs}) for the different measuring locations used in section 2;

$$TR = \frac{k_{sgs}}{k_{resolved} + k_{sgs}}$$

Average k_{sgs} is calculated based on direct output from FDS of the instant k_{sgs} for each time-step (&DEVC ID='SKE_*location*', QUANTITY='SUBGRID KINETIC ENERGY', XYZ=x,y ,z). $k_{resolved}$ is calculated based on the following equation;

Equation 2

$$k_{resolved} = \frac{Var(u) + Var(v) + Var(w)}{2}$$

Sensitivity analysis with respect to grid-size is normally performed, and strongly recommended, when performing FDS simulations. For this assignment the recommendations for grid-size, i.e. $4 < D^*/\delta x < 16$, where D^* is the characteristic fire diameter and δx represent the grid-size [1], is included to assess the relationship between the recommendations and turbulent resolution. The equation for D* is given by [1];

Equation 3

$$D^* = \left(\frac{Q}{\rho_\infty \, c_p \, T_\infty \sqrt{g}}\right)^{\frac{2}{5}}$$

In our example, with a 100 kw fire, this gives D*=0.383, when assuming ρ_∞=1.2, c_p= 1.0 and T_∞=293 (20°C). The resulting $D^*/\delta x$ for cell sizes used, is given in Table 9 along with the calculated turbulence resolution.

Table 10. TR for the given scenario for different grid-sizes and different simulation types (LES and DNS).

Cell size	$D^*/\delta x$	**Fire**	**Room**	**Door up**	**Door low**
0.1 m	3,83	0,2758	0,1587	0,1964	0,0216
0.05 m	7,66	0,1845	0,0158	0,1691	0,0123
0.025/0.05 m*	15,32/7,66	0,1054	0,0180	0,2071	0,0227

* This simulation was done with 2 meshes, where the fire-area was divided in smaller cells, half of the other mesh, to possibly get a better resolution of the high-turbulent fire area.

As expected, the subgrid energy being modelled in the simulations becomes smaller with decreasing cell size, i.e. a larger part of the turbulent structures are being resolved and calculated directly instead of being "modelled". The grid acts as a filter with respect to the turbulent structures, i.e. finer grid (smaller cell-sizes) will capture more of the eddies which varies in size, time and velocity.

The difference between 0.1 m and 0.05 m grid is significant, and supports the use of the recommended sensitivity analysis given in the FDS user-guide [5]. The 0.1 m grid will in fact be outside the recommended range for $D^*/\delta x$ (4-16), but as one can see from the turbulent resolution of the fire-area for the split mesh simulation, further refinement will have great impact. The conclusion from section 2 regarding the difficulties arising when splitting meshes is further supported by the calculation of turbulence resolution.

The "size" of the subgrid is largest for the fire and the upper door areas, which was the locations one expected the most turbulence to occur in section 2 of this report. In fact, when accounting for the subgrid, the difference in intensity between different locations becomes smaller, as shown in *Table 11* below. This shows the importance of sufficient resolving. The recommended degree of resolution is 80 %, corresponding to a TR of 0,2 (20 %).

Table 11. Turbulence intensity, comparing intensity calculated without and with subgrid.

Cell size	**0.1 m**	**0.1 m incl. subgrid**	**0.05 m**	**0.05 m incl. subgrid**	**0.025/0.05 m**	**0.025/0.05 m incl. subgrid**
Fire	0,2414	0,3135	0,3580	0,4226	0,3929	0,4318
Room	0,3941	0,3975	0,4938	0,4941	0,3052	0,3053
Door upper	0,2965	0,3266	0,2694	0,2855	0,2540	0,2699
Door lower	0,1333	0,1334	0,1278	0,1278	0,1040	0,1041

As can be seen from the results, the high-velocity locations, i.e. fire and upper door, have a significantly higher turbulence intensity when the subgrid is taken into account whilst the low-velocity locations do not change much. The difference between turbulence intensity with and without including the subgrid becomes smaller for smaller grid-sizes, of course.

Attachments (not included)

[1] FDS input file 0.1 m cells
[2] Excel-sheet output 0.1 m cells
[3] FDS input file 0.05 m cells
[4] Excel-sheet output 0.5 m cells
[5] FDS input file 0.025/0.05 m cells
[6] Excel-sheet output 0.025/0.05 m cells

References

[1] *Computational Methods for Fluid Dynamics*, Fertziger, J., H. & Peric, M., third revision, 2002.
[2] *ing4006_turbulens_bph_2016*, lecture notes, Husted, B., 2016.
[3] Environmental fluid dynamics, Cushman-Roisin, B., John Wiley & Sons, ch. 8, under preparation; http://engineering.dartmouth.edu/~d30345d/books/EFM.html
[4] *Example of turbulence*, Lecture notes, Fronter, Husted, B., 2016.
[5] *FDS user guide*, sixth edition, NIST, 2016.
[6] *Numerical Heat Transfer and Fluid Flow*, lecture note on Fronter 2016.
[7] *Advanced Fire and Egress Modelling (ING 4006). Home assignment 3.* Assignment given on Fronter 2016.

Appendix B. FDS input file for 1.5 m/s ventilation scenario

Vent_tox_1.5m_s.fds

Generated by PyroSim - Version 2017.2.1115

20.feb.2018 21:32:32

```
&HEAD CHID='Vent_tox_1_5m_s', TITLE='Tunnel fire ventilation'/

&TIME T_END=3600.0/

&DUMP RENDER_FILE='Vent_tox_1_5m_s.ge1', COLUMN_DUMP_LIMIT=.TRUE., DT_DEVC=1.0, DT_HRR=1.0, DT_ISOF=1.0, DT_PL3D=5.0,
DT_RESTART=100.0, DT_SLCF=1.0, WRITE_XYZ=.TRUE., PLOT3D_QUANTITY='VOLUME FRACTION','VOLUME FRACTION','VOLUME FRACTION','W-
VELOCITY','HRRPUV', PLOT3D_SPEC_ID(1:3)='CARBON DIOXIDE','CARBON MONOXIDE','OXYGEN'/

&MISC TMPA=15.0, VISIBILITY_FACTOR=8.0, RESTART=.TRUE./

&MESH ID='Mesh2', IJK=56,500,36, XB=0.0,11.2,170.0,270.0,0.0,7.0/

&MESH ID='Mesh3', IJK=28,575,18, XB=0.0,11.2,270.0,500.0,0.0,7.0/

&MESH ID='Mesh1', IJK=28,435,18, XB=0.0,11.2,-4.0,170.0,0.0,7.0/

&MESH ID='Mesh4', IJK=28,500,18, XB=0.0,11.2,500.0,700.0,0.0,7.0/

&MESH ID='Mesh5', IJK=28,760,18, XB=0.0,11.2,700.0,1004.0,0.0,7.0/

&REAC ID='Reaction1',
    FUEL='REAC_FUEL',
    C=4.56,
    H=6.56,
    O=2.34,
    N=0.4,
    CO_YIELD=0.1,
    SOOT_YIELD=0.09,
    HEAT_OF_COMBUSTION=2.0E4/

&DEVC ID='FED', QUANTITY='FED', XYZ=1.5,200.0,2.0/

&DEVC ID='FIC', QUANTITY='FIC', XYZ=1.5,200.0,2.0/

&DEVC ID='FED01', QUANTITY='FED', XYZ=10.1,200.0,2.0/

&DEVC ID='FIC01', QUANTITY='FIC', XYZ=10.1,200.0,2.0/

&DEVC ID='FED02', QUANTITY='FED', XYZ=1.5,230.0,2.0/

&DEVC ID='FIC02', QUANTITY='FIC', XYZ=1.5,230.0,2.0/

&DEVC ID='FED03', QUANTITY='FED', XYZ=10.1,230.0,2.0/

&DEVC ID='FIC03', QUANTITY='FIC', XYZ=1.5,230.0,2.0/

&DEVC ID='FED04', QUANTITY='FED', XYZ=1.5,350.0,2.0/

&DEVC ID='FIC04', QUANTITY='FIC', XYZ=1.5,350.0,2.0/

&DEVC ID='FED05', QUANTITY='FED', XYZ=10.1,350.0,2.0/

&DEVC ID='FIC05', QUANTITY='FIC', XYZ=10.1,350.0,2.0/
```

```
&DEVC ID='FED06', QUANTITY='FED', XYZ=1.5,500.0,2.0/
&DEVC ID='FIC06', QUANTITY='FIC', XYZ=1.5,500.0,2.0/
&DEVC ID='SOOT VOLUME CONCENTRATION', QUANTITY='VOLUME FRACTION', SPEC_ID='SOOT', XYZ=1.5,20.0,2.0/
&DEVC ID='SOOT VOLUME CONCENTRATION01', QUANTITY='VOLUME FRACTION', SPEC_ID='SOOT', XYZ=1.5,230.0,2.0/
&DEVC ID='SOOT VOLUME CONCENTRATION02', QUANTITY='VOLUME FRACTION', SPEC_ID='SOOT', XYZ=1.5,250.0,2.0/
&DEVC ID='SOOT VOLUME CONCENTRATION03', QUANTITY='VOLUME FRACTION', SPEC_ID='SOOT', XYZ=1.5,350.0,2.0/
&DEVC ID='SOOT VOLUME CONCENTRATION04', QUANTITY='VOLUME FRACTION', SPEC_ID='SOOT', XYZ=1.5,400.0,2.0/
&DEVC ID='SOOT VOLUME CONCENTRATION05', QUANTITY='VOLUME FRACTION', SPEC_ID='SOOT', XYZ=1.5,500.0,2.0/
&DEVC ID='SOOT VOLUME CONCENTRATION06', QUANTITY='VOLUME FRACTION', SPEC_ID='SOOT', XYZ=4.8,500.0,2.0/
&DEVC ID='SOOT VOLUME CONCENTRATION07', QUANTITY='VOLUME FRACTION', SPEC_ID='SOOT', XYZ=4.8,600.0,2.0/
&DEVC ID='SOOT VOLUME CONCENTRATION08', QUANTITY='VOLUME FRACTION', SPEC_ID='SOOT', XYZ=4.8,800.0,2.0/
&DEVC ID='VELOCITY', QUANTITY='VELOCITY', XYZ=3.7,215.0,6.0/
&DEVC ID='Sootvolume', QUANTITY='VOLUME FRACTION', SPEC_ID='SOOT', XYZ=10.1,205.0,2.0/
&DEVC ID='Sootvolume01', QUANTITY='VOLUME FRACTION', SPEC_ID='SOOT', XYZ=10.1,215.0,2.0/
&DEVC ID='Sootvolume02', QUANTITY='VOLUME FRACTION', SPEC_ID='SOOT', XYZ=10.1,230.0,2.0/
&DEVC ID='Sootvolume03', QUANTITY='VOLUME FRACTION', SPEC_ID='SOOT', XYZ=10.1,250.0,2.0/
&MATL ID='CONCRETE',
    FYI='Typisk betong',
    SPECIFIC_HEAT=1.04,
    CONDUCTIVITY=1.8,
    DENSITY=2280.0/
&SURF ID='TUNNELWALL',
    RGB=146,202,166,
    DEFAULT=.TRUE.,
    BACKING='VOID',
    MATL_ID(1,1)='CONCRETE',
    MATL_MASS_FRACTION(1,1)=1.0,
    THICKNESS(1)=1.0,
    ROUGHNESS=0.25/
&SURF ID='HGV Fire',
    COLOR='RED',
    HRRPUA=1890.0,
    RAMP_Q='HGV Fire_RAMP_Q'/
&RAMP ID='HGV Fire_RAMP_Q', T=0.0, F=0.0/
&RAMP ID='HGV Fire_RAMP_Q', T=30.0, F=0.012625/
```

```
&RAMP ID='HGV Fire_RAMP_Q', T=60.0, F=0.025249/
&RAMP ID='HGV Fire_RAMP_Q', T=90.0, F=0.037874/
&RAMP ID='HGV Fire_RAMP_Q', T=120.0, F=0.050499/
&RAMP ID='HGV Fire_RAMP_Q', T=121.0, F=0.051008/
&RAMP ID='HGV Fire_RAMP_Q', T=180.0, F=0.100692/
&RAMP ID='HGV Fire_RAMP_Q', T=210.0, F=0.138159/
&RAMP ID='HGV Fire_RAMP_Q', T=300.0, F=0.251883/
&RAMP ID='HGV Fire_RAMP_Q', T=420.0, F=0.403482/
&RAMP ID='HGV Fire_RAMP_Q', T=660.0, F=0.70678/
&RAMP ID='HGV Fire_RAMP_Q', T=892.0, F=1.0/
&RAMP ID='HGV Fire_RAMP_Q', T=1800.0, F=1.0/
&OBST ID='Obstruction', XB=0.6,10.9,0.0,1000.0,-0.4,0.0, THICKEN=.TRUE., SURF_ID='TUNNELWALL'/
&OBST ID='Obstruction', XB=0.6,1.0,0.0,1000.0,0.0,2.8, THICKEN=.TRUE., SURF_ID='TUNNELWALL'/
&OBST ID='Obstruction', XB=1.0,1.4,0.0,1000.0,2.8,3.6, THICKEN=.TRUE., SURF_ID='TUNNELWALL'/
&OBST ID='Obstruction', XB=1.4,1.8,0.0,1000.0,3.6,4.0, THICKEN=.TRUE., SURF_ID='TUNNELWALL'/
&OBST ID='Obstruction', XB=1.8,2.2,0.0,1000.0,4.0,4.8, THICKEN=.TRUE., SURF_ID='TUNNELWALL'/
&OBST ID='Obstruction', XB=2.2,2.6,0.0,1000.0,4.8,5.2, THICKEN=.TRUE., SURF_ID='TUNNELWALL'/
&OBST ID='Obstruction', XB=2.6,3.4,0.0,1000.0,5.2,5.6, THICKEN=.TRUE., SURF_ID='TUNNELWALL'/
&OBST ID='Obstruction', XB=3.4,4.2,0.0,1000.0,5.6,6.0, THICKEN=.TRUE., SURF_ID='TUNNELWALL'/
&OBST ID='Obstruction', XB=4.2,5.0,0.0,1000.0,6.0,6.4, THICKEN=.TRUE., SURF_ID='TUNNELWALL'/
&OBST ID='Obstruction', XB=5.0,6.6,0.0,1000.0,6.4,6.8, THICKEN=.TRUE., SURF_ID='TUNNELWALL'/
&OBST ID='Obstruction', XB=6.6,7.4,0.0,1000.0,6.0,6.4, THICKEN=.TRUE., SURF_ID='TUNNELWALL'/
&OBST ID='Obstruction', XB=7.4,8.2,0.0,1000.0,5.6,6.0, THICKEN=.TRUE., SURF_ID='TUNNELWALL'/
&OBST ID='Obstruction', XB=8.2,9.0,0.0,1000.0,5.2,5.6, THICKEN=.TRUE., SURF_ID='TUNNELWALL'/
&OBST ID='Obstruction', XB=9.0,9.4,0.0,1000.0,4.8,5.2, THICKEN=.TRUE., SURF_ID='TUNNELWALL'/
&OBST ID='Obstruction', XB=9.4,9.8,0.0,1000.0,4.0,4.8, THICKEN=.TRUE., SURF_ID='TUNNELWALL'/
&OBST ID='Obstruction', XB=9.8,10.2,0.0,1000.0,3.6,4.0, THICKEN=.TRUE., SURF_ID='TUNNELWALL'/
&OBST ID='Obstruction', XB=10.2,10.6,0.0,1000.0,2.8,3.6, THICKEN=.TRUE., SURF_ID='TUNNELWALL'/
&OBST ID='Obstruction', XB=10.6,11.0,0.0,1000.0,0.0,2.8, THICKEN=.TRUE., SURF_ID='TUNNELWALL'/
&OBST ID='FIREOBST', XB=2.4,5.0,205.0,225.0,0.4,0.8, SURF_ID='INERT'/
&OBST ID='Obstruction duct 1', XB=5.4,6.2,50.0,53.0,5.6,6.4, SURF_ID='INERT'/
&OBST ID='Obstruction duct 2', XB=5.4,6.2,150.0,153.0,5.6,6.4, SURF_ID='INERT'/
&OBST ID='Obstruction duct 3', XB=5.4,6.2,250.0,253.0,5.6,6.4, SURF_ID='INERT'/
&OBST ID='Obstruction duct 4', XB=5.4,6.2,350.0,353.0,5.6,6.4, SURF_ID='INERT'/
&OBST ID='Obstruction duct 5', XB=5.4,6.2,450.0,453.0,5.6,6.4, SURF_ID='INERT'/
```

```
&OBST ID='Obstruction duct 6', XB=5.4,6.2,550.0,553.0,5.6,6.4, SURF_ID='INERT'/
&OBST ID='Obstruction duct 7', XB=5.4,6.2,650.0,653.0,5.6,6.4, SURF_ID='INERT'/
&OBST ID='Obstruction duct 8', XB=5.4,6.2,750.0,753.0,5.6,6.4, SURF_ID='INERT'/
&OBST ID='Obstruction duct 9', XB=5.4,6.2,850.0,853.0,5.6,6.4, SURF_ID='INERT'/
&OBST ID='Obstruction duct 10', XB=5.4,6.2,950.0,953.0,5.6,6.4, SURF_ID='INERT'/
&VENT ID='Vent01', SURF_ID='HVAC', XB=5.4,6.2,50.0,50.0,5.6,6.4/
&VENT ID='Vent02', SURF_ID='HVAC', XB=5.4,6.2,53.0,53.0,5.6,6.4/
&VENT ID='Vent03', SURF_ID='HVAC', XB=5.4,6.2,150.0,150.0,5.6,6.4/
&VENT ID='Vent04', SURF_ID='HVAC', XB=5.4,6.2,153.0,153.0,5.6,6.4/
&VENT ID='Vent05', SURF_ID='HVAC', XB=5.4,6.2,250.0,250.0,5.6,6.4/
&VENT ID='Vent06', SURF_ID='HVAC', XB=5.4,6.2,253.0,253.0,5.6,6.4/
&VENT ID='Vent07', SURF_ID='HVAC', XB=5.4,6.2,350.0,350.0,5.6,6.4/
&VENT ID='Vent08', SURF_ID='HVAC', XB=5.4,6.2,353.0,353.0,5.6,6.4/
&VENT ID='Vent09', SURF_ID='HVAC', XB=5.4,6.2,450.0,450.0,5.6,6.4/
&VENT ID='Vent10', SURF_ID='HVAC', XB=5.4,6.2,453.0,453.0,5.6,6.4/
&VENT ID='Vent11', SURF_ID='HVAC', XB=5.4,6.2,550.0,550.0,5.6,6.4/
&VENT ID='Vent12', SURF_ID='HVAC', XB=5.4,6.2,553.0,553.0,5.6,6.4/
&VENT ID='Vent13', SURF_ID='HVAC', XB=5.4,6.2,650.0,650.0,5.6,6.4/
&VENT ID='Vent14', SURF_ID='HVAC', XB=5.4,6.2,653.0,653.0,5.6,6.4/
&VENT ID='Vent15', SURF_ID='HVAC', XB=5.4,6.2,750.0,750.0,5.6,6.4/
&VENT ID='Vent16', SURF_ID='HVAC', XB=5.4,6.2,753.0,753.0,5.6,6.4/
&VENT ID='Vent17', SURF_ID='HVAC', XB=5.4,6.2,850.0,850.0,5.6,6.4/
&VENT ID='Vent18', SURF_ID='HVAC', XB=5.4,6.2,853.0,853.0,5.6,6.4/
&VENT ID='Vent19', SURF_ID='HVAC', XB=5.4,6.2,950.0,950.0,5.6,6.4/
&VENT ID='Vent20', SURF_ID='HVAC', XB=5.4,6.2,953.0,953.0,5.6,6.4/
&VENT ID='Mesh Vent: Mesh15 [XMAX]', SURF_ID='OPEN', XB=11.2,11.2,-4.0,1004.0,0.0,7.0, OUTLINE=.TRUE./
&VENT ID='Mesh Vent: Mesh15 [XMIN]', SURF_ID='OPEN', XB=0.0,0.0,-4.0,1004.0,0.0,7.0, OUTLINE=.TRUE./
&VENT ID='Mesh Vent: Mesh15 [YMAX]', SURF_ID='OPEN', XB=0.0,11.2,1004.0,1004.0,0.0,7.0, OUTLINE=.TRUE./
&VENT ID='Mesh Vent: Mesh15 [YMIN]', SURF_ID='OPEN', XB=0.0,11.2,-4.0,-4.0,0.0,7.0, OUTLINE=.TRUE./
&VENT ID='Mesh Vent: Mesh15 [ZMAX]', SURF_ID='OPEN', XB=0.0,11.2,-4.0,1004.0,7.0,7.0, COLOR='INVISIBLE', OUTLINE=.TRUE./
&VENT ID='100MW Tunnel fire', SURF_ID='HGV Fire', XB=2.4,5.0,205.0,225.0,0.8,0.8/
&HVAC ID='Node01', TYPE_ID='NODE', DUCT_ID='Duct01', VENT_ID='Vent01'/
&HVAC ID='Node02', TYPE_ID='NODE', DUCT_ID='Duct01', VENT_ID='Vent02'/
&HVAC ID='Node03', TYPE_ID='NODE', DUCT_ID='Duct02', VENT_ID='Vent03'/
&HVAC ID='Node04', TYPE_ID='NODE', DUCT_ID='Duct02', VENT_ID='Vent04'/
```

```
&HVAC ID='Node05', TYPE_ID='NODE', DUCT_ID='Duct03', VENT_ID='Vent05'/

&HVAC ID='Node06', TYPE_ID='NODE', DUCT_ID='Duct03', VENT_ID='Vent06'/

&HVAC ID='Node07', TYPE_ID='NODE', DUCT_ID='Duct04', VENT_ID='Vent07'/

&HVAC ID='Node08', TYPE_ID='NODE', DUCT_ID='Duct04', VENT_ID='Vent08'/

&HVAC ID='Node09', TYPE_ID='NODE', DUCT_ID='Duct05', VENT_ID='Vent09'/

&HVAC ID='Node10', TYPE_ID='NODE', DUCT_ID='Duct05', VENT_ID='Vent10'/

&HVAC ID='Node11', TYPE_ID='NODE', DUCT_ID='Duct06', VENT_ID='Vent11'/

&HVAC ID='Node12', TYPE_ID='NODE', DUCT_ID='Duct06', VENT_ID='Vent12'/

&HVAC ID='Node13', TYPE_ID='NODE', DUCT_ID='Duct07', VENT_ID='Vent13'/

&HVAC ID='Node14', TYPE_ID='NODE', DUCT_ID='Duct07', VENT_ID='Vent14'/

&HVAC ID='Node15', TYPE_ID='NODE', DUCT_ID='Duct08', VENT_ID='Vent15'/

&HVAC ID='Node16', TYPE_ID='NODE', DUCT_ID='Duct08', VENT_ID='Vent16'/

&HVAC ID='Node17', TYPE_ID='NODE', DUCT_ID='Duct09', VENT_ID='Vent17'/

&HVAC ID='Node18', TYPE_ID='NODE', DUCT_ID='Duct09', VENT_ID='Vent18'/

&HVAC ID='Node19', TYPE_ID='NODE', DUCT_ID='Duct10', VENT_ID='Vent19'/

&HVAC ID='Node20', TYPE_ID='NODE', DUCT_ID='Duct10', VENT_ID='Vent20'/

&HVAC ID='Duct01', TYPE_ID='DUCT', AREA=0.64, PERIMETER=3.2, VOLUME_FLOW=5.4, NODE_ID='Node01','Node02', REVERSE=.TRUE.,
ROUGHNESS=1.0E-3, LENGTH=3.0/

&HVAC ID='Duct02', TYPE_ID='DUCT', AREA=0.64, PERIMETER=3.2, VOLUME_FLOW=5.4, NODE_ID='Node03','Node04', REVERSE=.TRUE.,
ROUGHNESS=1.0E-3, LENGTH=3.0/

&HVAC ID='Duct03', TYPE_ID='DUCT', AREA=0.64, PERIMETER=3.2, VOLUME_FLOW=5.4, NODE_ID='Node05','Node06', REVERSE=.TRUE.,
ROUGHNESS=1.0E-3, LENGTH=3.0/

&HVAC ID='Duct04', TYPE_ID='DUCT', AREA=0.64, PERIMETER=3.2, VOLUME_FLOW=5.4, NODE_ID='Node07','Node08', REVERSE=.TRUE.,
ROUGHNESS=1.0E-3, LENGTH=3.0/

&HVAC ID='Duct05', TYPE_ID='DUCT', AREA=0.64, PERIMETER=3.2, VOLUME_FLOW=5.4, NODE_ID='Node09','Node10', REVERSE=.TRUE.,
ROUGHNESS=1.0E-3, LENGTH=3.0/

&HVAC ID='Duct06', TYPE_ID='DUCT', AREA=0.64, PERIMETER=3.2, VOLUME_FLOW=5.4, NODE_ID='Node11','Node12', REVERSE=.TRUE.,
ROUGHNESS=1.0E-3, LENGTH=3.0/

&HVAC ID='Duct07', TYPE_ID='DUCT', AREA=0.64, PERIMETER=3.2, VOLUME_FLOW=5.4, NODE_ID='Node13','Node14', REVERSE=.TRUE.,
ROUGHNESS=1.0E-3, LENGTH=3.0/

&HVAC ID='Duct08', TYPE_ID='DUCT', AREA=0.64, PERIMETER=3.2, VOLUME_FLOW=5.4, NODE_ID='Node15','Node16', REVERSE=.TRUE.,
ROUGHNESS=1.0E-3, LENGTH=3.0/

&HVAC ID='Duct09', TYPE_ID='DUCT', AREA=0.64, PERIMETER=3.2, VOLUME_FLOW=5.4, NODE_ID='Node17','Node18', REVERSE=.TRUE.,
ROUGHNESS=1.0E-3, LENGTH=3.0/

&HVAC ID='Duct10', TYPE_ID='DUCT', AREA=0.64, PERIMETER=3.2, VOLUME_FLOW=5.4, NODE_ID='Node19','Node20', REVERSE=.TRUE.,
ROUGHNESS=1.0E-3, LENGTH=3.0/

&ISOF QUANTITY='VISIBILITY', VALUE=1.0,3.0,4.0,6.0/

&SLCF QUANTITY='VISIBILITY', PBX=1.5/

&SLCF QUANTITY='VISIBILITY', PBX=5.8/
```

```
&SLCF QUANTITY='TEMPERATURE', PBX=5.8/
&SLCF QUANTITY='VELOCITY', VECTOR=.TRUE., PBX=5.8/
&SLCF QUANTITY='VOLUME FRACTION', SPEC_ID='CARBON MONOXIDE', PBX=5.8/
&SLCF QUANTITY='VOLUME FRACTION', SPEC_ID='CARBON DIOXIDE', PBX=5.8/
&SLCF QUANTITY='VOLUME FRACTION', SPEC_ID='OXYGEN', PBX=5.8/
&SLCF QUANTITY='VOLUME FRACTION', SPEC_ID='SOOT', PBX=5.8/
&SLCF QUANTITY='VISIBILITY', PBX=10.1/
&SLCF QUANTITY='TEMPERATURE', PBX=1.5/
&SLCF QUANTITY='TEMPERATURE', PBX=3.7/
&SLCF QUANTITY='TEMPERATURE', PBX=10.1/
&SLCF QUANTITY='VELOCITY', VECTOR=.TRUE., PBX=1.5/
&SLCF QUANTITY='VELOCITY', VECTOR=.TRUE., PBX=10.1/
&SLCF QUANTITY='VOLUME FRACTION', SPEC_ID='CARBON MONOXIDE', PBX=1.5/
&SLCF QUANTITY='VOLUME FRACTION', SPEC_ID='CARBON MONOXIDE', PBX=10.1/
&SLCF QUANTITY='VOLUME FRACTION', SPEC_ID='CARBON DIOXIDE', PBX=1.5/
&SLCF QUANTITY='VOLUME FRACTION', SPEC_ID='CARBON DIOXIDE', PBX=10.1/
&SLCF QUANTITY='VOLUME FRACTION', SPEC_ID='OXYGEN', PBX=1.5/
&SLCF QUANTITY='VOLUME FRACTION', SPEC_ID='OXYGEN', PBX=10.1/
&SLCF QUANTITY='VOLUME FRACTION', SPEC_ID='SOOT', PBX=1.5/
&SLCF QUANTITY='VOLUME FRACTION', SPEC_ID='SOOT', PBX=10.1/
&SLCF QUANTITY='TEMPERATURE', PBY=200.0/
&SLCF QUANTITY='TEMPERATURE', PBY=206.0/
&SLCF QUANTITY='TEMPERATURE', PBY=212.0/
&SLCF QUANTITY='TEMPERATURE', PBY=218.0/
&SLCF QUANTITY='TEMPERATURE', PBY=224.0/
&SLCF QUANTITY='TEMPERATURE', PBY=230.0/
&SLCF QUANTITY='VELOCITY', VECTOR=.TRUE., PBY=50.0/
&SLCF QUANTITY='VELOCITY', VECTOR=.TRUE., PBY=150.0/
&SLCF QUANTITY='VELOCITY', VECTOR=.TRUE., PBY=200.0/
&SLCF QUANTITY='VELOCITY', VECTOR=.TRUE., PBY=215.0/
&SLCF QUANTITY='VELOCITY', VECTOR=.TRUE., PBY=230.0/
&SLCF QUANTITY='VELOCITY', VECTOR=.TRUE., PBY=300.0/
&SLCF QUANTITY='VELOCITY', VECTOR=.TRUE., PBY=400.0/
&SLCF QUANTITY='VISIBILITY', PBY=200.0/
&SLCF QUANTITY='VISIBILITY', PBY=215.0/
```

```
&SLCF QUANTITY='VISIBILITY', PBY=230.0/

&SLCF QUANTITY='VISIBILITY', PBY=325.0/

&SLCF QUANTITY='VISIBILITY', PBY=425.0/

&SLCF QUANTITY='VISIBILITY', PBY=525.0/

&SLCF QUANTITY='VISIBILITY', PBY=625.0/

&SLCF QUANTITY='VISIBILITY', PBY=725.0/

&SLCF QUANTITY='VISIBILITY', PBY=825.0/

&SLCF QUANTITY='VISIBILITY', PBY=925.0/

&SLCF QUANTITY='VELOCITY', VECTOR=.TRUE., PBZ=5.8/

&SLCF QUANTITY='VISIBILITY', PBZ=2.0/

&SLCF QUANTITY='VOLUME FRACTION', SPEC_ID='SOOT', PBZ=2.0/

&SLCF QUANTITY='VOLUME FRACTION', SPEC_ID='CARBON DIOXIDE', PBZ=2.0/

&SLCF QUANTITY='VOLUME FRACTION', SPEC_ID='CARBON MONOXIDE', PBZ=2.0/

&SLCF QUANTITY='VOLUME FRACTION', SPEC_ID='OXYGEN', PBZ=2.0/

&SLCF QUANTITY='DENSITY', SPEC_ID='SOOT', PBZ=2.0/

&SLCF QUANTITY='EXTINCTION COEFFICIENT', PBZ=2.0/

&SLCF QUANTITY='TEMPERATURE', PBZ=2.0/

&SLCF QUANTITY='TEMPERATURE', PBZ=6.0/

&SLCF QUANTITY='TEMPERATURE', PBZ=3.0/

&SLCF QUANTITY='TEMPERATURE', PBZ=4.0/

&SLCF QUANTITY='TEMPERATURE', PBZ=5.0/

&TAIL /
```